

Anti-biofilm activity of the tick-derived antimicrobial peptide Os(11-22)NH₂
against *Candida albicans* ATCC 90028

Court Kudakwashe Chiramba

Student number: 13328507

Submitted in partial fulfilment of the degree:

Magister Scientiae Biochemistry

in the Faculty of Natural and Agricultural Sciences

Department of Biochemistry, Genetics and Microbiology

University of Pretoria

Date: 15 February 2019

DECLARATION OF ORIGINALITY UNIVERSITY OF PRETORIA

The Department of Biochemistry, Genetics and Microbiology places great emphasis upon integrity and ethical conduct in the preparation of all written work submitted for academic evaluation.

While academic staff teach you about referencing techniques and how to avoid plagiarism, you too have a responsibility in this regard. If you are at any stage uncertain as to what is required, you should speak to your lecturer before any written work is submitted.

You are guilty of plagiarism if you copy something from another author's work (e. g a book, an article or a website) without acknowledging the source and pass it off as your own. In effect you are stealing something that belongs to someone else. This is not only the case when you copy work word-for-word (verbatim), but also when you submit someone else's work in a slightly altered form (paraphrase) or use a line of argument without acknowledging it. You are not allowed to use work previously produced by another student. You are also not allowed to let anybody copy your work with the intention of passing it off as his/her work.

Students who commit plagiarism will not be given any credit for plagiarized work. The matter may also be referred to the Disciplinary Committee (Students) for a ruling. Plagiarism is regarded as a serious contravention of the University's rules and can lead to expulsion from the University.

The declaration which follows must accompany all written work submitted while you are a student of the Department of Biochemistry. No written work will be accepted unless the declaration has been completed and attached.

Full names of student: Court Kudakwashe Chiramba

Student number: 13328507

Topic of work: Anti-biofilm activity of the tick-derived antimicrobial peptide Os(11-22)NH₂ against *Candida albicans* ATCC 90028

1. I understand what plagiarism is and am aware of the University's policy in this regard.
2. I declare that this dissertation is my own original work. Where other people's work has been used (either from a printed source, Internet or any other source), this has been properly acknowledged and referenced in accordance with departmental requirements.
3. I have not used work previously produced by another student or any other person to hand in as my own.
4. I have not allowed, and will not allow, anyone to copy my work with the intention of passing it off as his or her own work.

SIGNATURE:

DATE: 15 February 2019

Acknowledgements

I would like to express my thanks to the following:

- My supervisor, Prof. ARM Gaspar for her guidance, patience and constant encouragement. Her kind-hearted nature has created an environment for me to become a better scientist and to express my research in a way that is simple and can be easily understood.
- My co-supervisor, Prof. MJ Bester, for her insightful questions that challenged me to think more and gain a deeper understanding about the research I was doing. Her support during this project has been nothing short of incredible.
- Ms Sandra van Wyngaardt and Ms Sonya September for their technical assistance.
- The members (current and former) of the Biotherapeutics research group (Dr A Ibrahim, Ms R Mbuayama, Ms D Mwiria, Mr S Ramafoko, Miss S Watson, Miss J van Heerden, Miss M van de Walt and Mr D Möller) for their unwavering support during this project. From their assistance in the lab to scientific and non-scientific discussions, every moment has been enjoyable.
- Mr A Hall and Dr E Venter from the Lab for Microscopy and Microanalysis, University of Pretoria. Mr A Hall provided assistance with obtaining light microscopy images and Dr E Venter assisted with obtaining confocal microscopy images.
- The University of Pretoria, National Research Foundation and South African Medical Research Council for their financial support of this project.

My parents for their love and support during this project, even though they did not understand what my research was about, their unending belief in me has been amazing.

Table of Contents

Acknowledgements.....	ii
Summary.....	v
List of Tables	vii
List of Figures.....	viii
List of Abbreviations	x
1. Literature Review.....	1
1.1 Introduction.....	1
1.2 Antimicrobial resistance.....	2
1.3 Fungal infections	3
1.3.1 <i>Candida albicans</i> -related fungal infections	3
1.4 Current antifungal drugs	4
1.5 Fungal biofilms and antimicrobial resistance	8
1.5.1 Biofilm development	8
1.5.2 Role of biofilms in antimicrobial resistance	9
1.6 Antimicrobial peptides: a potential alternative to antimicrobial therapy.....	10
1.7 Mechanisms of action of antimicrobial peptides.....	11
1.7.1 Membrane targeting antimicrobial peptides.....	12
1.7.2 Antimicrobial peptides with intracellular targets.....	14
1.7.3 Mechanisms of action of antifungal peptides	15
1.8 Antimicrobial peptides that possess anti-biofilm activity	15
1.9 Therapeutic applications of antimicrobial peptides: limitations and possible solutions... 16	16
1.10 Background to the study.....	18
1.11 Aim of the study	19
1.12 Objectives of the study.....	19
2. Materials and Methods	20
2.1 <i>C. albicans</i> growth and culture conditions.....	20
2.2 Preparation of synthetic peptides	20
2.3 Screening of peptides for anti-planktonic activity	20
2.4 Optimization of biofilm formation	22
2.4.1 Determination of biofilm biomass	22
2.4.2 Determination of biofilm cell viability	23
2.5 Screening for anti-biofilm activity.....	24
2.5.1 Biofilm inhibition assay	24
2.5.2 Biofilm eradication assay.....	24

2.6 Mode of action studies	24
2.6.1 Membrane integrity: Confocal laser scanning microscopy.....	24
2.6.2 Reactive oxygen species production: 2',7'-Dichlorodihydrofluorescein diacetate assay.....	26
2.7 Data analysis.....	27
3. Results	29
3.1 Anti-planktonic activity.....	29
3.2 Optimization of biofilm formation	30
3.2.1 Biofilm biomass	30
3.2.2 Biofilm viability	33
3.3 Anti-biofilm activity.....	34
3.3.1 Biofilm inhibiting activity.....	34
3.3.2 Biofilm eradicating activity	36
3.4 Mode of action studies	37
3.4.1 Membrane permeabilization.....	37
3.4.2 Induction of reactive oxygen species formation	40
4. Discussion.....	44
5. Conclusions and Future Perspectives.....	50
6. References	53
7. Appendix.....	67

Summary

The growing occurrence of antimicrobial resistance (AMR) is a global cause for concern due to the decreased availability of effective antimicrobial drugs. Therefore, treating resistant infections can become costly or even impossible. Furthermore, the increase in resistant infections leads to longer hospital stays and higher mortality rates. Resistance is prevalent because microorganisms can form biofilms; communities of cells bound to a surface and covered in an extracellular matrix (ECM), that protects cells from the effects of antimicrobial agents. Besides the ECM, biofilm cells further resist antimicrobial drugs by rapidly developing a number of mechanisms. Therefore, development of novel antimicrobial agents is key to overcoming AMR. One potential alternative to conventional antimicrobial drugs are cationic antimicrobial peptides (AMPs) which are short and amphipathic molecules. Some AMPs possess both anti-planktonic and anti-biofilm activity among other beneficial properties which make them a suitable alternative to conventional antimicrobial drugs. In this study, the anti-biofilm activity of Os(11-22)NH₂, a short peptide derived from Os, a derivative of a defensin identified in the tick *Ornithodoros savignyi*, was investigated. For the purpose of this study, the opportunistic fungal pathogen *Candida albicans*, one of the leading causes of hospital-acquired infections, was used as the model microorganism.

Os was inactive, while the derivative Os(11-22)NH₂ was active against planktonic (free-floating) *C. albicans* with a minimum inhibitory concentration that reduces growth by 50% (MIC₅₀) of 47 µM. The CellTiter Blue (CTB) cell viability assay was used to determine the biofilm inhibiting and eradicating activity. Os(11-22)NH₂ inhibited biofilm formation with a minimum concentration of the antifungal agent that reduced biofilm formation by 50% (BIC₅₀) of 81 µM. Inverted light microscopy images confirmed CTB cell viability results and reduced hyphal formation was observed. Treatment of preformed biofilms with Os(11-22)NH₂ led to biofilm eradication by Os(11-22)NH₂ with a minimum concentration of the antifungal agent that decreased cell viability in a pre-grown biofilm by 50% (BEC₅₀) of 210 µM.

Most AMPs target the cell membrane, therefore, membrane permeabilizing activity was investigated using confocal laser scanning microscopy (CLSM) and the DNA binding dyes propidium iodide (PI) and 4',6-diamidino-2-phenylindole (DAPI). Results indicated that cell membranes were permeabilized by treatment with Os(11-22)NH₂ during biofilm inhibition and eradication.

Some AMPs are known to induce the production of reactive oxygen species (ROS) in microorganisms, leading to cell death. Therefore, the fluorescence producing dye 2,7-dichlorodihydrofluorescein diacetate (DCFH-DA) was used to determine whether Os(11-22)NH₂ induces ROS production. Os(11-22)NH₂ induced ROS production during biofilm inhibition and eradication. In the presence of ascorbic acid, a scavenger of ROS, the production of ROS by the peptide was significantly reduced ($p < 0.0001$).

Furthermore, the effect of ascorbic acid on the biofilm inhibiting and eradicating activity of Os(11-22)NH₂ was determined using the CTB cell viability assay. For biofilm inhibition, no significant difference was observed between treatments in the presence and absence of ascorbic acid, therefore killing during biofilm inhibition was not due to ROS production. For eradication, a significant increase ($p < 0.0001$) in biofilm eradicating activity was observed in the presence of ascorbic acid indicating that the biofilm eradicating activity of Os(11-22)NH₂ was enhanced by ascorbic acid.

In conclusion, anti-biofilm activity of Os(11-22)NH₂ was determined at micromolar concentrations, indicating a potential antifungal application for this peptide. Future research should reveal its mode of action and combination with other antifungal agents.

List of Tables

Table 1.1: Examples of antifungal peptides and their sources, structures and modes of action.....	15
Table 1.2: Physicochemical properties of OsDef2, Os and Os(11-22)NH ₂	19
Table 3.1: MIC ₅₀ and MIC _{max} values of caspofungin, Os(11-22)NH ₂ and Os.....	30
Table 3.2: BIC ₅₀ and BIC _{max} values of amphotericin B and Os(11-22)NH ₂	34
Table 3.3: BEC ₅₀ and BEC _{max} values of amphotericin B and Os(11-22)NH ₂	36
Table 3.4: The influence of ascorbic acid on the biofilm inhibiting activity of Os(11-22)NH ₂	41
Table 5.1: Summary of results from this study.....	52
Table 7.1: Components of double strength (2X) RPMI-1640 2% glucose for anti-planktonic assay.....	67
Table 7.2: Components of single strength RPMI-1640 for biofilm studies.....	67
Table 7.3: Components of 10 mM phosphate buffered saline (PBS) for biofilm studies.....	67

List of Figures

Figure 1.1: Structure of amphotericin B and three-dimensional structures of amphotericin B, cholesterol and ergosterol	5
Figure 1.2: Structures of (A) ketoconazole and (B) isavuconazole.....	6
Figure 1.3: Structures of (A) micafungin, (B) anidulafungin and (C) caspofungin.....	7
Figure 1.4: Overview of biofilm development in <i>C. albicans</i>	8
Figure 1.5: Structural classes of antimicrobial peptides.....	11
Figure 1.6: Models of membrane disruption by antimicrobial peptides.....	13
Figure 2.1: Structure of crystal violet.....	22
Figure 2.2: Reduction of resazurin to resorufin in the CellTiter Blue cell viability assay.....	23
Figure 2.3: Structures of (A) propidium iodide and (B) 4',6-diamidino-2-phenylindole.....	25
Figure 2.4: Structured detail of the 2',7'-Dichlorodihydrofluorescein diacetate assay.....	27
Figure 3.1: Anti-planktonic activity of (A) caspofungin and (B) Os and Os(11-22)NH ₂	29
Figure 3.2: Light microscopy visualization of the kinetics of <i>C. albicans</i> biofilm development.....	31
Figure 3.3: <i>C. albicans</i> biofilm formation over time in terms of biomass assessed by crystal violet staining.....	32
Figure 3.4: <i>C. albicans</i> biofilm formation over time in terms of viability assessed with the CellTiter Blue cell viability assay.....	33
Figure 3.5: Biofilm inhibiting activity of (A) amphotericin B and (B) Os(11-22)NH ₂	34
Figure 3.6: Light microscopy images showing biofilm inhibiting effect of amphotericin B and Os(11-22)NH ₂	35
Figure 3.7: Biofilm eradicating activity of (A) amphotericin B and (B) Os(11-22)NH ₂	36
Figure 3.8: Confocal laser scanning microscopy images of treated and untreated biofilms during biofilm inhibition.....	38
Figure 3.9: Confocal laser scanning microscopy images of treated and untreated biofilms during biofilm eradication.....	39

Figure 3.10: Induction of reactive oxygen species formation during biofilm inhibition.....	40
Figure 3.11: Induction of reactive oxygen species formation during biofilm eradication.....	42
Figure 3.12: Effect of ascorbic acid addition on biofilm eradication.....	43

List of Abbreviations

ϵ	Extinction coefficient
μg	Microgram
μL	Microlitre
μm	Micrometre
μM	Micromolar
ABC	ATP binding cassette
Abs	Absorbance
AFP	Antifungal peptide
AMB	Amphotericin B
AMP	Antimicrobial peptide
AMR	Antimicrobial resistance
ANOVA	Analysis of variance
ATCC	American Type Culture Collection
AU	Arbitrary unit
BEC_{50}	Minimum concentration of antifungal that decreased cell viability in a pre-grown biofilm by 50%
BIC_{50}	Minimum concentration of antifungal that reduced biofilm formation by 50%
CFU/mL	Colony forming unit per millilitre
CLSM	Confocal laser scanning microscopy
CTB	CellTiter Blue
CV	Crystal violet
DAPI	4',6-diamidino-2-phenylindole
DCF	2,7-dichlorofluorescein
DCFH	2,7-dichlorodihydrofluorescein
DCFH-DA	2,7-dichlorodihydrofluorescein diacetate
df	Dilution factor
DMSO	Dimethyl sulfoxide
DNA	Deoxyribonucleic acid
ECM	Extracellular matrix
g	Gram
HBD	Human β -defensin
HNP	Human neutrophil peptide
IC_{50}	Inhibitory concentration that relates to a response which is the average of the top and bottom values
KCl	Potassium chloride
kDa	Kilodalton
L	Litre
m/v	Mass per volume
MFS	Major facilitator superfamily
MgSO_4	Magnesium sulfate
MIC	Minimum inhibitory concentration

MIC ₅₀	Minimum inhibitory concentration of antifungal that reduced growth by 50%
mM	Millimolar
mmol	Millimole
MOPS	3-(N-morpholino) propanesulfonic acid
mV	Millivolts
MW	Molecular weight
NaOH	Sodium hydroxide
n	Number of amino acid residues
nm	Nanometre
OD	Optical density
PBS	Phosphate buffered saline
PI	Propidium iodide
RNA	Ribonucleic acid
ROS	Reactive oxygen species
RP-HPLC	Reverse phase high performance liquid chromatography
RPMI-1640	Roswell Park Memorial Institute 1640
RPMI-DMSO	RPMI-1640 containing 0.5% DMSO
SA	South Africa
SEM	Standard error of the mean
Trp	Tryptophan
Tyr	Tyrosine
v/v	Volume per volume
WHO	World Health Organization
YPD	Yeast peptone dextrose

1. Literature Review

1.1 Introduction

Antimicrobial resistance (AMR) is currently a worldwide threat to human health due to the decreasing efficacy of antimicrobial agents used to treat infections. Globally, approximately 700 000 deaths per year are attributed to antimicrobial resistant infections. However, this number is inaccurate due to the lack of epidemiological data from a number of countries. If solutions are not developed, the number of deaths due to AMR are predicted to reach 10 million by 2050, with a staggering 4.1 million of these deaths occurring in Africa (1). AMR can be caused by numerous factors such as the misuse and abuse of antimicrobial agents, the sale of counterfeit and substandard antimicrobial agents, genetic mutations and acquisition of AMR-encoding genes. All of the previously mentioned factors contribute to greater mortality, prolonged hospital stays and increased treatment costs (2). In particular, increased cases of resistance to antifungal drugs has led to greater concern. Currently, there are three main classes of antifungal drugs: polyenes, azoles and echinocandins. Resistance to antifungal drugs belonging to all three classes has been reported. Species in the genus *Candida* are the most common hospital-acquired fungal pathogens. In South Africa, the World Health Organization (WHO) reported resistance to fluconazole, a first line treatment of *Candida* infections, to be as high as 49% (2). Furthermore, several epidemiological studies in African hospitals have reported resistance of *Candida* species to all three antifungal classes and both planktonic (free-floating) and biofilm forms have become resistant (3-6). A biofilm is a community made up of many microorganisms that are attached to a living or non-living surface and are covered by an extracellular matrix (ECM) which provides protection from the external environment. In addition, biofilms possess unique resistance mechanisms that enable them to survive antifungal treatment (7). Given the high incidence of antifungal resistance, the development of novel antifungal agents that possess anti-biofilm activity is of great importance.

Antimicrobial peptides (AMPs) are short, amphipathic and cationic molecules that have been identified in various organisms and have been found to be active against bacteria, viruses and fungi (8). AMPs possess broad-spectrum activity, multiple killing targets and develop little to no resistance against target cells (9). In addition, AMPs have been found to act against planktonic and biofilm forms of microorganisms. Some AMPs display strong antifungal activity and are therefore classified as antifungal peptides (AFPs). In previous studies, the peptide Os which was derived from a defensin identified in the soft tick *Ornithodoros savignyi*, displayed antifungal activity against planktonic (10) and biofilm (11) forms of *C. albicans*. Os was shortened and amidated at the carboxy terminus to form Os(11-22)NH₂, which also displayed anti-planktonic activity (10). Therefore, the aim of this study was to further investigate the antifungal activity of Os(11-22)NH₂ against *C. albicans* biofilms.

1.2 Antimicrobial resistance

According to the WHO, AMR occurs when a microorganism (bacterium, virus, fungus or parasite) is able to survive and even grow in the presence of an antimicrobial drug (antibiotic, antiviral, antifungal or antiparasitic) that it was once susceptible to (2). As a result, the treatment of infections becomes complicated, costly and even impossible in severe cases. Moreover, the period of illness is extended, and the likelihood of mortality becomes greater. The development of AMR in microorganisms occurs naturally, however, the acquisition of resistance can be sped up by misuse and abuse of antimicrobial agents in both humans and animals. Another factor that contributes to increasing AMR is the lack of development of novel antimicrobial agents that can replace antimicrobial agents that are no longer effective (2).

Accelerated resistance brought about by the misuse and abuse of antimicrobial agents can occur in a number of ways. Firstly, antimicrobial agents are one of the most frequently prescribed drugs in human medicine. However, almost half of these prescriptions are not necessary (12). Furthermore, the use of antimicrobial agents in veterinary medicine, aquaculture and agriculture has led to greater AMR (2). The failure to complete a prescribed course of antimicrobial agents can also lead to resistance since the microorganisms that survived the initial antimicrobial treatment could gain resistance to the antimicrobial agent. Lastly, the production and prescription of substandard and counterfeit antimicrobial agents has also contributed to increasing AMR. Substandard drugs are defined as medicines that are authentic, however, they have not been subjected to standards and quality testing protocols. Counterfeit drugs, on the other hand, are drugs that have been incorrectly labelled in order to mislead consumers. Counterfeit drugs may possess insufficient amounts of the active ingredient or contain no active ingredient at all (13). The use of substandard or counterfeit drugs can promote AMR due to the lack of sufficient doses of the antimicrobial agents, therefore, the period of sickness may persist and the occurrence of infections may increase (14).

In addition to the misuse and abuse of antimicrobial agents, AMR can be obtained by natural processes such as mutations and horizontal gene transfer. The transfer of genetic material can occur by transformation and conjugation. Transformation involves the uptake of deoxyribonucleic acid (DNA) outside the cell followed by incorporation of the DNA into the chromosome. Conjugation is the most common mechanism of transferring genes that encode for AMR. In this form of gene transfer, a pilus is formed between two cells and a plasmid containing resistance encoding genes is transferred from the donor cell to the recipient cell (12).

1.3 Fungal infections

The increasing occurrence of mycoses (fungal infections) and resistance of fungal pathogens to conventional antifungal agents poses a threat to public health. Fungal infections can be categorized as hypersensitive reactions to proteins produced by fungi or reactions to fungal toxins. Healthy individuals can be predisposed to a variety of infections which can be cutaneous, subcutaneous or systemic (15). Severe cases of fungal infections can result from other health related challenges such as AIDS, diabetes, organ transplantation and cancer (16). Approximately 1.4 million deaths per year can be attributed to fungal infections, most of which are caused by *Pneumocystis*, *Candida*, *Aspergillus* and *Cryptococcus* species (17). However, most infections that have been recorded are caused by species belonging to *Aspergillus* and *Candida*, the causative agents of aspergillosis and candidiasis, respectively. In a clinical setting, it was found that in patients with impaired immunity, aspergillosis and candidiasis were responsible for between 80-90% of systemic fungal infections (18).

1.3.1 *Candida albicans*-related fungal infections

C. albicans is a dimorphic fungus that belongs to the Saccharomycetae family of ascomycete fungi (19). This fungus is part of the normal microbiota and can be found in a number of areas in the human body such as the oral cavity, and gastrointestinal and genitourinary tracts. In healthy individuals, *C. albicans* is a harmless microorganism. However, when host immunity is compromised, *C. albicans* can overgrow and cause a variety of infections. *C. albicans* related infections can be either superficial or systemic (20). Systemic infections pose a greater threat to human health and can be caused by the presence of implanted medical devices such as prosthetic heart valves, endotracheal tubes, joint replacements and catheters (21). In some cases, yeast cells can disperse into the bloodstream, causing candidemia. In more serious cases, cells can spread to other parts of the body and infect other internal organs, causing disseminated candidiasis (19).

Infections caused by the genus *Candida* are amongst the leading causes of nosocomial (hospital-acquired) infections, most of which are caused by *C. albicans* (22). This emphasizes the importance of developing therapies that are effective against *C. albicans*. However, effective therapies are difficult to develop due to the ability of *C. albicans* to form biofilms which consist of yeast cells, pseudohyphae and hyphae (23). A biofilm is defined as a community made up of many microorganisms that are attached to either a living or non-living surface and are covered by the ECM which provides protection from the external environment (24). Besides forming monomicrobial biofilms, *C. albicans* can also form polymicrobial biofilms with other fungi and bacteria, making the treatment of infections more complicated. In addition, biofilms are highly resistant to antimicrobial treatment. Therefore, to treat infections, higher doses of antimicrobial drugs are

required, and this often happens when medical devices are removed. The resistant nature of these biofilms presents a twofold problem. Firstly, removal of implanted medical devices can be an expensive procedure and secondly, the dispensation of higher doses of antifungal drugs can cause side effects, such as kidney and liver damage (20).

1.4 Current antifungal drugs

In order to combat the threat posed by growing cases of fungal infections, antifungal drugs have been developed. However, the development of antifungal drugs fails to match the constraints imposed by managing fungal infections in patients (25). Antifungal drugs have multiple targets including the fungal cell wall, membrane components, DNA and ribonucleic acid (RNA) synthesis, microtubule assembly, and protein synthesis (26). Currently, there is a wide range of antifungal drugs used to treat fungal infections with the most focus being on three classes: polyenes, azoles and echinocandins.

Polyene antifungal drugs are a natural product from the soil actinomycete *Streptomyces nodosus* (27). This class of antifungal drugs acts on fungal cells by binding to ergosterol, a sterol found in fungal membranes. Hydrophobic interactions between polyenes and ergosterol leads to the formation of a complex, which has a detrimental effect on membrane function, resulting in pore formation. Formation of pores leads to the efflux of the cellular contents, which leads to cell death.

An example from this class is amphotericin B (AMB), an antifungal drug prescribed as a first line treatment for patients affected by severe, life threatening infections (28-30). AMB (Figure 1.1A) exhibits a broad spectrum of activity against fungal infections such as cryptococcosis, invasive and mucosal candidiasis, blastomycosis and histoplasmosis (31). Due to its high selectivity for fungal cells, AMB is a good antifungal drug despite toxicity issues. Although AMB does bind to cholesterol, a sterol found in human cell membranes, it has a greater binding affinity for ergosterol. Higher specificity for ergosterol can be attributed to differences in the respective structures of cholesterol and ergosterol, as shown in Figure 1.1B (32). A major concern that surrounds the use of AMB is toxicity, especially the toxic effect on the kidneys, lowering of blood potassium levels and infusion reactions (33). In order to overcome these side effects, new formulations of AMB have been developed. A lipid-based formulation of AMB has been found to be highly effective in reducing kidney toxicity (34).

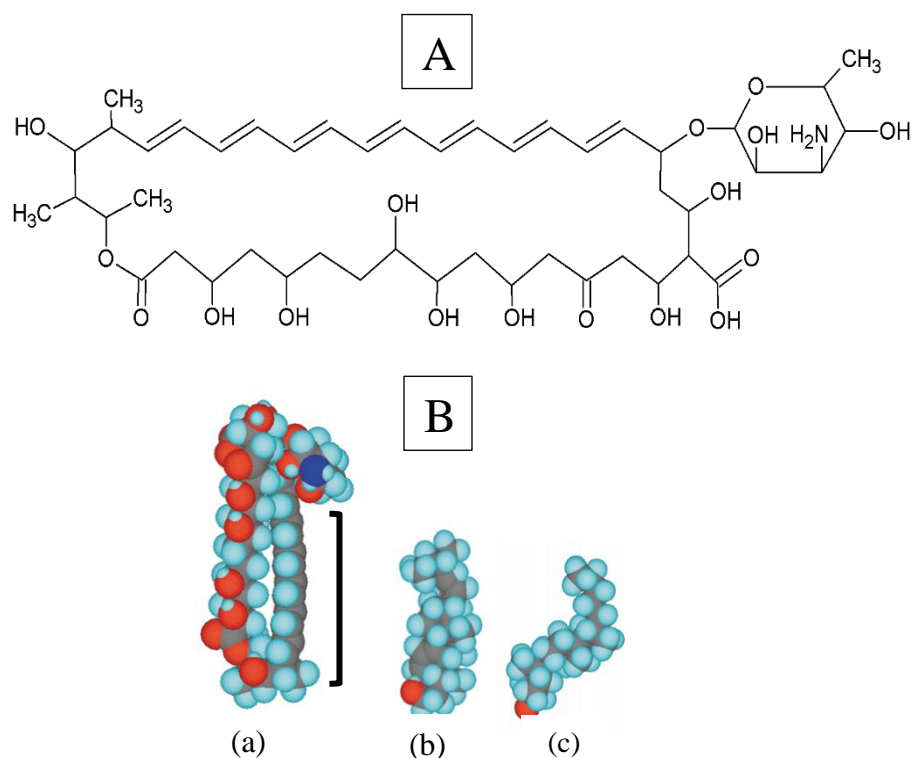


Figure 1.1: (A) Structure of amphotericin B. Structure of amphotericin B was drawn using ChemSketch (ACD/Labs). (B) Three-dimensional structures of (a) amphotericin B, (b) cholesterol and (c) ergosterol. Ergosterol has a cylindrical shape, whereas cholesterol has a sigmoidal shape. The cylindrical shape of ergosterol facilitates better binding to the hydrophobic portion (grey) of amphotericin B (indicated by the bracket) compared to cholesterol. Adapted from Odds *et al.* (26).

The azole class of antifungal drugs consists of two types of azoles: imidazoles such as ketoconazole, and triazoles such as isavuconazonium sulfate (isavuconazole) (35). Azoles act on fungal cells by inhibiting the enzyme lanosterol 14 α -demethylase, which catalyzes the elimination of the 14- α methyl group of lanosterol in the biosynthesis of ergosterol (36). Inhibition of lanosterol 14- α demethylase leads to a decrease in ergosterol and a build-up of ergosterol precursors, which affects the regular fluidity and permeability of the fungal cell membrane. The decreased availability of ergosterol also has a detrimental effect on membrane bound enzymes that are involved in cell wall synthesis (37).

Ketoconazole (Figure 1.2A), the first imidazole that could be taken orally, has a broad spectrum of activity and was especially effective in treating endemic mycoses, oral candidiasis, superficial skin infections and coccidioidomycosis (38). Despite its broad-spectrum activity, the use of ketoconazole was associated with adverse side effects. In order to overcome this problem, new triazoles such as fluconazole, posaconazole and isavuconazole (Figure 1.2B) were developed. Isavuconazole was first introduced in 2015, making it the latest azole antifungal drug to be developed. Like ketoconazole, isavuconazole has broad spectrum activity, with notable activity against most *Candida*, *Cryptococcus* and *Aspergillus* species (39).

Two issues surround the use of azole drugs, namely toxicity and resistance. Side effects associated with the use of imidazoles and triazoles include inflammation of the liver, rash and gastrointestinal problems (40). Compared to older azole drugs, these effects are not as prominent in newer azole drugs. Despite the reduced risks of toxicity, the use of azole drugs in pregnant women is not advised due to potential birth defects (41). Concerning the issues of resistance, two common mechanisms have been identified. The first mechanism is mutation of the target enzyme, lanosterol 14 α -demethylase, a mechanism seen in *Cryptococcus*, *Aspergillus* and *Candida* species (16). Another mechanism involves exclusion of the drug from fungal cells through expression of genes that encode efflux pumps (31).

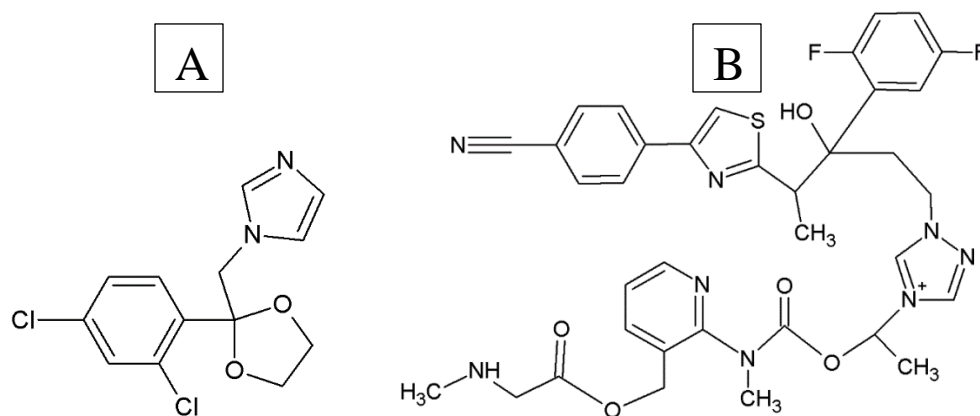


Figure 1.2: Structures of (A) ketoconazole and (B) isavuconazole. Ketoconazole was one of the first azole drugs to be developed, however, due to issues with toxicity, it was replaced by newer azole drugs such as isavuconazole. Structures of ketoconazole and isavuconazole were drawn using ChemSketch (ACD/Labs).

The echinocandins are the most recent class of antifungal drugs, having been introduced in the late 1990s. Echinocandins are semisynthetic lipopeptides that are made up of a cyclic hexapeptide linked to a fatty acid side chain. The side chain plays a critical role in the antifungal activity of echinocandins (26). The main target of the echinocandins is 1,3- β -D-glucan synthase, an enzyme responsible for synthesizing 1,3- β -D-glucan, a polysaccharide that is a critical component of fungal cell walls (42). Inhibition of 1,3- β -D-glucan synthase interferes with the structure of the growing cell wall, which negatively affects osmotic stability and eventually leads to cell death (43).

The echinocandins consist of three antifungal drugs: caspofungin, anidulafungin and micafungin, all of which exhibit similar antifungal activity (Figure 1.3). All three exhibit fungicidal activity against numerous *Candida* species, however, a fungistatic effect is observed against *Aspergillus* species (44). In the case of *Candida*-related diseases such as candidemia and invasive candidiasis, echinocandins are recommended as

an initial treatment for patients (31). Resistance to echinocandin drugs is low, but is slowly rising in *Candida* species with resistance in *C. glabrata*, rising from 3% to 15% (45). Resistance to echinocandins can be attributed to mutations in the gene that codes for 1,3- β -D-glucan synthase (16). Toxicity of echinocandin drugs is minimal, with mild side effects such as headaches, rash, fever and nausea being reported. Side effects are less severe compared to the azole and polyene drugs as 1,3- β -D-glucan synthase is not present in mammalian cells (46).

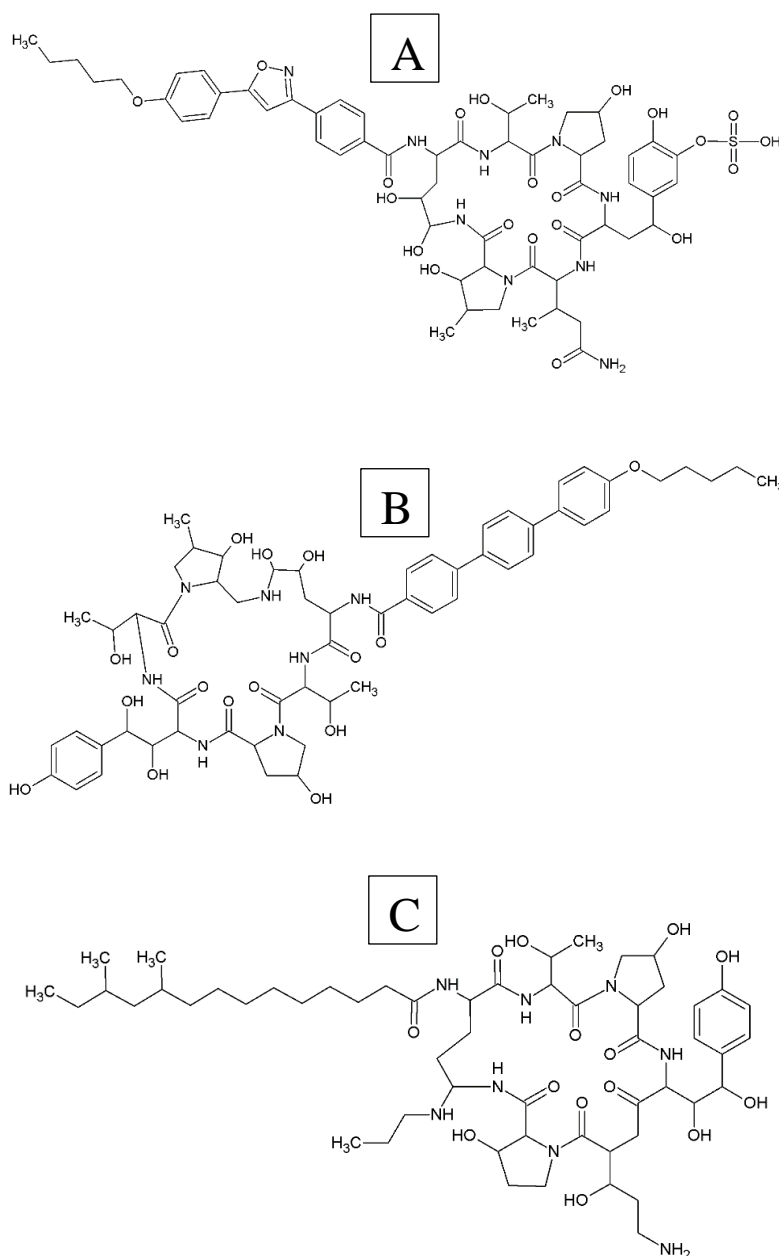


Figure 1.3: Structures of echinocandin drugs, (A) micafungin, (B) anidulafungin and (C) caspofungin. Echinocandins are semisynthetic lipopeptides that consist of a cyclic hexapeptide coupled to a fatty acid side chain. Structures of micafungin, anidulafungin and caspofungin were drawn using ChemSketch (ACD/Labs).

1.5 Fungal biofilms and antimicrobial resistance

1.5.1 Biofilm development

As previously mentioned, a biofilm is a community made up of many microorganisms that are attached to either a living or non-living surface and are covered by an ECM which provides protection from the external environment (24). Biofilms can be found in a number of environments such as aquatic environments, artificial structures, biomaterials as well as plant and mammalian tissue (20). The development of biofilms occurs sequentially involving four key steps: adherence, initiation, maturation and dispersal. An overview of this process is shown in Figure 1.4. Initially, yeast cells adhere to a surface through weak van der Waals forces. After the adherence step, cells begin to grow on the surface and form a layer of cells that will anchor the biofilm to the surface. When the basal layer is formed, the biofilm enters the initiation step, in which growth of hyphae occurs. Over time, further growth of hyphae and the production of the ECM occurs once the maturation stage is reached (20). Finally, when the biofilm is mature, some of the yeast cells are dispersed from the biofilm to other tissues, organs or surfaces to form new biofilms (47).

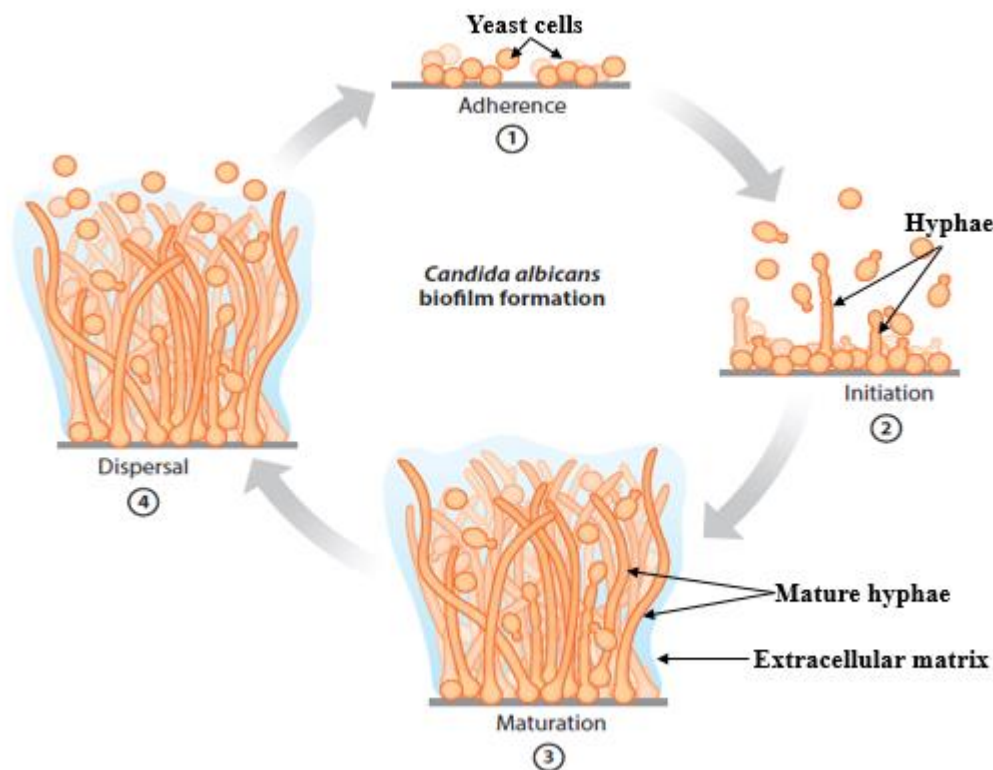


Figure 1.4: Overview of biofilm development in *C. albicans*. Initially, yeast cells will adhere to a substrate. Once the adherence stage is complete, cells begin to grow and develop pseudohyphae and hyphae in the initiation stage. In the maturation stage, further hyphal growth and ECM production occurs. Finally, when the biofilm is mature, yeast cells will disperse to form a new biofilm. Adapted from Nobile and Johnson (20).

1.5.2 Role of biofilms in antimicrobial resistance

A notable characteristic of biofilms is that they are less susceptible to chemical and physical attack compared to their planktonic counterparts. Therefore, higher doses of antimicrobial drugs are required to kill cells in biofilms. This resistance can be attributed to a number of resistance mechanisms employed by biofilm cells. Mechanisms include efflux pumps, the presence of the ECM, persister cells, starvation-induced stress responses and extracellular DNA (7).

The main purpose of efflux pumps is to transport drugs out of the cell into the extracellular environment. In planktonic cells, efflux pumps are only upregulated when antimicrobial drugs enter cells. However, in biofilms, efflux pumps are upregulated throughout the entire process of biofilm development (20). In fungi, two classes of efflux pumps exist: ATP-binding cassette (ABC) pumps and major facilitator superfamily (MFS) transporters (48). It has been noted in a number of *Candida* species, including *C. albicans*, that the presence of low intracellular concentrations of antifungal drugs is due to constant upregulation of efflux pumps (49). For example, the ABC transporters CDR1 and CDR2 and the MFS transporter MDR1 have been found to play a role in the resistance of *C. albicans* to azoles (50).

The ECM plays a role in the resistance of biofilms to antimicrobial drugs by reducing the rate of antimicrobial diffusion, which in turn reduces the efficacy of the antimicrobial. Furthermore, reducing the rate of antimicrobial diffusion means that cells in the biofilm are initially exposed to a low concentration of the antimicrobial, giving cells time to produce a response to the antimicrobial (51). The interaction of ECM components such as polysaccharides with antimicrobials leads to a reduction in the rate of diffusion of the antimicrobial. An example of such a polysaccharide is β -1, 3-glucan, a polymer of β -1, 3-glucose, which is found in *C. albicans* biofilms (7). In addition to polysaccharides, *C. albicans* biofilms also contain proteins, glycoproteins, lipids and nucleic acids. In some cases, extracellular nucleic acids play a role in antimicrobial resistance by interacting with positively charged antimicrobials (52). Besides serving as a physical barricade to drug entry, the ECM is also responsible for preserving the biofilm structure (53) and enabling biofilm cells to resist host immune defences (54). In some microorganisms, the ECM has been shown to play a role in water retention and the absorption of nutrients for cells in the biofilm. In extreme cases of nutrient deprivation, cells in the biofilm will produce enzymes that will break down the ECM, which in turn provides nutrients for the cells, enabling cell survival under nutrient-limiting conditions (55).

Persister cells are a subpopulation of cells in the biofilm that are capable of surviving doses much higher than the minimum inhibitory concentration (MIC) of antimicrobials. This extreme resistance to antimicrobial drugs is not due to changes in the structure of the cell membrane, instead, it is due to the cells entering a state of metabolic dormancy which enables them to survive antimicrobial attack. In *C. albicans*, persister cells were found in biofilms but not in planktonic cultures, indicating that these cells play a crucial

role in the survival of *C. albicans* biofilms (56). Persister cells are not mutants, however, they are a phenotypic variant of wild type cells. This was illustrated in an experiment by LaFleur *et al.* (56) where the surviving population of cells after antimicrobial treatment of a *C. albicans* biofilm exhibited tolerance to a number of antimicrobial agents. When surviving cells were inoculated to form a new biofilm, a new subpopulation of persisters was produced, indicating that persister cells are phenotypic variants of wild type cells that possess a genotype that can be passed onto progeny cells.

The reduced susceptibility of biofilms to antimicrobial agents has resulted in the development of new antimicrobial agents in order to combat the increasing incidence of resistance. This has also led to the proposal of novel alternatives to antimicrobial therapy, overcoming the barrier of resistance. One proposed alternative is the use of AMPs.

1.6 Antimicrobial peptides: a potential alternative to antimicrobial therapy

AMPs are short, amphipathic molecules (10-50 amino acids) that possess a net positive charge (+2 to +9) and a considerable proportion of hydrophobic amino acids (57). These characteristics enable the peptide to fold into a three-dimensional amphipathic structure, usually when the peptide comes into contact with membranes. This allows the peptide to form separate patches which are abundant in cationic and hydrophobic amino acids (58). AMPs have been isolated from a wide variety of organisms including plants, bacteria, fungi, insects and vertebrates. Invertebrates lack some components of the adaptive immune system; therefore, AMPs provide an important defence mechanism (59). In plants, AMPs play a key role in preventing attacks from bacteria and fungi (60).

As more AMPs were discovered, further research was conducted concerning peptide structure and the relationship between structure and function. This led to the discovery of four distinct classes of AMPs: α -helix, β -sheet, extended and loop structures (61). Examples of these structures are shown in Figure 1.5. The β -sheet peptides consist of an antiparallel β -sheet that is held in place by disulfide bonds. In the case of larger β -sheet AMPs, such as human β -defensin-3, a few helical segments exist. An example of β -sheet AMPs are the tachyplesins, a group of AMPs isolated from the Japanese horseshoe crab, *Tachypleus tridentatus* (62). The α -helix peptides have α -helical conformations and usually have a minor curvature in the middle of the structure due to the presence of a proline or glycine residue. The magainins, isolated from the skin of the African clawed frog *Xenopus laevis* (63) are examples of AMPs that possess the α -helical conformation.

Extended AMPs do not have a secondary structure; however, these peptides contain a high proportion of certain residues such as arginine, tryptophan and proline in their structures. A well-studied extended AMP

is indolicidin, a 13-amino acid long peptide with an amidated C-terminus that was isolated from cytoplasmic granules of bovine neutrophils (64). Loop AMPs are characterized by their loop structures imparted by the presence of either a disulfide, amide or isopeptide bond. Thanatin, a 21-amino acid AMP was isolated from the spined soldier bug, *Podisus maculiventris*, and contains an antiparallel β -sheet which is stabilised by a single disulfide bond (65).

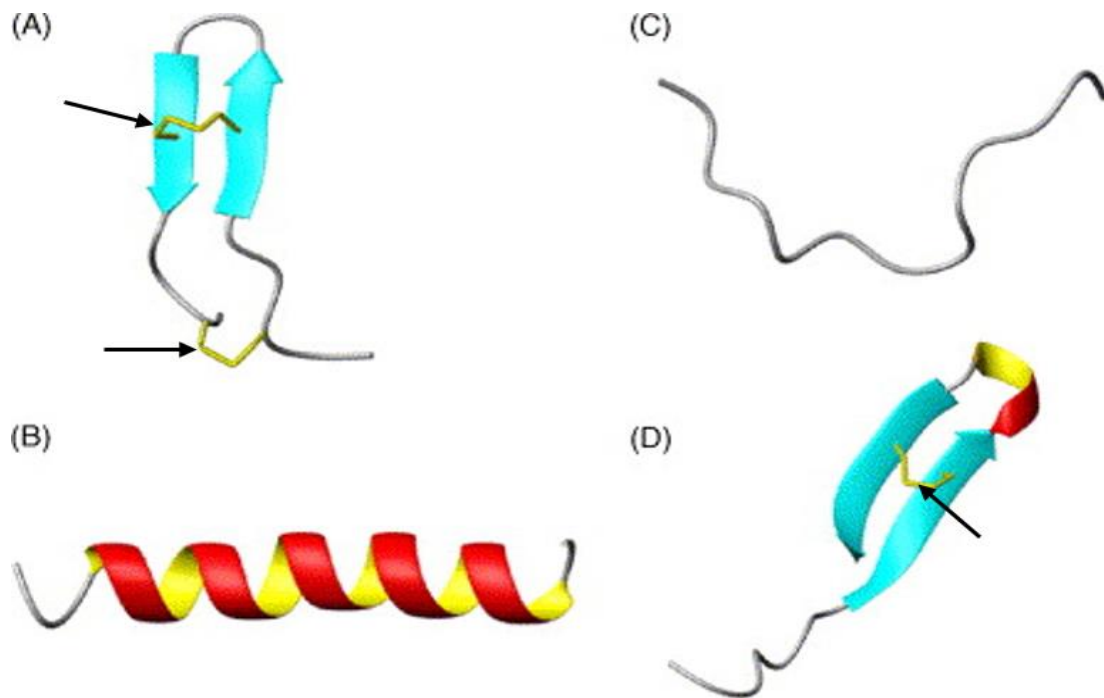


Figure 1.5: Structural classes of antimicrobial peptides. (A) β -sheet, (B) α -helix, (C) extended and (D) loop structures. Disulfide bonds are indicated by the arrows. Adapted from Powers and Hancock (61).

AFPs are a subset of AMPs that possess antifungal activity and have similar natural and structural diversity as AMPs. Furthermore, AFPs include cyclic lipopeptides, linear peptides and open-ended cysteine-rich peptides (66).

1.7 Mechanisms of action of antimicrobial peptides

AMPs have been shown to be active against a number of microorganisms, including bacteria and fungi (67). Despite the membrane being a general target for most AMPs, some AMPs have been found to interact with components of the cell wall and various intracellular targets. For the purpose of this study, AMPs that target the membrane and intracellular components will be discussed.

1.7.1 Membrane targeting antimicrobial peptides

The first interaction between AMPs and target cells is electrostatic where the positively charged peptides interact with the negatively charged cell surface components (68). Once this interaction has occurred, the peptides must pass through cell wall components in order to gain access to the cell membrane. Examples of cell wall components include lipoteichoic acids and peptidoglycan in Gram-positive bacteria, lipopolysaccharide in Gram-negative bacteria and chitin in fungi. Once the AMPs have passed through the cell wall, they are then able to interact with the cell membrane, inducing pore formation (68). Various models have been proposed as to how AMPs form pores and these have been reviewed extensively by Nguyen *et al.* (67) and are shown in Figure 1.6.

The ‘barrel stave’ model of pore formation involves the alignment of a bundle of peptide helices in the membrane along with a central lumen. To form the pore, hydrophobic areas of the peptide will interact with the lipid portion of the bilayer and hydrophilic areas of the peptide will form the inner portion of the pore (68).

In the carpet model, peptides bind electrostatically to the negatively charged phospholipid head groups and cover the membrane surface. At high peptide concentrations, it is speculated that the peptides on the surface disturb the bilayer in the same way as a detergent, leading to micelle formation (69). At threshold peptide concentrations, some peptides can access the membrane due to the development of transient holes in the membrane. Eventually, the membrane collapses as a result of disturbances affecting bilayer curvature (68).

The toroidal pore model can be subdivided into the ordered and disordered toroidal model. In the ordered toroidal pore model, AMPs insert into the membrane and cause lipid monolayers to curve in such a way that the water core is lined by both inserted peptides and lipid head groups. This is different from the barrel stave model where only inserted peptides line the water pore. To form the toroidal pore, the polar faces of the peptides interact with the polar lipid head groups. The lipids from both leaflets are induced to bend out of their usual configuration and are connected to form a single bend from top to bottom consisting of both peptides and lipid head groups (68). Conversely, in the disordered toroidal pore model, lipid molecules are bent inwards, however, the formation of pores is more stochastic, and a few peptides are situated close to the middle of the water pore. In this model, more peptides are located at the mouth of the pore than on the external leaflet. As the peptides move into the cell interior, peptides stay parallel to the plane of the bilayer (70).

In some cases, peptides can cause membranes to become thinner or thicker. Research has shown that the frog skin peptide PGLa induces membrane thickening (71), while the human cathelicidin peptide LL-37 induces membrane thinning (72).

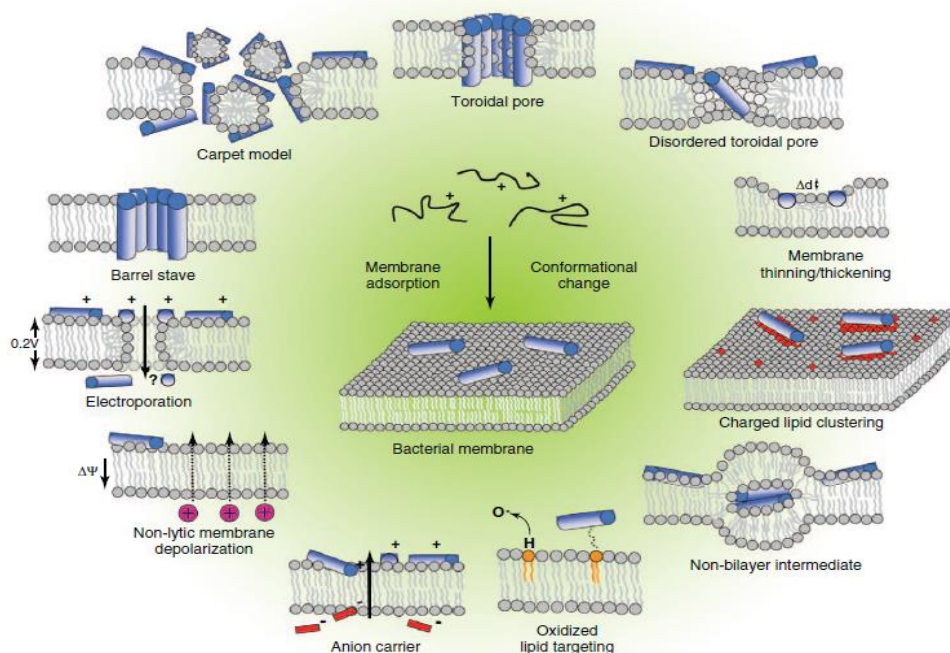


Figure 1.6: Models of membrane disruption. The initial interaction occurs between positively charged AMPs (blue rods) and the negatively charged components of the membrane. After the initial interaction, membrane disruption can occur in a variety of ways as shown in the figure. Adapted from Nguyen *et al.* (67).

Anionic lipid clustering is observed in positively charged peptides that have a high density of positive charges and also have a conformation that is flexible. The accumulation of negatively charged lipids in an area of the membrane leads to the concentration of negative charges which in turn attracts positively charged peptides. The concentration of positively charged peptides in this negatively charged area might lead to the formation of a pore. If the peptides manage to break through the membrane, further damage in the form of cell content leakage and membrane depolarization can occur (73). Some AMPs, such as indolicidin permeabilize membranes by means of an anion carrier mechanism. In this mechanism, peptides will form complexes with hydrophilic negatively charged molecules and then these molecules are transported across the membrane out of the cell (74).

Bilayer phospholipids can become oxidised in cases of infection and inflammation making them a potential target for membrane disrupting peptides. In membranes that contain oxidised phosphatidylcholine lipids, the peptides temporin B and L were able to slot more effectively into membranes. This could have been due to the formation of a Schiff base between lipid aldehyde groups and peptide amino groups. In some cases, AMPs cause the formation of non-bilayer intermediates in the membrane (75).

The cyclic AMP, daptomycin, disturbs membrane integrity by causing the efflux of potassium ions and the dissipation of membrane potential. The activity of daptomycin is linked to a change in membrane potential

from -165 mV to -100 mV across the cell membrane (76). Finally, some AMPs can disrupt the membrane by means of the electroporation model. In this model, positively charged peptides associate with the membrane and produce an electrical potential difference across the membrane. When the potential difference reaches a particular voltage, pores form in the membrane. NK-lysin is an example of an AMP that acts by this model of membrane disruption (77).

1.7.2 Antimicrobial peptides with intracellular targets

Some AMPs have the ability to enter the cell without permeabilizing the cell membrane and can act on intracellular targets. Examples of intracellular targets include organelles, proteins or the disruption of vital cellular processes such as DNA synthesis.

Buforin II, a 21 residue AMP derived from the Asian toad, *Bufo bufo gargarizans*, kills *Escherichia coli* by binding to DNA and RNA without permeabilizing the cell membrane. Some AMPs can inhibit cell division by causing cellular filamentation, resulting in cells having an elongated morphology. AMPs that cause *Salmonella typhimurium* filamentation are the porcine derived proline and arginine-rich AMPs, PR-39 and PR-26 (78). Other intracellular targets of PR-39 include protein synthesis and DNA replication. At a concentration of 25 μM , PR-39 prevented protein synthesis and caused the breakdown of proteins that play a role in DNA replication (79). In addition to its membrane permeabilizing activity, indolicidin induced the filamentation of *E. coli*. Indolicidin also prevented DNA and RNA synthesis at a concentration of 100 $\mu\text{g/mL}$ (52.5 μM). At higher concentrations (150 $\mu\text{g/mL}$ (78.8 μM) and 200 $\mu\text{g/mL}$ (105 μM)), there was significant inhibition of protein synthesis (80). The human neutrophil peptides, HNP-1 and HNP-2, reduce DNA, RNA and protein synthesis while HNP-1 also prevents the synthesis of the periplasmic enzyme β -galactosidase (81).

Histatins are AMPs that are abundant in histidine, a positively charged amino acid. Through binding to a receptor on the fungal cell membrane, histatins can enter the cell. As a result, histatins can enter the cytoplasm and cause respiring cells to lose ATP without inducing membrane lysis. Histatins can also disrupt the cell cycle and stimulate the production of reactive oxygen species (ROS), leading to killing of fungal cells (82). Pyrrocoricin (VDKGSYLPRPTPPRPIYNRN), is a 20-amino acid long, proline-rich peptide that exerts antibacterial activity by binding to DNaK, a heat shock protein, which leads to a decrease in the ATPase activity of DNaK. Drosocin (GKPRPYSPRPTSHPRPIRV), another proline-rich AMP, interacts with GroEL, a bacterial chaperone protein which plays a role in protein folding. Interactions between drosocin and GroEL lead to changes in the refolding of proteins that were initially misfolded (83). Lantibiotics are Gram-positive bacteria derived AMPs that possess lanthionine, an amino acid that contains

a thioether group. The lantibiotic, mersacidin, prevents the synthesis of peptidoglycan, a structural component of Gram-positive bacterial cell walls (84).

1.7.3 Mechanisms of action of antifungal peptides

Generally, AFPs exert selective toxicity towards their microbial target by interacting with molecular determinants of pathogens that have been conserved such as components of the cell wall, cell membrane and intracellular targets (85). Although their main targets are components of the fungal cell, some AFPs also target components of bacterial cells. Examples of AFPs are shown in Table 1.1.

Table 1.1: Examples of antifungal peptides and their sources, structures and modes of action.

Peptide family	Example	Source	Structure	Mode of action	Reference
Pneumocandins	Pneumocandin A ₀	<i>Zalerion asboricola</i> (Fungus)	Lipopeptide	Inhibits 1,3- β -glucan synthesis	(86)
Aureobasidins	Aureobasidin A	<i>Aureobasidium pullulans</i> (Fungus)	Cyclic depsipeptide	Alters assembly of chitin and actin	(87)
Histidine-rich peptides	Histatin	Human saliva	Linear peptide	Cell cycle disruption, formation of ROS	(82)
Membrane selective peptides	Iturin A	<i>Bacillus subtilis</i> (Bacterium)	Cyclic lipopeptide	Pore formation	(88)
	Drosomycin	<i>Drosophila melanogaster</i> (Insect)	Cysteine-rich peptide	Pore formation	(89)
	HsAFP1	<i>Heuchera sanguinea</i> (Plant)	Mixed α -helix and β -sheet, cysteine-rich peptide	Pore formation	(90)

1.8 Antimicrobial peptides that possess anti-biofilm activity

AMPs generally possess activity against planktonic cells, however, some AMPs possess activity against microbial biofilms. AMPs that possess anti-biofilm activity are medically important because chronic infections are usually resistant to treatment due to the presence of biofilms (24). Therefore, biofilm-active AMPs provide a potential therapeutic alternative to conventional antibiotics.

The human cathelicidin, LL-37, inhibited the development of biofilms at concentrations 16 times less than its MIC against planktonic bacteria (91). LL-37 inhibited biofilm formation against *E. coli* and

Staphylococcus aureus at concentrations lower than the respective MICs of both microorganisms (92). KT2 and RT2 are two cationic peptides and are 17 amino acids long and rich in tryptophan residues (six tryptophan residues in each peptide). Both peptides exhibited anti-biofilm activity against a multidrug resistant *E. coli* strain and were able to inhibit biofilm development and destroyed preformed biofilms, at concentrations as low as 1 μ M (93).

AMPs are not only active against bacterial biofilms, some are active against fungal biofilms. AS-10, a mouse cathelicidin-derived peptide, showed anti-biofilm activity against *C. albicans* biofilms. Anti-biofilm activity was observed at a concentration of 0.22 μ M, more than 200 times lower than its MIC against planktonic *C. albicans*. In addition to antifungal activity, AS-10 also inhibited the development of a polymicrobial biofilm consisting of *C. albicans* and *Staphylococcus epidermidis* (94).

In order to augment the activity of AMPs against microorganisms, some AMPs have been used in combination with conventional antimicrobials. Combination therapy can lead to greater efficacy (especially if the compounds have different targets), reduce toxic effects, lower costs of dosage and potentially have better activity against resistant microorganisms (95). A combination of bacillomycin D, a lipopeptide, and AMB showed a synergistic effect against *C. albicans* biofilms (96). AS-10 showed a synergistic effect against *C. albicans* biofilms when used in combination with both caspofungin and AMB (94). The tyrocidines, a group of cyclic decapeptides derived from *Bacillus aneurinolyticus*, eradicated preformed *C. albicans* biofilms when used in combination with caspofungin and AMB. Although synergistic activity was observed with both antifungal drugs, it was found that the tyrocidines had a more significant effect on caspofungin activity (97). The plant defensin rHsAFP1 from *H. sanguinea* displayed anti-biofilm activity when used alone and in combination with caspofungin or AMB against *C. albicans*. More pronounced synergistic activity was observed when rHsAFP1 was used in combination with caspofungin (90).

1.9 Therapeutic applications of antimicrobial peptides: limitations and possible solutions

Despite the growing potential of AMPs as therapeutic molecules either alone or in combination with other conventional antibiotics, a number of issues need to be addressed. First, the high cost of producing AMPs has limited their use, consequently more cost-effective methods of synthesis must be developed, especially considering quantities required for clinical trials and eventual patient treatment. One approach is recombinant production (98), where a recombinant expression system is used to produce higher quantities of peptides while reducing production costs. However, there are shortcomings with regards to recombinant production. In some cases, the expressed AMP can be toxic to the host cell, resulting in its death. In addition to potential death of the cell producing the AMP, the C-terminus must be neutralized due to its negatively

charged carboxyl group. As the AMP is produced in a host cell, only naturally occurring amino acids can be used in the AMP synthesis and this eliminates the incorporation of non-natural amino acids and peptidomimetics often required to enhance peptide stability and activity (98). Despite these obstacles, there has been some success where for example, the fungal peptide plectasin was produced using a fungal expression system (99). Another solution is to reduce the size of peptide to the smallest amino acid sequence that still has antimicrobial activity. The tick defensin OsDef2 was identified in the midgut of *O. savignyi* and was found to have antibacterial activity. OsDef2 was shortened to form the derivatives Os and Os-C which were 22 and 19 amino acids long, respectively, and both peptides retained antibacterial activity (100).

Despite AMPs having considerable *in vitro* activity, this activity often is lost when peptides are exposed to physiological salt and serum concentrations (9) and this limits their systemic use. AMPs that are insensitive to these conditions are for example the tachyplesins and polymuphesins that exhibit activity in the presence of salts (101). The synthesis of salt-insensitive AMPs is possible, but involves altering peptide hydrophobicity, amphipathicity, charge and helicity (102).

The issue of AMP toxicity is of concern, and studies on peptide mediated toxicity are limited to the effects on erythrocytes and cell lines. Therefore, further research must be undertaken in order to understand the potential mechanisms of toxicity and the development of toxicity profiles (9). The cell membrane is a common target for AMPs, however, AMPs disturb prokaryotic membranes to a more pronounced extent than eukaryotic membranes. Reduced specificity for eukaryotic membranes is due to the lack of anionic lipids on the cell surface, a weak membrane potential gradient and the presence of cholesterol (57). One approach that has been proposed to reduce toxic effects is the synthesis of liposomal formulations which could enable the use of AMPs in systemic applications (103).

The greatest hindrance to the use of AMPs as an alternative to antimicrobials is their susceptibility to degradation by proteases. If administered orally, AMPs can be degraded by pepsin, trypsin and chymotrypsin. If administered intravenously, proteases in the blood can degrade AMPs. In addition to this, some bacterial species resist the action of AMPs by producing proteases that render AMPs inactive (98). A number of strategies to make AMPs resistant to the action of proteases have been developed. One method is to add an acetyl group to the N-terminus which makes the peptide less susceptible to the action of aminopeptidases (104). However, the addition of an acetyl group reduces the overall charge of the peptide, which may negatively affect peptide activity. Another approach to make peptides less susceptible to proteases is cyclization. Peptides can be cyclized in two ways: through disulfide bonds between cysteine residues or through joining the backbone at the C- and N-terminus. Both methods were found to improve the stability of short synthetic peptides in serum (105).

The incorporation of D-amino acids into peptide sequences is another method often used to reduce the susceptibility of peptides to proteases. D-amino acids are mirror images of the more common L-amino acids. The use of D-amino acids has proven beneficial because the antimicrobial activity is preserved since interactions with target membranes are not dependent on the stereochemistry of the AMP (98). In some cases, it has been reported that D-enantiomers of AMPs exhibit greater antimicrobial activity than their L-enantiomer counterparts. One example is the peptide M33, where the protease-resistant D-enantiomer was more active against Gram-positive pathogens than the L-enantiomer (106).

Another method to reduce protease susceptibility is the use of peptidomimetics, which are polymeric molecules that resemble peptides but have different backbone structures. The benefits are improved stability and retention of the biological characteristics of parent peptides. Peptidomimetics ensure that the spatial alignment of peptides is conserved while changes to the backbone structure confers resistance to protease activity. Examples of peptidomimetics include β -peptides, peptoids, and oligoacyllysines (98).

Another strategy to increase peptide stability is replacing some amino acids with non-natural amino acids. The addition of non-natural amino acids improves metabolic stability and increases the range of physicochemical properties that can be used to improve peptides as antimicrobial agents. In the case of arginine and lysine, changes can be made that alter the length of the side chain while the positive charge is retained. The substitution of a single arginine residue in Api88, an analogue of apiadaecin 16, by L-ornithine or L-homoarginine increased stability in serum without changing activity against *E. coli* (107).

1.10 Background to the study

Two defensin isoforms, OsDef1 and OsDef2, were identified in the midgut of the soft tick *O. savignyi*. Both peptides were 37 residues long and possessed cysteine residues that are representative of the defensin class of AMPs. When tested for antibacterial activity, both peptides were active against Gram-positive bacteria, however, OsDef2 was more active than OsDef1 (100). In an attempt to design shorter peptides with equivalent or more pronounced antibacterial activity, OsDef2 was used as a template to synthesize the analogue Os. Properties of the peptides are shown in Table 1.2.

In a study conducted by Prinsloo *et al.* (100), Os was found to be active against Gram-positive and Gram-negative bacteria; was non-toxic to mammalian cells and did not cause erythrocyte haemolysis. Furthermore, Os also exhibited antioxidant and anti-inflammatory activity (108).

Table 1.2: Physicochemical properties of OsDef2, Os and Os(11-22)NH₂.

Peptides	Sequence	Mass (Da)	Length	Charge	<H> ^a
OsDef2	GYGCPFNQYQCHSHCKGIRGYKGGYCKGAFKQTCKCY	4185.80	37	+ 6	0.371
Os	KGIRGYKGGYCKGAFKQTCKCY	2459.92	22	+ 6	0.249
Os(11-22)NH ₂	CKGAFKQTCKCY-NH ₂	1378.69	12	+ 4	0.396

^aHydrophobicity. Data obtained from HeliQuest [heliquest.ipmc.cnrs.fr/].

The mechanism of action of Os was investigated by Taute *et al.* (109), and in this study, transmission electron microscopy studies showed that Os affected the outer membrane of *E. coli* and *B. subtilis* and induced cell membrane permeabilization. Peptide localization experiments revealed that Os crosses the membrane and enters both *E. coli* and *B. subtilis* cells.

Os was also found to possess antifungal activity, against planktonic cells (10) and biofilms (11). In an attempt to reduce costs and design a more efficient antifungal peptide, Os was shortened further and amidated at the carboxy terminus to form the peptide Os(11-22)NH₂ (Table 1.2) in order to investigate if this shortened derivative retained antifungal activity.

1.11 Aim of the study

The aim of this study was to investigate the anti-biofilm activity of the peptide Os(11-22)NH₂ against *C. albicans*.

1.12 Objectives of the study

The objectives of this study were to determine whether Os(11-22)NH₂:

- (i) Possesses anti-planktonic activity against *C. albicans*.
- (ii) Inhibits *C. albicans* biofilm formation.
- (iii) Eradicates preformed *C. albicans* biofilms.
- (iv) Inhibits biofilm formation and eradicates preformed biofilms by membrane permeabilization.
- (v) Inhibits biofilm formation and eradicates preformed biofilms by inducing the formation of ROS.

2. Materials and Methods

2.1 *C. albicans* growth and culture conditions

C. albicans (ATCC 90028) was grown aerobically at 30°C in yeast peptone dextrose (YPD; yeast extract, 0.5% (m/v), peptone, 1% (m/v) and dextrose, 2% (m/v)) medium purchased from Sigma-Aldrich (Johannesburg, South Africa (SA)).

2.2 Preparation of synthetic peptides

The peptides used for this study were synthesized by GenScript (Piscataway, NJ, USA) using FlexPeptide™ synthesis technology. The molecular mass and purity of the peptides were determined using mass spectrometry and reverse phase high performance liquid chromatography (RP-HPLC), respectively. Amino acid analysis was performed for Os(11-22)NH₂ in order to determine the amount of peptide in a 1 mg of lyophilized powder. Stock solutions of the peptide were prepared using sterile distilled water. Aliquots of the stock solution were stored at -20°C. For Os, peptide concentration was determined by measuring the absorbance and using the following equation:

$$c = \frac{MW \times df \times Abs}{n(\epsilon_{Tyr}) + n(\epsilon_{Trp})}$$

where *c* is the peptide concentration in mg/mL, *MW* is the molecular weight in mg/mmol, *df* is the dilution factor, *Abs* is the absorbance at 280 nm, and *n* represents the number of tyrosine (Tyr) or tryptophan (Trp) residues and ϵ represents the extinction coefficients of tyrosine and tryptophan which are 1200 and 5560 AU/mmol/mL, respectively (110). Stock solutions were prepared using sterile distilled water and aliquots were stored at -20°C.

2.3 Screening of peptides for anti-planktonic activity

The microbroth dilution assay is used to test the susceptibility of microorganisms to antimicrobial agents in 96-well plates. The method was performed according to the EUCAST Definitive Document EDef 7.1 (111). The medium, double strength Roswell Park Memorial Institute 1640 (RPMI-1640) medium with L-glutamine and phenol red and without sodium bicarbonate (Sigma-Aldrich, Johannesburg, SA) was used.

Double strength RPMI-1640 was buffered with 3-(N-morpholino) propanesulfonic acid (MOPS, Sigma-Aldrich, Johannesburg, SA), adjusted using sodium hydroxide (NaOH) to pH 7.0 and supplemented with 2% (m/v) glucose (2X RPMI-1640 2% glucose). The solution was filter sterilized using a 0.22 μm filter (Pall Corporation, Ann Arbor, MI, USA) and stored at 4°C.

For Os and Os(11-22)NH₂, working concentrations were prepared by diluting stock solutions with 2X RPMI-1640 2% glucose. Twofold dilutions were made in 2X RPMI-1640 2% glucose until eight concentrations of peptide ranging from 1.56 μM to 200 μM (double the final concentration) were prepared. Os and Os(11-22)NH₂ were added to their respective test wells. To prepare working concentrations of caspofungin (Sigma-Aldrich, Johannesburg, SA), the stock solution was diluted eight times with sterile distilled water. A twofold dilution series (50 μL) ranging from 0.004 μM to 0.625 μM (double the final concentrations) was prepared in 2X RPMI-1640 2% glucose. Twofold dilutions of caspofungin were added to separate test wells.

The inoculum was prepared by streaking *C. albicans* on YPD agar plates and incubating the cells at 37°C for 24 hours. The next day, single colonies were suspended in sterile distilled water to prepare a yeast suspension. Afterwards, the inoculum was suspended by vigorous vortexing. The optical density (OD) of the suspension was measured at 530 nm using a spectrophotometer (VWR, Radnor, PA, USA) (111). To obtain an OD between 0.12 and 0.15, the yeast suspension was diluted in sterile distilled water. An OD between 0.12 and 0.15 indicated that the suspension contained $1-5 \times 10^6$ CFU/mL. To prepare a working suspension, the yeast suspension was diluted ten times in distilled water to a cell concentration of $1-5 \times 10^5$ CFU/mL.

To the wells that contained Os(11-22)NH₂, Os and caspofungin, final working concentrations were obtained by adding an equal volume of the yeast suspension (50 μL) to the test wells resulting in a final cell density of $0.5-2.5 \times 10^5$ CFU/mL. For the growth control, equal volumes of the yeast suspension and 2X RPMI-1640 2% glucose were added to wells. Afterwards, cells were incubated at 37°C without agitation for 24 hours. After incubation, OD was measured at 530 nm using the SpectraMax® Paradigm® Multi-Mode Microplate Reader (Molecular Devices, Sunnyvale, CA, USA). Using the OD measurements, the minimum inhibitory concentration that reduced growth by 50% (MIC₅₀) (90) was determined.

To ensure that test wells contained $0.5-2.5 \times 10^5$ CFU/mL, viable counts were performed. A diluted cell suspension was prepared in sterile distilled water. The suspension was homogenized by vortexing and plated on YPD agar. After 24 hours incubation, the colonies were counted.

2.4 Optimization of biofilm formation

Before anti-biofilm activity was investigated, the optimum time for growing *C. albicans* was determined by measuring biofilm biomass and viability. Biofilm biomass was measured using crystal violet (CV) staining and viability was measured using the CellTiter Blue (CTB) cell viability assay.

2.4.1 Determination of biofilm biomass

Biofilm biomass was determined using CV staining according to the method by Jose *et al.* (112), with modifications. CV is a basic dye that can interact with anionic surface molecules and polysaccharides in the ECM. Despite being suitable for determining biomass, it is not a good indicator of viability since it stains both live and dead cells (113). The structure of CV is shown in Figure 2.1.

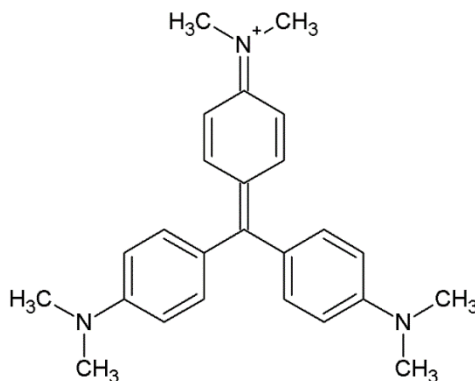


Figure 2.1: Structure of crystal violet. CV is a basic dye used to quantify biofilm biomass and binds to negatively charged components of the cell such as negatively charged proteins, RNA and DNA. Structure of CV was drawn using ChemSketch (ACD/Labs).

An overnight *C. albicans* culture was aliquoted and centrifuged at $2000 \times g$ for 10 minutes. Afterwards, the supernatant was discarded, and the pellet was washed with single strength RPMI-1640 adjusted to pH 7.0 with NaOH. Afterwards, the pellet was centrifuged at $14\ 100 \times g$ for 2 minutes. After washing, the supernatant was discarded, and the pellet was resuspended in RPMI-1640. The OD of the cell suspension was measured at 620 nm and the suspension was diluted to a cell density of 1×10^6 CFU/mL using RPMI-1640. To the wells of a clear, 96-well polystyrene plate (Greiner Bio-One, Kremsmunster, Austria), 100 μ L cell suspension was added and cells were incubated for 1.5 hours at 37°C to allow for cell adhesion to the plate wells. After adhesion, RPMI-1640 was aspirated, and biofilms were washed with phosphate buffered saline (PBS; 10 mM, pH 7.4) to remove cells that did not adhere. RPMI-1640 (100 μ L) was added and biofilms were allowed to grow for 2, 12, 24 and 48 hours at 37°C. After biofilm growth, biofilms were

washed with PBS, then fixed with 20% (v/v) formaldehyde and incubated at room temperature for 20 minutes. The formaldehyde was then removed, and the plates were left to dry. Afterwards, biofilms were stained with 0.1% (m/v) CV (Sigma-Aldrich, Johannesburg, SA) for 20 minutes. To remove excess CV, plates were immersed in a tub of water and blot dried on a stack of paper towels. Afterwards, qualitative analysis of biomass was performed using an inverted light microscope (Optika Microscopes, Ponteranica, Italy). Quantitative analysis of biomass was performed by solubilizing CV that was bound to biofilms using 30% (v/v) acetic acid and leaving plates to stand for 15 minutes. Afterwards, biomass was determined by measuring the absorbance of the solubilized CV at 550 nm using a SpectraMax® Paradigm® Multi-Mode Microplate Reader.

2.4.2 Determination of biofilm cell viability

The viability of cells in the biofilm was determined using the CTB (Promega, Madison, WI, USA) cell viability assay, an assay which can be used to quantify cells that are metabolically active. In the CTB assay, NADH in viable cells reduces the blue, non-fluorescent dye resazurin to resorufin, a pink, fluorescent dye (114). The reduction of resazurin to resorufin is shown in Figure 2.2.

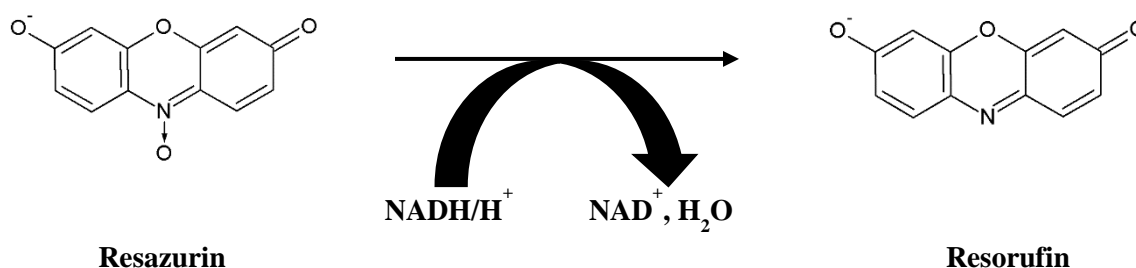


Figure 2.2: Reduction of resazurin to resorufin in the CellTiter Blue cell viability assay. In viable cells, the non-fluorescent dye resazurin is reduced by NADH to form the fluorescent product resorufin. Structures of resazurin and resorufin were drawn using ChemSketch (ACD/Labs).

C. albicans biofilms were grown according to the method by Troskie *et al.* (97), with modifications. Biofilms were grown for 2, 12, 24 and 48 hours as described in section 2.4.1. After biofilm growth, biofilms were washed with PBS and 100 μ L RPMI-1640 was added. A volume (20 μ L) of CTB was added to the biofilms followed by incubation in the dark for an hour at 37°C. Viability was determined by measuring the fluorescence at an excitation wavelength of 535 nm and an emission wavelength of 590 nm using a SpectraMax® Paradigm® Multi-Mode Microplate Reader.

2.5 Screening for anti-biofilm activity

2.5.1 Biofilm inhibition assay

The biofilm inhibiting ability of Os(11-22)NH₂ against *C. albicans* was evaluated by using the CTB cell viability assay according to the method by Troskie *et al.* (97), with modifications. Biofilms were grown as described in section 2.4.1, however, after allowing biofilms to adhere for 1.5 hours, biofilms were treated with either 0.019 μM to 5 μM AMB in RPMI-1640 containing dimethyl sulfoxide (DMSO) (RPMI-DMSO) or 1.56 μM to 200 μM Os(11-22)NH₂ in RPMI-1640 and incubated for 24 hours at 37°C. Since AMB is not water-soluble, AMB was dissolved in DMSO. The final concentration of DMSO was 0.5%. After incubation, biofilms were aspirated, washed with PBS then quantified with CTB as described in section 2.4.2. The fluorescence values obtained from CTB quantification were used to calculate the minimum concentration of each antifungal that reduced biofilm formation by 50% (BIC₅₀) (90).

Biofilm inhibition by Os(11-22)NH₂ and AMB was further investigated using CV staining and light microscopy as described in section 2.4.1. Biofilms were grown in the presence of the calculated BIC₅₀ concentrations of Os(11-22)NH₂ and AMB.

2.5.2 Biofilm eradication assay

The biofilm eradicating ability of Os(11-22)NH₂ against *C. albicans* was evaluated by using the CTB cell viability assay according to the method by Troskie *et al.* (97), with modifications. Biofilms were grown for 24 hours at 37°C as described in section 2.4.1. After washing biofilms with PBS, serial dilutions of 0.039 μM to 10 μM AMB in RPMI-DMSO or 1.56 μM to 400 μM Os(11-22)NH₂ in RPMI-1640 were added to biofilms followed by further incubation for 24 hours at 37°C. For AMB, the final concentration of DMSO was 0.5%. After incubation, biofilms were aspirated, washed with PBS and quantified with CTB as described in section 2.4.2. The fluorescence values obtained from CTB quantification were used to calculate the minimum concentration of each antifungal that decreased cell viability in a pre-grown biofilm by 50% (BEC₅₀) (90).

2.6 Mode of action studies

2.6.1 Membrane integrity: Confocal laser scanning microscopy

The cell membrane is a target for most AMPs, therefore, to investigate whether Os(11-22)NH₂ affects membrane integrity, confocal laser scanning microscopy (CLSM) was used. A cell concentration of 1 × 10⁶ CFU/mL was added to polystyrene coverslips coated with poly-L-lysine (Sigma-Aldrich, Johannesburg, SA). Biofilm inhibition and eradication experiments were carried out as described in sections 2.5.1 and

2.5.2, respectively. For inhibition, biofilms were grown in the presence of Os(11-22)NH₂ at the concentration equivalent to the BIC₅₀ for 24 hours and for eradication the 24-hour biofilms were exposed to the BEC₅₀ of Os(11-22)NH₂ for 24 hours. The non-ionic surfactant Triton X-100, a membrane permeabilizing agent, was used as a positive control. The polar head group of Triton X-100 disturbs hydrogen bonding in the lipid bilayer of the cell, which in turn compromises the compactness and integrity of the membrane (115). Since Triton X-100 rapidly permeabilizes membranes, 24-hour biofilms were treated with 1% (v/v) Triton X-100 for 2 and for 24 hours. Following incubation, biofilms were washed with PBS then stained with 1.5 µg/mL propidium iodide (PI; Sigma-Aldrich, Johannesburg, SA) for 15 minutes then stained with 10 µg/mL 4',6-diamidino-2-phenylindole (DAPI; Sigma-Aldrich, Johannesburg, SA) for 5 minutes. Both PI and DAPI bind to DNA and emit fluorescence. The cells are first stained with PI, which freely enters cells with damaged cell membranes, but not cells with intact cell membranes and intercalates with DNA (116). Subsequent addition of DAPI, which can enter cells with damaged or intact membranes, stains cells with intact cell membranes (117). The red staining of PI and blue staining of DAPI indicate cells with damaged and intact cell membranes, respectively. The structures of PI and DAPI are shown in Figure 2.3.

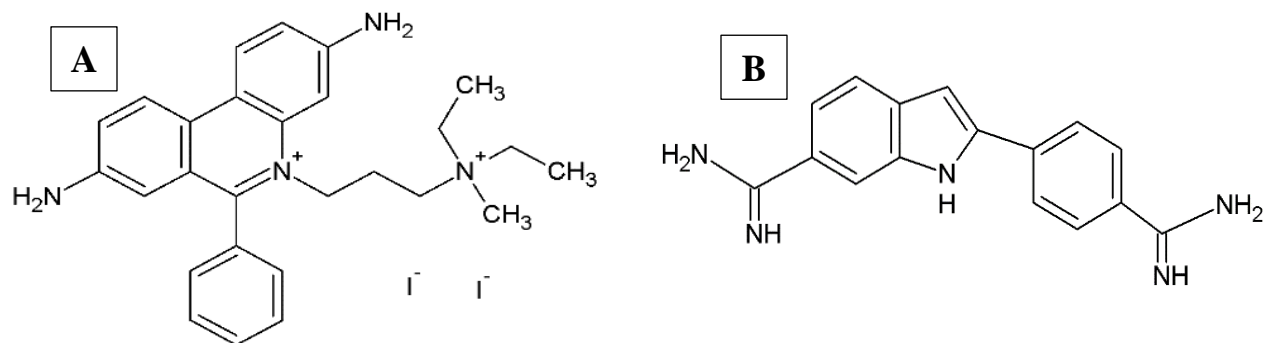


Figure 2.3: Structures of (A) propidium iodide (PI) and (B) 4',6-diamidino-2-phenylindole (DAPI). PI and DAPI are molecules that can bind to DNA and form fluorescent complexes. DAPI can enter all cells, both cells with damaged and intact membranes while PI can only enter cells with damaged membranes. Structures of PI and DAPI were drawn using ChemSketch (ACD/Labs).

After staining with PI and DAPI, biofilms were washed twice with PBS and mounted onto microscope slides with anti-fade mounting medium (Sigma-Aldrich, Johannesburg, SA). Following mounting, cells were visualized using a Zeiss LSM 510 META Confocal Microscope (Carl Zeiss NTS GmbH, Oberkochen, Germany). PI was detected at an excitation wavelength of 535 nm and an emission wavelength of 617 nm while DAPI was detected at an excitation wavelength of 364 nm and an emission wavelength of 454 nm. Images were viewed using Zeiss LSM Image Browser software.

2.6.2 Reactive oxygen species production: 2',7'-Dichlorodihydrofluorescein diacetate assay

Many organisms are known to produce ROS which are chemically reactive molecules that are generated within biological systems (118). ROS formation is a common mechanism of biofilm inhibition or eradication. As shown in Figure 2.4, the fluorogenic compound 2',7'-dichlorodihydrofluorescein diacetate (DCFH-DA), an indicator of oxidative stress, was used to investigate whether Os(11-22)NH₂ induces ROS formation in *C. albicans* biofilms. DCFH-DA is a non-fluorescent compound that can diffuse through the cell membrane. Once in the cell, intracellular esterases hydrolyze DCFH-DA to 2,7-dichlorodihydrofluorescein (DCFH), which is also non-fluorescent. In the presence of ROS, DCFH is oxidized to 2,7-dichlorofluorescein (DCF), a fluorescent compound (119) that can be quantified to determine the extent of induced ROS formation.

Biofilm inhibition and eradication were carried out in black, polystyrene 96-well plates (Greiner Bio-One, Kremsmunster, Austria) as described in sections 2.5.1 and 2.5.2, respectively. For inhibition experiments, adhered cells were grown in the presence of concentrations of Os(11-22)NH₂ and AMB that inhibited biofilm formation by 50%. For eradication experiments, preformed biofilms were treated with concentrations of Os(11-22)NH₂ and AMB that eradicated preformed biofilms by 50%. Following treatment, biofilms were washed with PBS to remove non-adhered cells. The PBS and non-adhered cells were aspirated and 100 μ L of DCFH-DA (10 μ M, prepared in PBS) was added to each test well. Biofilms were incubated at 37°C for 1 hour with shaking at 80 rpm and the fluorescence was measured using a plate reader set to an excitation wavelength of 485 nm and an emission wavelength of 525 nm (120).

To investigate whether induction of ROS contributes to biofilm inhibition and eradication, the ROS scavenging molecule ascorbic acid was added to cells treated with Os(11-22)NH₂ and AMB, and viability was determined. For biofilm inhibition, biofilms were grown in the presence of Os(11-22)NH₂ and AMB at their respective BIC₅₀ values in the presence and absence of 10 mM ascorbic acid. Likewise, for biofilm eradication, preformed biofilms were treated with Os(11-22)NH₂ and AMB at their respective BEC₅₀ values in the presence and absence of 10 mM ascorbic acid. Induction of ROS was determined using DCFH-DA as described previously and viability was determined using CTB as described in section 2.4.2. To ensure that changes in pH did not contribute to killing, 10 mM citric acid was used as a pH control (97).

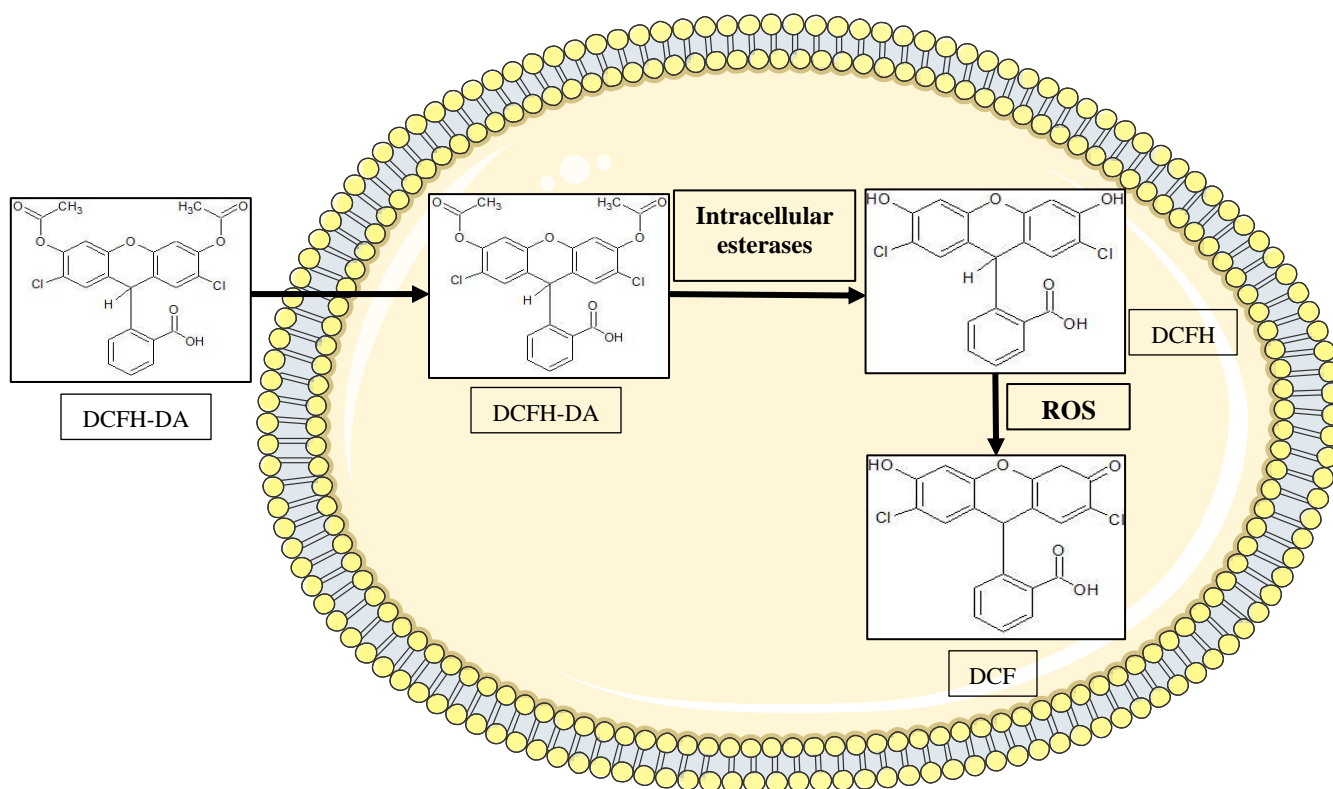


Figure 2.4: Structured detail of the 2',7'-dichlorodihydrofluorescein diacetate assay. 2',7'-dichlorodihydrofluorescein diacetate (DCFH-DA) enters cells by diffusing through the cell membrane. In the cell, esterases convert DCFH-DA to 2',7'-dichlorofluorescein (DCFH). In the presence of reactive oxygen species (ROS), DCFH is oxidized to 2',7'-dichlorofluorescein (DCF) (119). Structures of DCFH-DA, DCFH and DCF were drawn using ChemSketch (ACD/Labs).

2.7 Data analysis

To determine the percentage of inhibition or eradication, OD and fluorescence values were converted to percentage inhibition or eradication using the formula below (121):

$$\% \text{ inhibition/eradication} = 100 - \frac{100 \times (\text{Average absorption of test wells} - \text{blank})}{\text{Average absorption of growth control wells} - \text{blank}}$$

GraphPad Prism 7 software (GraphPad Software, San Diego, CA, USA) was used to construct sigmoidal dose-response curves of log (inhibitor) versus response (% inhibition or eradication) using non-linear regression analysis. The response (Y) was calculated using the formula (122):

$$Y = \frac{Top - Bottom}{1 + 10^{[\log(IC_{50} - X) \times A_s]}}$$

where the terms “top” and “bottom” refer to the maximum and minimum response, respectively. The 50% inhibitory concentration (IC_{50}) is the concentration that relates to a response which is the average of the top and bottom values. X is the logarithm (10-base) of the peptide concentration and A_s represents the Hill slope which is calculated as a best-fit value by the software.

Two to three independent experiments were performed in triplicate and results were presented as the mean \pm standard error of the mean (SEM). Statistical analysis was carried out using GraphPad Prism 7. Statistical significance included 95% confidence intervals and one-way analysis of variance (ANOVA) using Tukey’s multiple comparisons test.

3. Results

3.1 Anti-planktonic activity

Prior to the evaluation of the anti-biofilm activity of Os(11-22)NH₂, it was necessary to investigate the activity of the peptide against planktonic *C. albicans* cells. Caspofungin was used as a positive control and the parent peptide, Os, was included for comparison. Caspofungin (Figure 3.1A) and Os(11-22)NH₂ (Figure 3.1B) showed potent activity against the planktonic cells in the micromolar range. No growth inhibition was observed when cells were treated with Os, even at 100 μM, the highest concentration tested (Figure 3.1B).

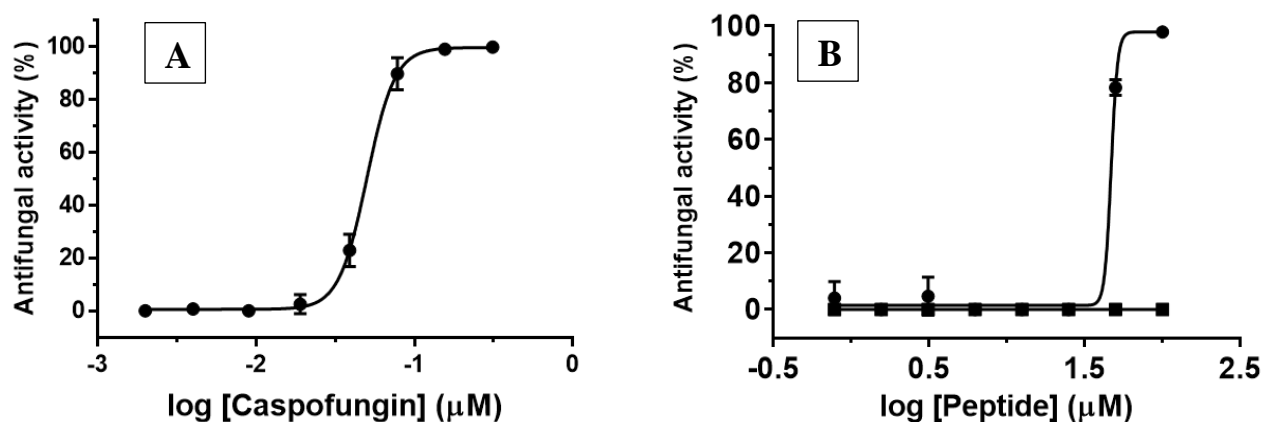


Figure 3.1: Anti-planktonic activity of (A) caspofungin and (B) Os and Os(11-22)NH₂. Planktonic *C. albicans* was incubated with (A) caspofungin (0.002 μM to 0.312 μM), (B) Os (0.78 μM to 100 μM) (■) or Os(11-22)NH₂ (0.78 μM to 100 μM)(●). Error bars indicate the mean ± SEM. Data are results of two independent experiments performed in triplicate.

The inhibition parameters MIC₅₀ and MIC_{max} (Table 3.1) were calculated from the full dose-response curves (Figure 3.1). Caspofungin exhibited antifungal activity against *C. albicans*, characterized by a MIC₅₀ and MIC_{max} of 0.05 μM and 0.08 μM, respectively. For Os(11-22)NH₂, MIC₅₀ and MIC_{max} values were 47 μM and 53 μM, respectively.

Table 3.1: MIC₅₀ and MIC_{max} values of caspofungin and Os(11-22)NH₂.

Antifungal agent	MIC ₅₀ ^a (μM)	MIC _{max} ^b (μM)
Caspofungin	0.05 ± 0.00	0.08 ± 0.01
Os(11-22)NH ₂	47 ± 0.30	53 ± 0.00

Each value represents the mean ± SEM of two independent experiments, each performed in triplicate.

^a The MIC₅₀ values were derived from full dose-response curves and are the concentrations necessary to cause 50% growth inhibition (90).

^b The MIC_{max} values were calculated as the value at the intercept between the slope and the top plateau of a full dose-response curve and represents the concentrations necessary to cause total inhibition (121).

3.2 Optimization of biofilm formation

Before anti-biofilm assays were performed, it was necessary to determine the optimal time required to establish *C. albicans* biofilms. CV was used for both qualitative and quantitative analysis of biofilm biomass, whereas biofilm viability was evaluated using the CTB cell viability assay.

3.2.1 Biofilm biomass

Biofilms were grown for 2, 12, 24 and 48 hours and the increase in biomass was evaluated with light microscopy following CV staining. In Figures 3.2A to 3.2D, the process of biofilm development is shown. Initially, yeast cells adhered to the surface of the growth substrate, which in this case was a polystyrene plate well and after 2 hours had formed microcolonies (Figure 3.2A). This was followed by budding and filamentation, which led to the formation of pseudohyphae and some hyphae after 12 hours (Figure 3.2B). Microcolonies started to combine with each other, forming a meshed network of interwoven hyphae with yeast cells being aggregated along the hyphae after 24 hours (Figure 3.2C). After 48 hours, the meshed hyphal network was denser, indicating the formation of a mature biofilm (Figure 3.2D).

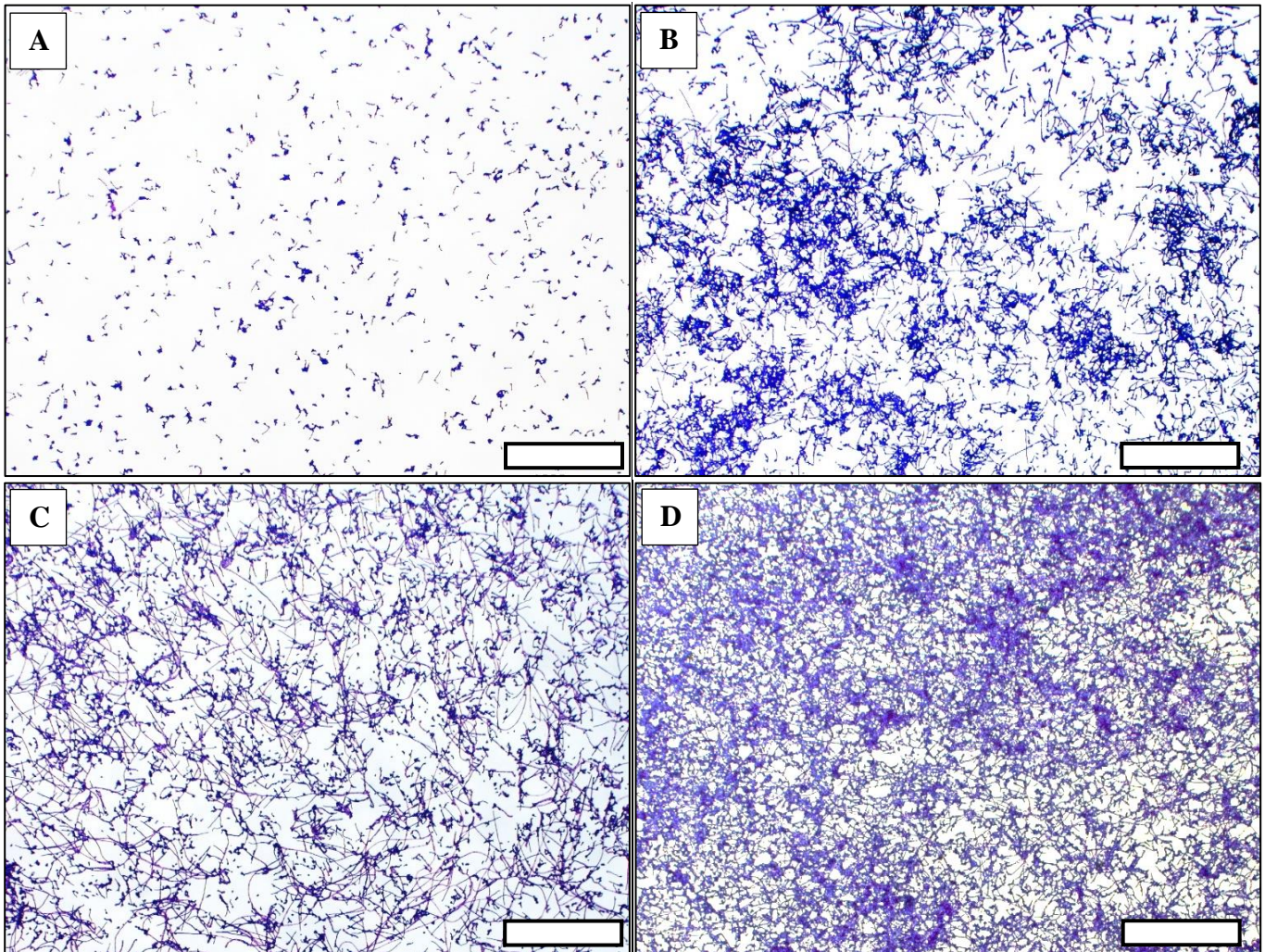


Figure 3.2: Light microscopy visualization of the kinetics of *C. albicans* biofilm development. Biofilms were grown for (A) 2, (B) 12, (C) 24, and (D) 48 hours after cell adhesion and then the biofilms were stained using CV. Scale bar = 1000 μm .

To obtain quantitative data regarding the biofilm biomass, CV was extracted, and the solubilized dye was quantified by measuring absorbance at 550 nm. Increase in biomass was observed at each of the time points (Figure 3.3). No significant difference was observed between 12 and 24 hours. Significant differences were observed between 2 and 12 hours ($p < 0.05$) and between 24 and 48 hours ($p < 0.01$).

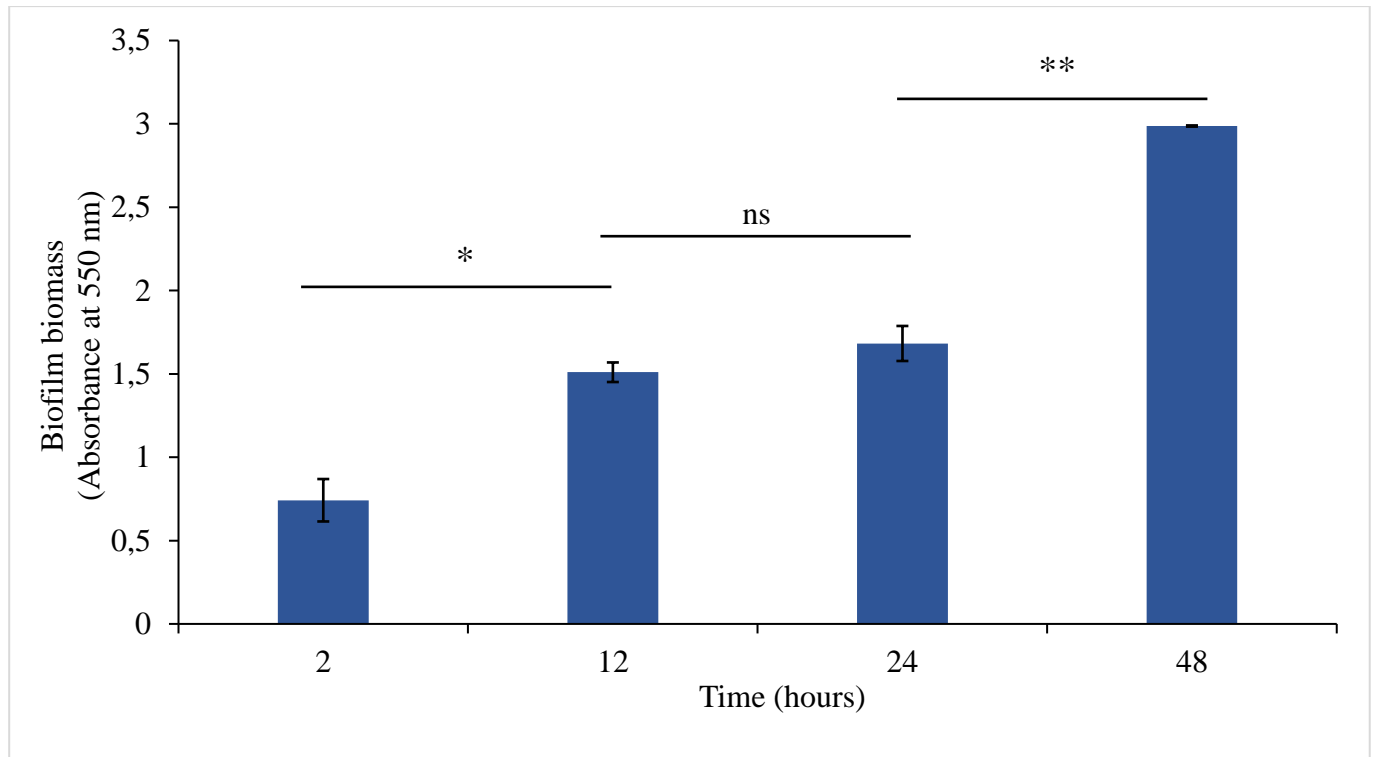


Figure 3.3: *C. albicans* biofilm formation over time in terms of biomass assessed by CV staining. The biomass of *C. albicans* biofilms grown for 2, 12, 24 and 48 hours after cell adhesion was determined by measuring the absorbance of the extracted CV. Error bars indicate the mean \pm SEM. Data are results of two independent experiments performed in triplicate. * $p < 0.05$, ** $p < 0.01$ and ns, not significant.

3.2.2 Biofilm viability

In addition to quantifying biofilm biomass, it was also necessary to quantify biofilm cell viability using the CTB cell viability assay. Biofilms were grown for 2, 12, 24 and 48 hours, after which the viability of biofilm cells was determined by measuring the fluorescence produced by the cells. The viability of *C. albicans* biofilms increased over time (Figure 3.4). An increase in fluorescence was observed between 2 and 12 hours, and between 24 and 48 hours. There was no significant difference in viability between 12 and 24 hours. However, significant differences were observed between 2 and 12 hours ($p < 0.001$) and between 24 and 48 hours ($p < 0.05$).

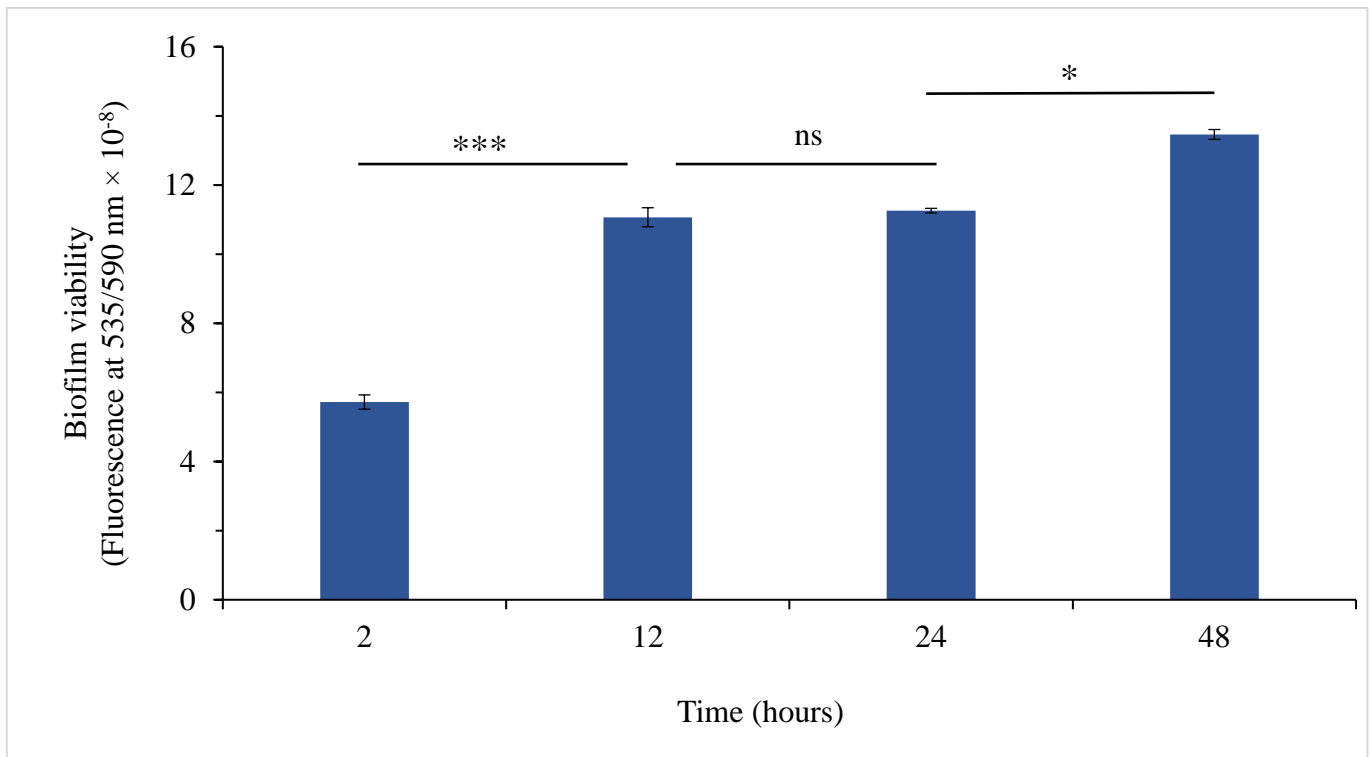


Figure 3.4: *C. albicans* biofilm formation over time in terms of viability assessed with CellTiter Blue. The viability of *C. albicans* biofilms was determined using the CTB cell viability assay. Biofilms were grown for 2, 12, 24 and 48 hours after cell adherence, after which CTB was added and the fluorescence was measured. Error bars indicate the mean \pm SEM. Data are results of two independent experiments performed in triplicate. * $p < 0.05$, *** $p < 0.001$, and ns, not significant.

3.3 Anti-biofilm activity

3.3.1 Biofilm inhibiting activity

The biofilm inhibiting potential of Os(11-22)NH₂ was determined by incubating adhered cells with AMB (positive control) or Os(11-22)NH₂ for 24 hours. The percentage of biofilm inhibition was determined using the CTB cell viability assay. AMB (Figure 3.5A) and Os(11-22)NH₂ (Figure 3.5B) inhibited *C. albicans* biofilm formation at micromolar concentrations in a dose-dependent manner.

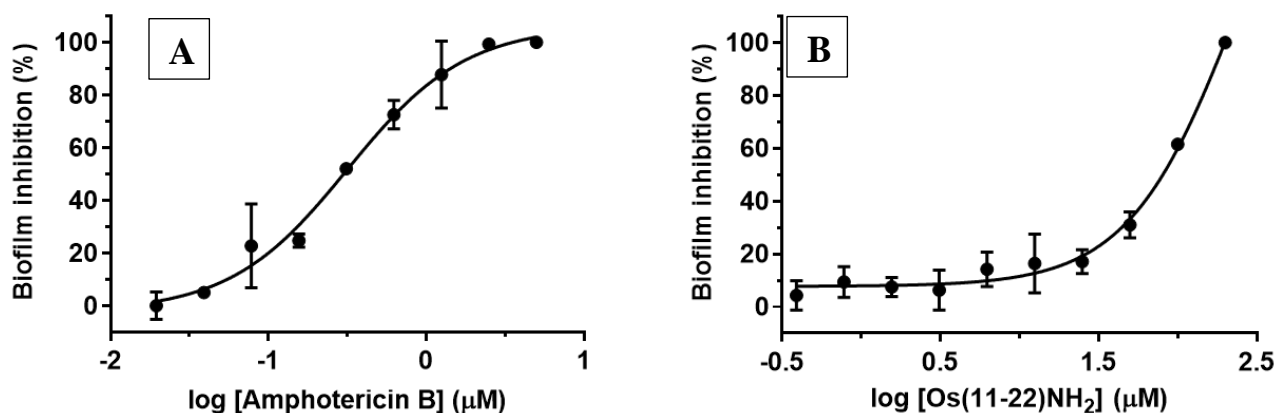


Figure 3.5: Biofilm inhibiting activity of (A) amphotericin B and (B) Os(11-22)NH₂. Adhered *C. albicans* cells were incubated with either AMB (0.019 μM to 5 μM) or Os(11-22)NH₂ (1.56 μM to 200 μM) for 24 hours and activity was determined using the CTB cell viability assay. Error bars indicate the mean ± SEM. Data are results of two independent experiments performed in triplicate.

The inhibition parameters BIC₅₀ and BIC_{max} (Table 3.2) were calculated from the full dose-response curves (Figure 3.5). AMB inhibited biofilm formation with respective BIC₅₀ and BIC_{max} values of 0.32 μM and 1.68 μM, whereas Os(11-22)NH₂ had BIC₅₀ and BIC_{max} values of 81 μM and 200 μM, respectively.

Table 3.2: BIC₅₀ and BIC_{max} values of amphotericin B and Os(11-22)NH₂.

Antifungal agent	BIC ₅₀ ^a (μM)	BIC _{max} ^b (μM)
Amphotericin B	0.32 ± 0.06	1.68 ± 0.6
Os(11-22)NH ₂	81 ± 2.71	200 ± 0.00

Each value is the mean ± SEM of two independent experiments, each performed in triplicate.

^a The BIC₅₀ values were derived from full dose-response curves and are the concentrations necessary to reduce biofilm formation by 50% (90).

^b The BIC_{max} values were calculated as the value at the intercept between the slope and the top plateau of a full dose-response curve and represents the concentrations necessary to cause total biofilm inhibition (121).

The biofilm inhibiting effect of AMB (positive control) and Os(11-22)NH₂ at their respective BIC₅₀ values was evaluated by light microscopy (Figure 3.6) of CV stained biofilms.

In the presence of AMB, shortened hyphae and many microcolonies were observed (Figure 3.6B), unlike the untreated control containing RPMI-DMSO, which had long hyphae and a few microcolonies (Figure 3.6A). The untreated control for Os(11-22)NH₂ also had a meshed hyphal network and very few microcolonies (Figure 3.6C) similar to the biofilm formed in the presence of RPMI-DMSO. Reduced biofilm formation was also seen after incubation with Os(11-22)NH₂, where a few long hyphae, shortened hyphae and microcolonies were present (Figure 3.6D).

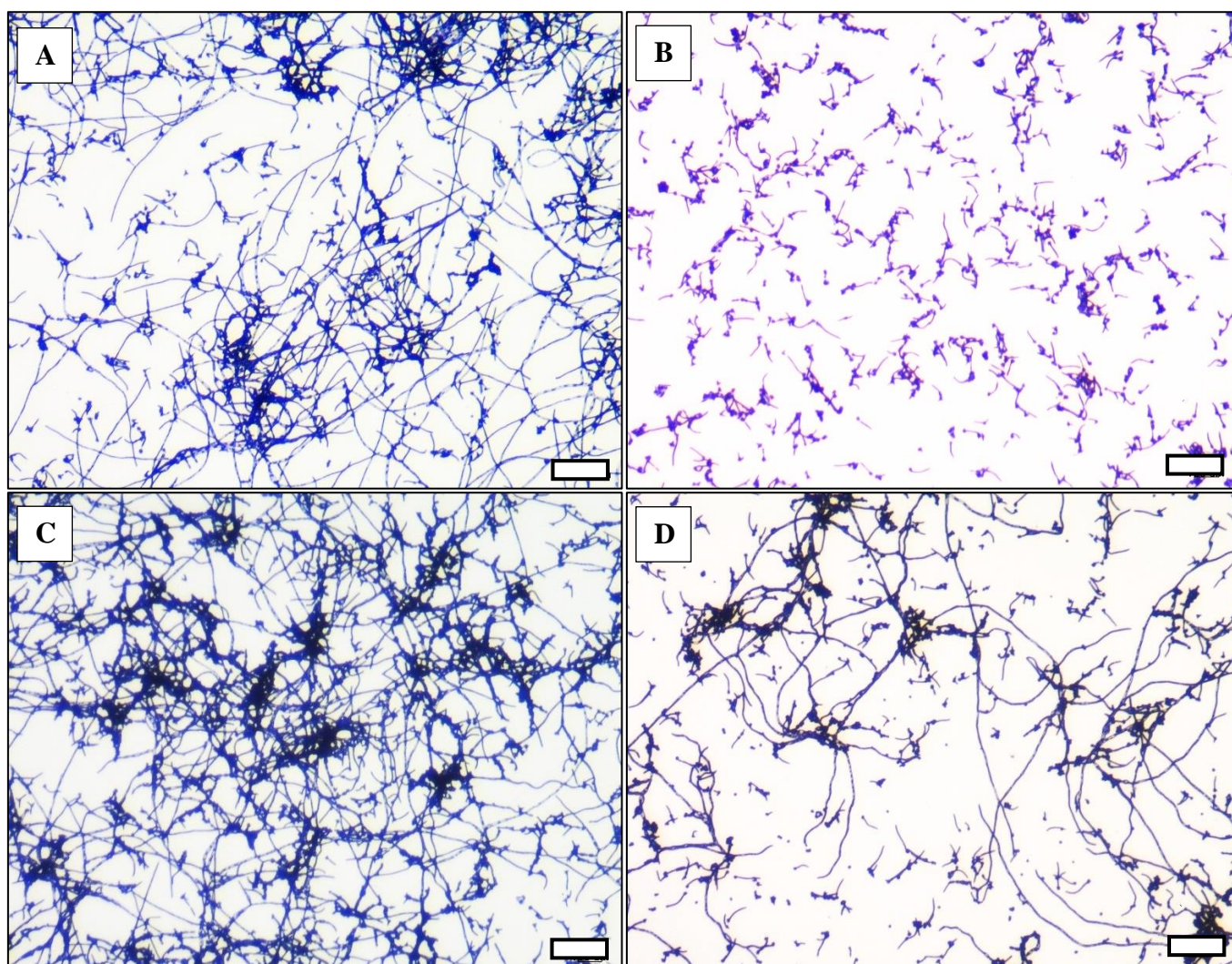


Figure 3.6: Light microscopy images showing biofilm inhibiting effect of amphotericin B and Os(11-22)NH₂. Adhered *C. albicans* cells were grown in the presence of concentrations of Os(11-22)NH₂ and AMB equivalent to the BIC₅₀ for 24 hours. Images represent cells grown in the presence of (A) RPMI-DMSO, (B) 0.32 μM AMB, (C) RPMI-1640 and (D) 81 μM Os(11-22)NH₂. Scale bar = 100 μm.

3.3.2 Biofilm eradicating activity

To investigate whether Os(11-22)NH₂ eradicates preformed biofilms, *C. albicans* biofilms were grown for 24 hours, treated with AMB (positive control) or Os(11-22)NH₂ for a further 24 hours and biofilm eradication was quantified using the CTB cell viability assay. AMB (Figure 3.7A) and Os(11-22)NH₂ (Figure 3.7B) eradicated preformed *C. albicans* biofilms at micromolar concentrations in a dose-dependent manner.

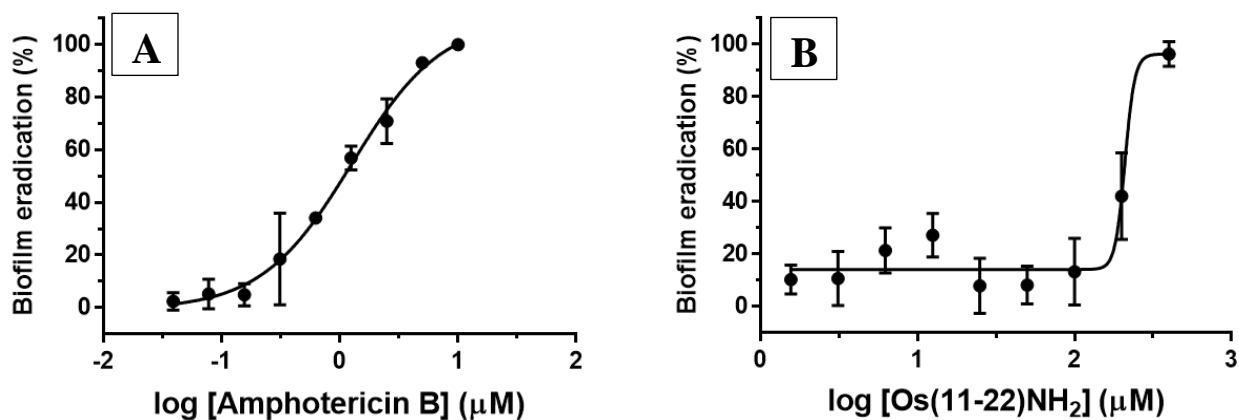


Figure 3.7: Biofilm eradicating activity of (A) amphotericin B and (B) Os(11-22)NH₂. Preformed *C. albicans* biofilms were incubated with either AMB (0.039 μM to 10 μM) or Os(11-22)NH₂ (1.56 μM to 400 μM). Error bars indicate the mean ± SEM. Data are results of three independent experiments performed in triplicate.

The biofilm eradication parameters BEC₅₀ and BEC_{max} (Table 3.3) were calculated from the full dose-response curves (Figure 3.7). AMB eradicated preformed *C. albicans* biofilms with BEC₅₀ and BEC_{max} values of 1.25 μM and 5.02 μM, respectively, whereas for Os(11-22)NH₂, the values were 210 μM and 277 μM, respectively.

Table 3.3: BEC₅₀ and BEC_{max} values of amphotericin B and Os(11-22)NH₂.

Antifungal agent	BEC ₅₀ ^a (μM)	BEC _{max} ^b (μM)
Amphotericin B	1.25 ± 0.24	5.02 ± 0.81
Os(11-22)NH ₂	210 ± 1.57	277 ± 43

Each value is the mean ± SEM of three independent experiments, each performed in triplicate.

^a The BEC₅₀ values were derived from full dose-response curves and are the concentrations necessary to decrease cell viability in a pre-grown biofilm by 50% (90).

^b The BEC_{max} values were calculated as the value at the intercept between the slope and the top plateau of a full dose-response curve and represents the concentrations necessary to cause total biofilm eradication (121).

3.4 Mode of action studies

3.4.1 Membrane permeabilization

Most AMPs tend to target the cell membrane which leads to the formation of pores, subsequent efflux of intracellular components and finally, cell death. Therefore, the membrane permeabilizing activity of Os(11-22)NH₂ was investigated using CLSM. For biofilm inhibition, biofilms grown for 24 hours were treated with 1% Triton X-100 for an hour as a positive control. Adhered cells were incubated with Os(11-22)NH₂ at the BIC₅₀ for 24 hours. Untreated cells were used as a negative control. The biofilms were stained with the fluorescent nuclear dyes PI (red) and DAPI (blue) and were viewed with CLSM. Images are shown in Figure 3.8.

In untreated biofilms (Figure 3.8, A-C), very little PI staining (Figure 3.8A) and more pronounced DAPI staining was observed (Figure 3.8B). Combined PI and DAPI staining is shown in Figure 3.8C. In contrast, cells that were treated with 1% Triton X-100 as a positive control (Figure 3.8, D-F), showed strong staining with PI (Figure 3.8D) which indicates that Triton X-100 caused membrane permeabilization. In similar fashion to Triton X-100, treatment with Os(11-22)NH₂ (Figure 3.8, G-I) led to PI staining (Figure 3.8G) indicating that Os(11-22)NH₂ inhibits biofilm formation by membrane permeabilization. Some DAPI staining was observed after treatment with 1% Triton X-100 and Os(11-11)NH₂ (Figures 3.8E and 3.8H). Combined DAPI and PI staining is shown in Figure 3.8I

Membrane permeabilization during biofilm eradication was evaluated by growing biofilms for 24 hours and treating the biofilms with Os(11-22)NH₂ at the BEC₅₀ for a further 24 hours. Triton X-100 (1%) was used as a positive control and was used to treat preformed biofilms for either 2 hours or 24 hours. Untreated biofilms were used as a negative control. In order to verify the presence of biofilms, transmitted light microscopy images were also taken. Images are shown in Figure 3.9.

Transmitted light microscopy images verified the formation of biofilms at all test conditions (Figures 3.9D, 3.9H, 3.9L and 3.9P). Untreated biofilms (Figure 3.9, A-D) showed DAPI staining (Figure 3.9B) and no PI staining (Figure 3.9A), indicating that the experimental conditions did not cause cellular damage. However, very little DAPI staining was observed in the untreated control compared to the treated biofilms (Figures 3.9F, 3.9J and 3.9N), indicating that the biofilms were very thick. Treatment of biofilms with Triton X-100 for 2 hours (Figure 3.9E) or 24 hours (Figure 3.9I) showed an increase in PI and DAPI staining which indicates that Triton X-100 caused membrane permeabilization. Treatment of biofilms with Os(11-22)NH₂ (Figure 3.9, M-P) at its BEC₅₀ led to PI staining (Figure 3.9M) compared to the untreated control, indicating that Os(11-22)NH₂ increased membrane permeability. Furthermore, in biofilms treated with either Triton X-100 or Os(11-22)NH₂ for 24 hours, the entirety of the yeast and hyphal cells was stained with either PI

(Figures 3.9I and 3.9M) or DAPI (Figures 3.9J and 3.9N). Combined images are shown in Figures 3.9C, 3.9G, 3.9K and 3.9O.

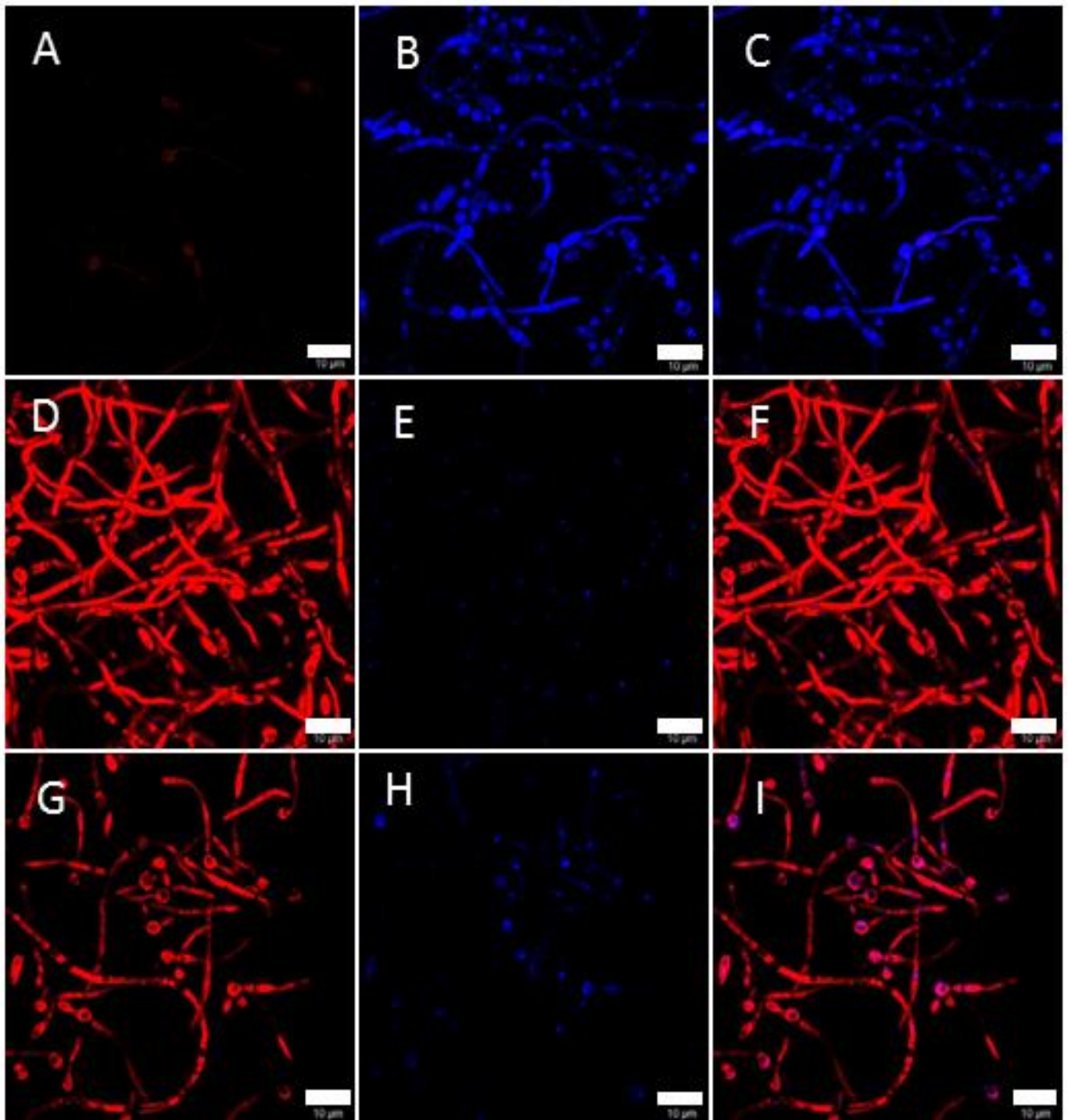


Figure 3.8: Confocal laser scanning images of treated and untreated biofilms during biofilm inhibition. Adhered *C. albicans* cells were grown in the presence of RPMI-1640 (A-C) and 81 μM Os(11-22) NH_2 (G-I). As a positive control, 24 hour preformed biofilms were treated with 1% Triton X-100 (D-F) for an hour. After treatment, biofilms were stained with propidium iodide (PI, red) and counterstained with 4',6-diamidino-2-phenylindole (DAPI, blue). Samples were mounted and viewed by CLSM. Images show samples stained with PI (A, D and G), DAPI (B, E and H) and DAPI and PI combined (C, F and I). Scale bars = 10 μm .

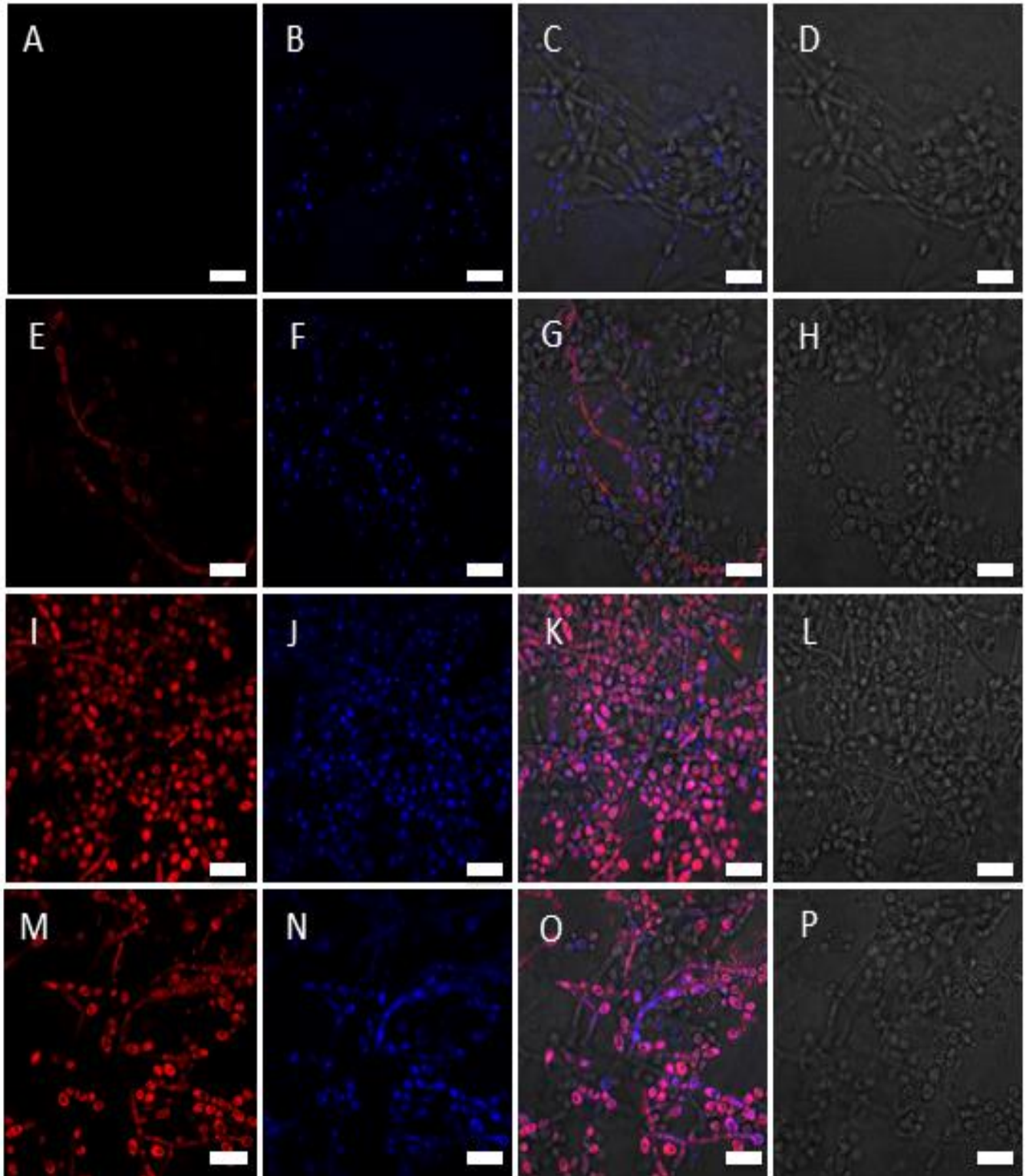


Figure 3.9: Confocal laser scanning microscopy images of treated and untreated biofilms during biofilm eradication. Preformed *C. albicans* biofilms were left untreated (A-D), treated with 1% Triton X-100 for 2 hours (E-H) or 24 hours (I-L) and treated with 210 μM Os(11-22) NH_2 (M-P). After treatment, biofilms were stained with PI (red) and counterstained with DAPI (blue). Samples were mounted and viewed by CLSM. Images show samples stained with PI (A, E, I and M), samples stained with DAPI (B, F, J and N), combined images (C, G, K and O) and samples viewed under transmitted light microscopy (D, H, L and P) to verify biofilm formation. Scale bars = 10 μm .

3.4.2 Induction of reactive oxygen species formation

A number of studies have shown that the mechanism of *C. albicans* killing by AMPs is via ROS formation. Therefore, the fluorescent dye DCFH-DA was used to detect whether Os(11-22)NH₂ induces ROS formation during biofilm inhibition. Adhered cells were incubated with AMB and Os(11-22)NH₂ at their respective BIC₅₀ values. Furthermore, a concentration corresponding to double the BIC₅₀ of AMB was included. To investigate whether there was a link between antifungal activity and ROS formation, ascorbic acid, a known ROS scavenging molecule was used (123). To ensure that ROS produced was not due to changes in pH, citric acid was included as a pH control.

For the untreated controls in RPMI-1640 and RPMI-DMSO, there was no significant difference between incubation without ascorbic acid, with ascorbic acid and with citric acid (Figure 3.10). Compared to the untreated control (RPMI-DMSO), AMB induction of ROS at its BIC₅₀ (0.32 μM) and at double the BIC₅₀ (0.64 μM) was not significant. Addition of 10 mM ascorbic acid did not induce a significant change in ROS formation by AMB at both concentrations. On the other hand, Os(11-22)NH₂ at its BIC₅₀ (81 μM) caused ROS formation that was significantly different compared to the untreated control ($p < 0.0001$). Furthermore, the presence of ascorbic acid significantly reduced ($p < 0.0001$) ROS formation.

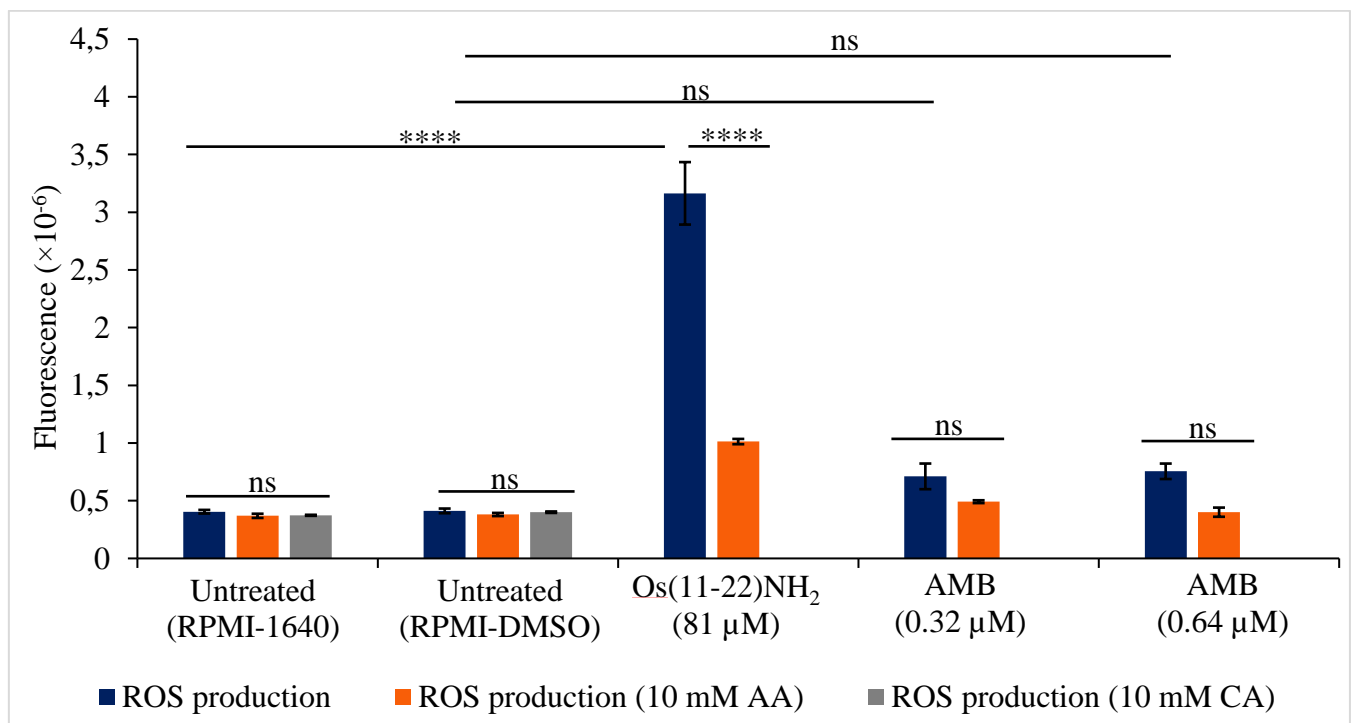


Figure 3.10: Induction of ROS formation during biofilm inhibition. Adhered *C. albicans* cells were incubated in the presence or absence of inhibitory concentrations of AMB and Os(11-22)NH₂ and ROS production was measured using the fluorescent dye DCFH-DA. The effect of adding 10 mM ascorbic acid (AA), a ROS scavenger, was also investigated. Citric acid (10 mM, CA) was used as a pH control. Error bars indicate the mean ± SEM. Data are results of three independent experiments performed in triplicate. **** $p < 0.0001$, ns, not significant.

To determine whether ROS produced by Os(11-22)NH₂ is responsible for biofilm inhibiting activity, adhered cells were incubated with the peptide at its BIC₅₀ in the absence or presence of ascorbic acid and activity was determined using the CTB cell viability assay. Irrespective of whether ascorbic acid was added or not, no significant difference in biofilm inhibition was observed for Os(11-22)NH₂, indicating that the peptide does not inhibit biofilm formation by ROS (Table 3.4).

Table 3.4: The influence of ascorbic acid on the biofilm inhibiting activity of Os(11-22)NH₂.

Treatment	Biofilm inhibition at 81 μM (%)
Os(11-22)NH ₂	35 ± 2.83
Os(11-22)NH ₂ + 10 mM ascorbic acid	28 ± 2.72

Each value is the mean ± SEM of three independent experiments, each performed in triplicate.

The induction of ROS formation was also investigated in 24 hour preformed biofilms which were treated with the BEC₅₀ concentrations of AMB (1.25 μM) and Os(11-22)NH₂ (210 μM) for 24 hours. In addition, double the BEC₅₀ of AMB (2.5 μM) was also tested. With regards to the untreated controls in RPMI-1640 and RPMI-DMSO, there was no significant difference between incubation without ascorbic acid, with ascorbic acid and with citric acid (Figure 3.11). ROS formation was observed at all concentrations of AMB and Os(11-22)NH₂ and was significantly different from ROS formation by untreated cells ($p < 0.0001$). At their respective BEC₅₀ concentrations, there was no significant difference in ROS formation by AMB and Os(11-22)NH₂. In the presence of 10 mM ascorbic acid, there was a significant difference ($p < 0.0001$) in ROS formation for both AMB concentrations and Os(11-22)NH₂.

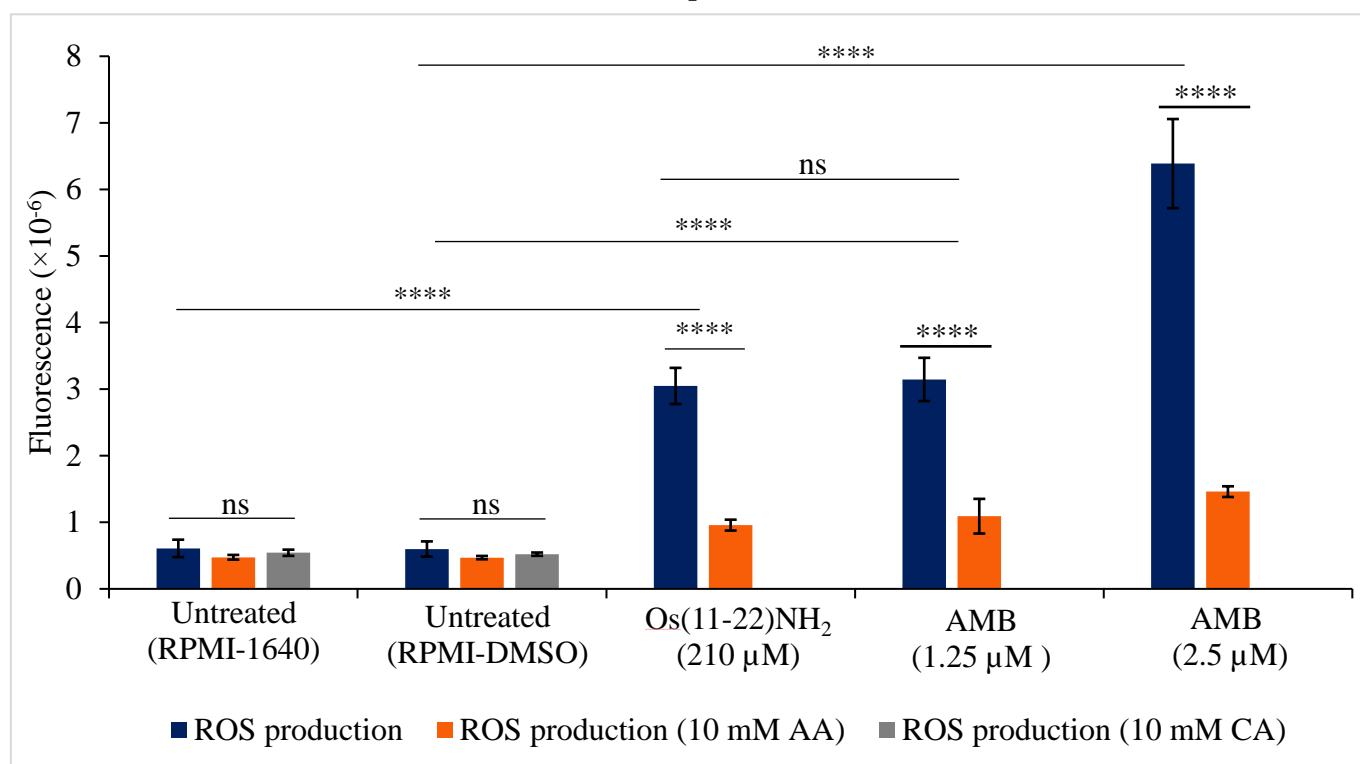


Figure 3.11: Induction of ROS formation during biofilm eradication. Preformed *C. albicans* biofilms were treated with eradicating concentrations of Os(11-22)NH₂ and AMB and ROS production was measured using DCFH-DA. The effect of adding 10 mM ascorbic acid (AA), a ROS scavenger, was also investigated. Citric acid (10 mM, CA) was used as a pH control. Error bars indicate the mean \pm SEM. Data are results of three independent experiments performed in triplicate. **** $p < 0.0001$, ns, not significant.

To investigate whether ROS contributes to killing during biofilm eradication, 24 hour preformed biofilms were treated with BEC₅₀ concentration of AMB (1.25 μ M) and Os(11-22)NH₂ (210 μ M) and double the BEC₅₀ of AMB (2.5 μ M) for 24 hours. Biofilm eradication in the presence and absence of 10 mM ascorbic acid was determined using the CTB cell viability assay. AMB eradicated preformed biofilms, however, there was no significant difference in the presence and absence of ascorbic acid (Figure 3.12). For Os(11-22)NH₂, biofilm eradication was significantly increased ($p < 0.0001$) in the presence of ascorbic acid, indicating that ascorbic acid enhanced the biofilm eradicating activity of Os(11-22)NH₂ (Figure 3.12). Overall, the results showed that although AMB and Os(11-22)NH₂ lead to ROS production during biofilm eradication, the activity is not as a result of ROS.

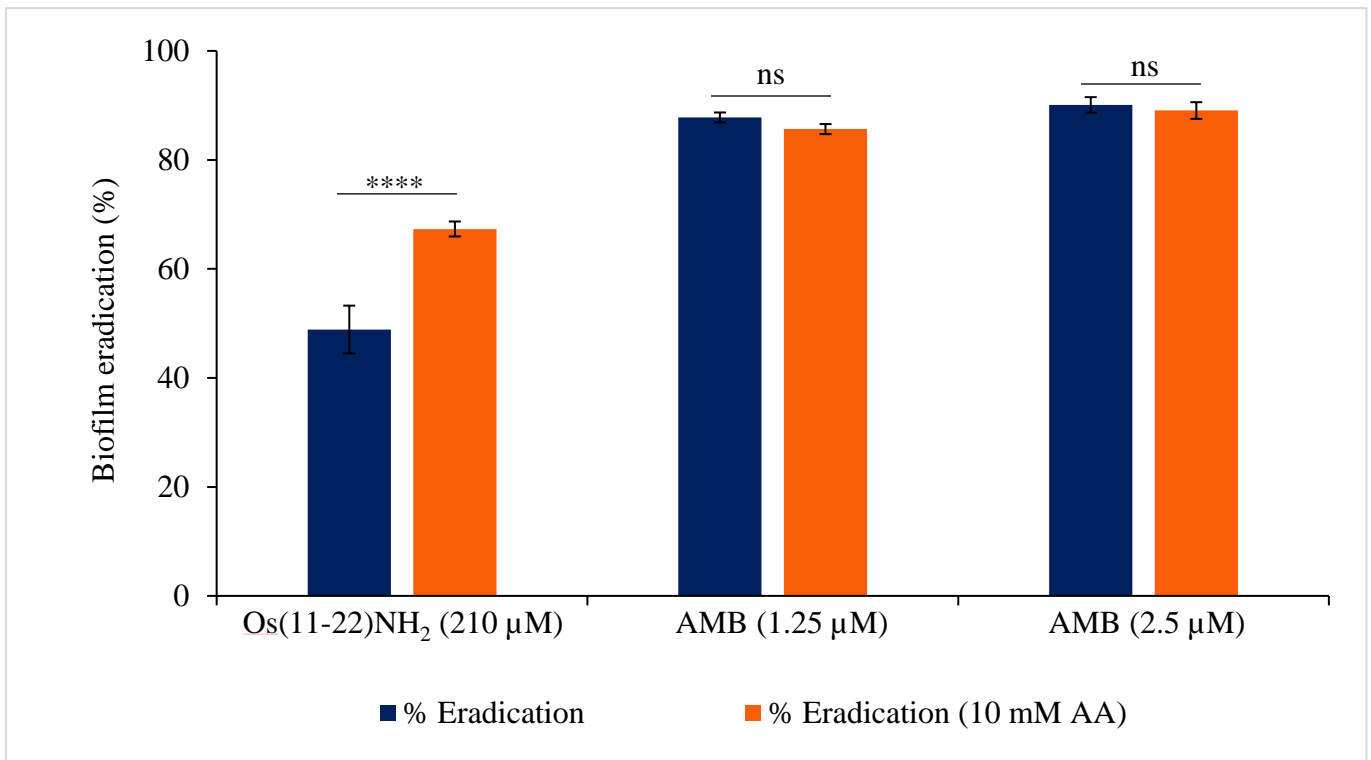


Figure 3.12: Effect of ascorbic acid addition on biofilm eradication. Preformed *C. albicans* biofilms were treated with biofilm eradicating concentrations of AMB and Os(11-22)NH₂. The effect of 10 mM ascorbic acid (AA) on biofilm eradication was investigated using CTB cell viability assay. Error bars indicate the mean ± SEM. Data are results of three independent experiments performed in triplicate. ****p < 0.0001, ns, not significant.

4. Discussion

The growing incidence of AMR has led to increased mortality, longer hospital stays, and more costly and complex treatments, as a result AMR has become a global health issue (2). Factors that influence AMR include the misuse and abuse of antimicrobial agents, the production of counterfeit and substandard drugs (13) and the acquisition of resistance encoding genes (12). Of great concern is antifungal resistance, which is responsible for millions of deaths due to fungal infections caused by biofilms. Resistance of fungal species to conventional antifungal drugs such as AMB, caspofungin and fluconazole is due to the highly resistant nature of biofilms. The presence of efflux pumps, the ECM, persister cells and extracellular DNA play a role in preventing antifungal activity, thus ensuring biofilm survival (7).

In order to tackle the issue of resistance to conventional antifungal drugs, it is necessary to discover or develop novel antifungal agents that possess anti-biofilm activity. A potential solution to overcome antifungal resistance is the use of cationic AMPs which are short and amphipathic molecules. AMPs have been found to be active against a number of bacteria, viruses and fungi (124). The development of resistance mechanisms by microorganisms is unlikely due to the diverse modes of killing such as targeting the cell wall, cell membrane and/or intracellular components (68). In this study, the anti-biofilm activity of Os(11-22)NH₂, a tick-derived AMP was investigated. Previous work has shown that Os(11-22)NH₂ possessed antibacterial activity and antifungal activity against planktonic *C. albicans*. Therefore, the aim of this study was to determine whether Os(11-22)NH₂ possessed activity against *C. albicans* biofilms.

Initially, it was necessary to determine the anti-planktonic activity of Os(11-22)NH₂ by means of the microbroth dilution assay. The parent peptide, (Os), was inactive at all concentrations tested (Figure 3.1 and Table 3.1) while the amidated, smaller analogue Os(11-22)NH₂ was active against planktonic *C. albicans* with a MIC₅₀ of 47 µM. For AMP induced killing to occur, the cationic AMP must interact with anionic components of the cell membrane. Lack of activity, as in the case of Os, is likely due to the presence of salts including sodium chloride (NaCl), potassium chloride (KCl) and magnesium sulfate (MgSO₄) in RPMI-1640 medium. The cations, Na⁺, K⁺ and Mg²⁺, will compete with Os for binding to negatively charged membrane components, thus preventing Os from killing planktonic *C. albicans*. The presence of cations has been found to have a negative effect on the antimicrobial activity of most, if not all defensin peptides. A study by Yacoub *et al.* (125) showed that the antimicrobial activity of two chicken β-defensin peptides is decreased in the presence of greater than 50 mM NaCl. Furthermore, human β-defensin peptides have been found to exhibit salt sensitivity in NaCl concentrations of 100 mM or more (126-128). However, killing was observed in the case of Os(11-22)NH₂, which has a lower overall positive charge of +4 compared to Os which has a charge of +6 (Table 1.2). In addition, Os(11-22)NH₂ (12 amino acids) is shorter than Os (22

amino acids), therefore, there is a possibility Os could have more difficulty interacting with specific cellular components and may have a different mode of killing.

Before anti-biofilm assays were performed, the optimum time for biofilm growth was determined. Therefore, biofilms were grown for 2, 12, 24 and 48 hours and the biomass and viability of biofilms was determined using CV and CTB cell viability assays, respectively. Biofilm formation over time was shown qualitatively by staining biofilms with CV and viewing under a light microscope (Figure 3.2). An increase in biomass over time was observed, indicating that the number of cells and amount of ECM increased (Figure 3.3). Images of biofilm development in Figure 3.2 follow a similar trend to the steps shown in Figure 1.4 in which planktonic cells first adhered to the surface (adherence, Figure 3.2A), followed by continued growth of cells and hyphae (initiation, Figure 3.2B). Finally, hyphal growth continues until a mature biofilm is formed (maturation, Figures 3.2C and 3.2D). However, biomass is not a suitable measure for determining the optimum time for the growth of viable biofilms. Therefore, the viability of the biofilms was also investigated using the CTB cell viability assay. Results indicated that as time increased, biofilm viability also increased (Figure 3.4), indicating the presence of more viable cells. No significant differences in biofilm biomass and viability at 12 hours and 24 hours were observed (Figures 3.3 and 3.4). However, biofilms grown for 24 hours were used for biofilm inhibition and eradication studies, as increased hyphal formation was observed after 24 hours than at 12 hours (Figures 3.2B and 3.2C). The presence of yeast and hyphal cells is vital for successful biofilm development (129). Furthermore, mature biofilms tend to be formed by 24 hours, and can usually be seen without the aid of a microscope (20). CLSM also confirmed the presence of a well-established biofilm after 24 hours and increased biomass after 48 hours (Figure 3.9).

Medical devices such as catheters and joint prostheses provide a suitable surface for the formation of biofilms, increasing the likelihood of infections in patients (130). Therefore, novel antifungal agents could be used to coat the surfaces of medical devices, thereby preventing biofilm formation. In this study, the biofilm inhibiting activity was investigated by growing biofilms in the presence of Os(11-22)NH₂. AMB and Os(11-22)NH₂ showed biofilm inhibiting activity in the micromolar range, with BIC₅₀ values of 0.32 μM and 81 μM, respectively (Figure 3.5 and Table 3.2). This was confirmed by inverted light microscopy images of CV stained biofilms in Figure 3.6, where fewer hyphae were present after growth in the presence of BIC₅₀ concentrations of AMB and Os(11-22)NH₂ (Figures 3.6B and 3.6D) compared to the untreated controls (Figures 3.6A and 3.6C). The transition of *C. albicans* from the yeast to the hyphal form enables virulence development during biofilm formation (131), therefore, preventing this transition will inhibit biofilm formation.

In situations where biofilm formation cannot be prevented, the biofilm can develop and mature, which can be problematic in patients suffering from fungal infections or have implanted medical devices. The presence

of a mature biofilm means that higher doses of antifungal drugs must be administered, which further complicates treatment. In the case of patients who have implanted medical devices, the presence of biofilms means that the device may have to be removed entirely, which can be a costly and uncomfortable process (20). For this reason, the ideal antifungal drugs should possess biofilm inhibiting and eradicating activity. The biofilm eradicating activity was evaluated by incubating preformed *C. albicans* biofilms with a range of AMB and Os(11-22)NH₂ concentrations (Figure 3.7). Experiments showed that AMB and Os(11-22)NH₂ eradicated preformed biofilms, with BEC₅₀ values of 1.25 μM and 210 μM (Table 3.3).

A number of studies investigating the anti-biofilm activity of AMPs against *C. albicans* have been documented. In a study by Paulone *et al.* (132), the synthetic peptide KP had BIC₅₀ and BEC₅₀ values of 14 μM and 138 μM, respectively. The tyrocidines (TrcA, TrcB and TrcC) had BIC₅₀ values that ranged between 5.7 – 17 μM and BEC₅₀ values between 133-164 μM (97). Although some AMPs inhibit *C. albicans* biofilm formation, they are unable to eradicate preformed biofilms. The plant defensin OSIP108 had a BIC₅₀ of 5.3 μM, however, failed to eradicate preformed biofilms (BEC₅₀ > 800 μM). In addition, analogues of OSIP108 either had higher BIC₅₀ values than 5.3 μM or were unable to inhibit biofilm formation (133). Furthermore, the mouse cathelicidin derivative AS-10 inhibited biofilm formation at a lower concentration than the MIC (BIC₅₀ = 0.22 μM) but did not eradicate preformed biofilms (BEC₅₀ > 400 μM) (94). In this study, Os(11-22)NH₂ inhibited biofilm formation and eradicated preformed biofilms. The MIC₅₀ of Os(11-22)NH₂ (47 μM) was almost two times less than the BIC₅₀ (81 μM) and four and a half times less than the BEC₅₀ (210 μM). Furthermore, the BEC₅₀ of Os(11-22)NH₂ was over two and a half times more than the BIC₅₀.

AMPs display broad spectrum antimicrobial activity. However, some AMPs exhibit activity against fungi and are referred to as AFPs. The targets of AFPs include components of the mannoproteins and chitin, components of the cell wall, glycerophospholipids such as glucosylceramide in the cell membrane and intracellular targets such as organelles and important cell functions such as protein synthesis (134). A common target for cationic AMPs and AFPs is the cell membrane. Cationic AMPs can interact with negatively charged components of the cell membrane, leading to decreased membrane integrity. Since Os(11-22)NH₂ possesses the characteristics of a membrane targeting AMP (cationic charge and amphipathicity), the membrane permeabilizing activity of Os(11-22)NH₂ at the BIC₅₀ was investigated. The DNA binding dye PI was used to indicate whether permeabilization occurred. PI can only enter cells where the integrity of the cell membrane has been compromised. Intracellularly, PI can bind both DNA and RNA (135) resulting in red fluorescence. On the other hand, DAPI can enter cells whether or not cell membrane integrity has been compromised and binds to regions of DNA that are abundant in adenine-thymine base pairings (117). In biofilm inhibition experiments, increased PI fluorescence in 1% Triton X-100 (Figure 3.8D) and Os(11-22)NH₂ (Figure 3.8G) treated cells indicated that membrane permeabilization had

occurred. Less DAPI fluorescence was seen in the Triton X-100 (Figure 3.8E) and Os(11-22)NH₂ (Figure 3.8H) treated cells compared to the untreated control (Figure 3.8B) because PI had already bound to nuclear DNA, therefore, DAPI could only bind to very small regions of DNA. Samples were first stained with PI, which can bind to four or five base pairs of DNA without specificity (116).

For the evaluation of biofilm eradication activity, biofilms were grown for 48 hours (grown for 24 hours, then RPMI-1640 medium was replenished, and the biofilm was grown for a further 24 hours) making it a fully mature biofilm (136). The biofilm at 48 hours had a higher biomass (Figure 3.3) and the cells were densely arranged (Figure 3.2D) which confirmed the establishment of a mature biofilm. In the untreated control, very little DAPI staining, weak and low levels of fluorescence were observed (Figure 3.9B) possibly because very little DAPI was able to traverse the thick ECM and enter the cells. In a study by Baillie and Douglas (137), biofilms grown on catheter discs were made up of a basal layer consisting of yeast cells and a thick upper layer made up of hyphae. Subsequently, when biofilms are viewed under the confocal microscope, only one layer is in focus meaning that only cells stained with DAPI in a particular focal plane could be observed and any DAPI fluorescence from cells that are out of focus will be blocked (138). Furthermore, it is also worth noting that extracellular DNA is present in the ECM, therefore, PI and DAPI might also interact with the extracellular DNA (52).

Triton X-100, is a non-ionic detergent that solubilizes proteins and can cause membrane permeabilization. Exposure of mature biofilms to Triton X-100 for 2 and 24 hours with a resulting increase in PI fluorescence after 24 hours indicates that the established ECM is dense. Once the ECM is solubilized, the nucleic acid binding dyes PI and DAPI have access to the intracellular DNA. Interestingly, the biofilm exposed to Os(11-22)NH₂ (Figure 3.9M) showed similar staining to the biofilm exposed to Triton X-100 for 24 hours (Figure 3.9I), indicating that the ECM is reduced, and intracellular DNA is more accessible for staining. Furthermore, the observed PI fluorescence indicates that membrane permeabilization had occurred. Therefore, more PI and DAPI could enter the cells, leading to higher fluorescence for both fluorescent dyes.

ROS are molecules that contain oxygen and are more potent and reactive than molecular oxygen (139). Common examples of ROS include the hydroxyl radical ([•]OH), superoxide (O₂^{•-}), hydrogen peroxide (H₂O₂) and singlet oxygen (¹O₂) (140). At regulated levels ROS play a critical role in the mediation of cellular responses such as apoptosis, cell growth and cell differentiation (141). However, when the cell is under oxidative stress, excess ROS is produced and can cause lipid peroxidation, damage to DNA and cell death (142). Numerous studies show that AMPs induce ROS formation in *C. albicans* (143-146). Furthermore, studies have shown a possible link between ROS production and membrane permeabilization. Troskie *et al.* (97) proposed that as tyrocidine peptides permeabilize the membrane, ROS production can occur due to osmotic stress or binding to cell membrane components. On the other hand, ROS production by the plant

defensin PvD1 was found to enhance membrane permeabilization (147). Therefore, it was necessary to investigate whether Os(11-22)NH₂ induced the formation of ROS using the fluorogenic dye DCFH-DA. During biofilm inhibition and eradication, results indicated that Os(11-22)NH₂ induced ROS production, which could play a role in the anti-biofilm activity of Os(11-22)NH₂. In the presence of ascorbic acid, a ROS scavenging antioxidant, ROS production by the peptide was significantly reduced during biofilm inhibition and eradication ($p < 0.0001$; Figures 3.10 and 3.11). For AMB, ROS production observed during biofilm inhibition was not significant compared to the untreated control (Figure 3.10), indicating that ROS production is not a key mode of action during biofilm inhibition. However, ROS production was observed in the presence of AMB during biofilm eradication, which is expected since AMB is known to induce ROS production (148). In the presence of ascorbic acid, however, a significant decrease in AMB-induced ROS production was observed during biofilm eradication at the BEC₅₀ (1.25 μM) and at double the BEC₅₀ (2.5 μM) (Figure 3.11).

In order to determine whether ROS production by Os(11-22)NH₂ contributes to killing during biofilm inhibition and eradication, the CTB cell viability assay was used. Biofilm inhibition and eradication experiments were performed in the presence and absence of ascorbic acid, a known ROS scavenger. With regards to biofilm inhibition, there was no significant difference in biofilm inhibiting activity in the presence and absence of ascorbic acid (Table 3.4), indicating that ROS production does not contribute to biofilm inhibition. However, increased ROS production following Os(11-22)NH₂ treatment could play a role in the induction of apoptosis since abnormally high levels of ROS are a common indicator of apoptosis in yeast cells (149). AMPs such as pleurocidin, psacothasin, scolopendin and melittin have been found to increase the levels of intracellular ROS, which in turn leads to apoptosis (144,150-152). The contribution of ROS production to biofilm eradication by Os(11-22)NH₂ was also investigated. If there is a significant decrease in biofilm eradication in the presence of ascorbic acid, it can be concluded that ROS production does play a role in biofilm eradication. On the other hand, if there is no change in biofilm eradication in the presence of ascorbic acid, then the peptide does not eradicate biofilms by ROS production. However, in this study, significantly more biofilm eradication ($p < 0.0001$) was observed in the presence of ascorbic acid than in the absence of ascorbic acid (Figure 3.12). The result indicated that addition of ascorbic acid enhanced the biofilm eradicating activity of Os(11-22)NH₂ which was unexpected. A similar observation was made in a study by Troskie *et al.* (97), where the biofilm eradicating activity of two tyrocidines (TrcA and TrcB) was significantly increased in the presence of 10 mM ascorbic acid. An explanation for increased biofilm eradicating activity was that ascorbic acid could have been acting as a chaotropic agent, which reduced aggregation and stabilized the structures of TrcA and TrcB. The same explanation could also be valid for increased biofilm eradication by Os(11-22)NH₂ in the presence of ascorbic acid. Ascorbic acid has been used in combination with antibiotics against *Pseudomonas aeruginosa* and was found to have synergistic

activity with chloramphenicol, tetracycline, streptomycin and kanamycin (153). Furthermore, Khalil *et al.* (154) showed that the presence of ascorbic acid decreases the MIC and increases the antioxidant activity of curcumin against *C. albicans* indicating that combination with ascorbic acid could potentially improve antifungal activity. When used on its own at high concentrations, ascorbic acid has been found to act as a pro-oxidant and exhibits antifungal activity against *C. albicans*. At concentrations ≥ 0.85 M, ascorbic acid inhibited *C. albicans* growth, and transition from the yeast to the hyphal form was prevented when cells were treated with concentrations as low as 0.085 M (155). However, in the present study a concentration of 10 mM ascorbic acid could have a pro-oxidant effect, especially when used in combination with antifungal agents. Therefore, the role of ascorbic acid as an antifungal agent should be considered.

Increased antifungal resistance and the limited variety of antifungal drugs have led to greater incidence of fungal infections. In order to combat these infections, higher doses of antifungal agents must be used which leads to toxic side effects. For example, the continuous administration of AMB is associated with nephrotoxicity which can lead to death (156). Therefore, novel antifungals must be developed to prevent resistance and toxicity. Cationic AMPs are a good alternative to conventional antifungals because these peptides are mostly water soluble, have multiple cellular targets and are less likely to be overcome by resistance mechanisms (9). In this study, the tick-derived AMP Os(11-22)NH₂ showed potent anti-biofilm activity against *C. albicans* and has shown potential for use in antifungal therapy as an alternative to conventional antifungal agents.

5. Conclusions and Future Perspectives

The anti-biofilm activity of the tick-derived AMP Os(11-22)NH₂ was evaluated in this study. Os(11-22)NH₂ exhibited activity against planktonic *C. albicans* (Table 5.1). Furthermore, Os(11-22)NH₂ demonstrated anti-biofilm activity by preventing *C. albicans* biofilm formation and eradicating preformed *C. albicans* biofilms (Table 5.1). The ability to inhibit biofilm formation indicates a potential application for Os(11-22)NH₂ as a coating agent for implanted medical devices. The inverted light microscopy image of cells grown in the presence of 81 µM Os(11-22)NH₂ indicated that reduced biofilm formation occurred compared to the untreated control. In particular, less hyphae were present in the treated sample, indicating that Os(11-22)NH₂ inhibits hyphal development. In similar fashion to a study by Morici *et al.* (157), the effect of Os(11-22)NH₂ treatment on the transcription of genes involved in cell adhesion, hyphal development and production of ECM in *C. albicans* biofilms can be investigated. Using quantitative real time RT-PCR, transcription levels of the genes of interest in treated and untreated biofilms can be investigated and compared. As a result, a better understanding of how Os(11-22)NH₂ affects *C. albicans* biofilm formation can be gained.

In order to improve activity, Os(11-22)NH₂ can be modified by cyclization (158), addition of D-isomers (106) and the addition of β-naphthylalanine (159), modifications that can be made to confer greater peptide stability.

Resistance to current antifungal drugs is a major issue due to the limited range of antifungal drugs. Currently, the azoles, echinocandins and polyenes are the major classes used, but resistance to drugs belonging to all three classes has been reported (31). A method to overcome resistance is the use of drugs in combination which can lead to more antifungal activity. In this study, Os(11-22)NH₂ has shown potential to be used in antifungal therapy due to its ability to inhibit biofilm formation and eradicate preformed biofilms. Therefore, Os(11-22)NH₂ could be used in combination with conventional antifungal drugs such as fluconazole (160), AMB (97) and caspofungin (161) against *C. albicans* strains that exhibit resistance to these antifungals. Combination studies could be carried out in the form of a checkerboard assay which would provide information whether interactions between Os(11-22)NH₂ and the antifungal drugs are synergistic.

The membrane permeabilizing activity of Os(11-22)NH₂ was investigated using CLSM. Results indicated that membrane permeabilization occurs during biofilm inhibition and eradication (Table 5.1). Further work should focus on investigating the ultrastructural effects of Os(11-22)NH₂ treatment on *C. albicans* using transmission electron microscopy (109). In addition, the interaction of Os(11-22)NH₂ with components of the membrane such as glycerophospholipids and sphingolipids should be considered. For example, the

peptides RsAFP2 and PvD1 interact with glucosylceramide, a fungal glycosphingolipid involved in fungal virulence. Interaction with glucosylceramide leads to ROS production, membrane permeabilization and apoptosis (143,147). The investigation of interactions between Os(11-22)NH₂ and membrane components could therefore provide more information on how Os(11-22)NH₂ permeabilizes fungal membranes.

Although Os(11-22)NH₂ induced ROS production during biofilm inhibition and eradication (Table 5.1), the production of ROS was significantly decreased in the presence of ascorbic acid. The presence of abnormally high levels of ROS is an indicator of apoptosis (162). Another indicator of apoptosis is the externalization of phosphatidylserine, a component of the cell membrane. During apoptosis, membrane integrity is compromised and leads to the movement of phosphatidylserine from the inner to the outer surface (163). Using Annexin V-FITC staining and flow cytometry, phosphatidylserine exposure can be determined. By comparing the fluorescence produced by treated and untreated *C. albicans* biofilms, it is possible to determine whether Os(11-22)NH₂ induces phosphatidylserine externalization. In addition, the results will give an indication whether Os(11-22)NH₂ causes apoptosis.

The effect of ascorbic acid on the anti-biofilm activity of Os(11-22)NH₂ was investigated using the CTB cell viability assay. During biofilm inhibition and eradication, no significant difference was observed between treatment in the presence and absence of ascorbic acid (Table 5.1). However, biofilm eradicating activity in the presence of ascorbic acid was enhanced indicating that the combination of Os(11-22)NH₂ and ascorbic acid resulted in improved activity. Ascorbic acid is an antioxidant, however, at higher concentrations, ascorbic acid acts as a pro-oxidant with potent antifungal activity. A previous study by Cursino *et al.* (153) showed that ascorbic acid had synergistic activity with conventional antibiotics. Therefore, the anti-biofilm activity of Os(11-22)NH₂ in combination with ascorbic acid could also be investigated using the checkerboard assay.

In conclusion, Os(11-22)NH₂ is an effective antifungal agent which inhibits biofilm formation and eradicates preformed biofilms. Future research should further investigate its mode of action and its combination with other antifungal agents.

Table 5.1: Summary of results from this study.

<u>Anti-planktonic activity</u>		
	Os(11-22)NH₂	Os
Activity	✓ (47 μM)	✗ (Inactive)
<u>Anti-biofilm activity</u>		
	Inhibition	Eradication
Activity	✓ (81 μM)	✓ (210 μM)
Membrane permeabilization	✓	✓
ROS production	✓	✓
Does ROS contribute to killing?	✗	✗

6. References

1. O'Neill, J. (2016) Tackling drug-resistant infections globally: final report and recommendations. In *Review on Antimicrobial Resistance*.
2. WHO. (2015) Global action plan on antimicrobial resistance.
3. dos Santos Abrantes, P. M., McArthur, C. P., and Africa, C. W. J. (2014) Multi-drug resistant oral *Candida* species isolated from HIV-positive patients in South Africa and Cameroon. *Diagnostic Microbiology and Infectious Disease* **79**, 222-227.
4. Njunda, A. L., Nsagha, D. S., Assob, J. C., Kamga, H. L., and Teyim, P. (2012) In vitro antifungal susceptibility patterns of *Candida albicans* from HIV and AIDS patients attending the Nylon Health District Hospital in Douala, Cameroon. *Journal of Public Health in Africa* **2**, 1-4.
5. Mulu, A., Kassu, A., Anagaw, B., Moges, B., Gelaw, A., Alemayehu, M., Belyhun, Y., Biadglegne, F., Hurissa, Z., and Moges, F. (2013) Frequent detection of 'azole' resistant *Candida* species among late presenting AIDS patients in northwest Ethiopia. *BMC Infectious Diseases* **13**, 82-91.
6. Mnge, P., Okeleye, B., Vasaikar, S., and Apalata, T. (2017) Species distribution and antifungal susceptibility patterns of *Candida* isolates from a public tertiary teaching hospital in the Eastern Cape Province, South Africa. *Brazilian Journal of Medical and Biological Research* **50**, e5797-e5803.
7. Sun, F., Qu, F., Ling, Y., Mao, P., Xia, P., Chen, H., and Zhou, D. (2013) Biofilm-associated infections: antibiotic resistance and novel therapeutic strategies. *Future Microbiology* **8**, 877-886.
8. Zaiou, M. (2007) Multifunctional antimicrobial peptides: therapeutic targets in several human diseases. *Journal of Molecular Medicine* **85**, 317-329.
9. Marr, A. K., Gooderham, W. J., and Hancock, R. E. W. (2006) Antibacterial peptides for therapeutic use: obstacles and realistic outlook. *Current Opinion in Pharmacology* **6**, 468-472.
10. Mbuayama, K. R. (2016) Antifungal properties of peptides derived from a defensin from the tick *Ornithodoros savignyi*. MSc dissertation, University of Pretoria.
11. Mwiria, D. (2017) Activity of tick antimicrobial peptides against *Candida albicans* biofilms. MSc dissertation, University of Pretoria.
12. Holmes, A. H., Moore, L. S. P., Sundsfjord, A., Steinbakk, M., Regmi, S., Karkey, A., Guerin, P. J., and Piddock, L. J. V. (2016) Understanding the mechanisms and drivers of antimicrobial resistance. *The Lancet* **387**, 176-187.
13. WHO. (1999) Counterfeit drugs: guidelines for the development of measures to combat counterfeit drugs.

14. Kelesidis, T., and Falagas, M. E. (2015) Substandard/counterfeit antimicrobial drugs. *Clinical Microbiology Reviews* **28**, 443-464.
15. Barrett, D. (2002) From natural products to clinically useful antifungals. *Biochimica et Biophysica Acta (BBA)-Molecular Basis of Disease* **1587**, 224-233.
16. Perlin, D. S., Shor, E., and Zhao, Y. (2015) Update on antifungal drug resistance. *Current Clinical Microbiology Reports* **2**, 84-95.
17. Brown, G. D., Denning, D. W., Gow, N. A. R., Levitz, S. M., Netea, M. G., and White, T. C. (2012) Hidden killers: human fungal infections. *Science Translational Medicine* **4**, 165rv113-165rv113.
18. Onnis, V., De Logu, A., Cocco, M. T., Fadda, R., Meleddu, R., and Congiu, C. (2009) 2-Acylhydrazino-5-arylpyrrole derivatives: Synthesis and antifungal activity evaluation. *European Journal of Medicinal Chemistry* **44**, 1288-1295.
19. Kim, J., and Sudbery, P. (2011) *Candida albicans*, a major human fungal pathogen. *The Journal of Microbiology* **49**, 171-177.
20. Nobile, C. J., and Johnson, A. D. (2015) *Candida albicans* biofilms and human disease. *Annual Review of Microbiology* **69**, 71-92.
21. Al-Fattani, M. A., and Douglas, L. J. (2004) Penetration of *Candida* biofilms by antifungal agents. *Antimicrobial Agents and Chemotherapy* **48**, 3291-3297.
22. Pfaller, M. A., Jones, R. N., Messer, S.A., Edmond, M.B., and Wenzel, R. P. (1998) National surveillance of nosocomial blood stream infection due to *Candida albicans*: frequency of occurrence and antifungal susceptibility in the SCOPE Program. *Diagnostic Microbiology and Infectious Disease* **31**, 327-332.
23. Finkel, J. S., and Mitchell, A. P. (2011) Genetic control of *Candida albicans* biofilm development. *Nature Reviews Microbiology* **9**, 109-118.
24. Harriott, M. M., and Noverr, M. C. (2011) Importance of *Candida*-bacterial polymicrobial biofilms in disease. *Trends in Microbiology* **19**, 557-563.
25. Kathiravan, M. K., Salake, A. B., Chothe, A. S., Dudhe, P. B., Watode, R. P., Mukta, M. S., and Gadhwe, S. (2012) The biology and chemistry of antifungal agents: a review. *Bioorganic & Medicinal Chemistry* **20**, 5678-5698.
26. Odds, F. C., Brown, A. J., and Gow, N. A. (2003) Antifungal agents: mechanisms of action. *Trends in Microbiology* **11**, 272-279.
27. Gallis, H. A., Drew, R. H., and Pickard, W. W. (1990) Amphotericin B: 30 years of clinical experience. *Reviews of Infectious Diseases* **12**, 308-329.

28. Chapman, S. W., Dismukes, W. E., Proia, L. A., Bradsher, R. W., Pappas, P. G., Threlkeld, M. G., and Kauffman, C. A. (2008) Clinical practice guidelines for the management of blastomycosis: 2008 update by the Infectious Diseases Society of America. *Clinical Infectious Diseases* **46**, 1801-1812.
29. Perfect, J. R., Dismukes, W. E., Dromer, F., Goldman, D. L., Graybill, J. R., Hamill, R. J., Harrison, T. S., Larsen, R. A., Lortholary, O., and Nguyen, M.-H. (2010) Clinical practice guidelines for the management of cryptococcal disease: 2010 update by the Infectious Diseases Society of America. *Clinical Infectious Diseases* **50**, 291-322.
30. Wheat, L. J., Freifeld, A. G., Kleiman, M. B., Baddley, J. W., McKinsey, D. S., Loyd, J. E., and Kauffman, C. A. (2007) Clinical practice guidelines for the management of patients with histoplasmosis: 2007 update by the Infectious Diseases Society of America. *Clinical Infectious Diseases* **45**, 807-825.
31. Nett, J. E., and Andes, D. R. (2016) Antifungal agents: spectrum of activity, pharmacology, and clinical indications. *Infectious Disease Clinics of North America* **30**, 51-83.
32. Brajtburg, J., Price, H., Medoff, G., Schlessinger, D., and Kobayashi, G. (1974) The molecular basis for the selective toxicity of amphotericin B for yeast and filipin for animal oils. *Antimicrobial Agents and Chemotherapy* **5**, 377-382.
33. Vincent, T. (2000) Current and future antifungal therapy: new targets for antifungal therapy. *International Journal of Antimicrobial Agents* **16**, 317-321.
34. Arikan, S., and Rex, J. H. (2001) Lipid-based antifungal agents: current status. *Current Pharmaceutical Design* **7**, 393-415.
35. Saag, M. S., and Dismukes, W. E. (1988) Azole antifungal agents: emphasis on new triazoles. *Antimicrobial Agents and Chemotherapy* **32**, 1-8.
36. Bossche, H. V., Koymans, L., and Moereels, H. (1995) P450 inhibitors of use in medical treatment: focus on mechanisms of action. *Pharmacology & Therapeutics* **67**, 79-100.
37. Marichal, P., Gorrens, J., and Vanden Bossche, H. (1985) The action of itraconazole and ketoconazole on growth and sterol synthesis in *Aspergillus fumigatus* and *Aspergillus niger*. *Sabouraudia: Journal of Medical and Veterinary Mycology* **23**, 13-21.
38. Shao, P.-L., Huang, L.-M., and Hsueh, P.-R. (2007) Recent advances and challenges in the treatment of invasive fungal infections. *International Journal of Antimicrobial Agents* **30**, 487-495.
39. Pettit, N. N., and Carver, P. L. (2015) Isavuconazole: a new option for the management of invasive fungal infections. *Annals of Pharmacotherapy* **49**, 825-842.
40. Ullmann, A., Cornely, O., Burchardt, A., Hachem, R., Kontoyiannis, D., Töpelt, K., Courtney, R., Wexler, D., Krishna, G., and Martinho, M. (2006) Pharmacokinetics, safety, and efficacy of

posaconazole in patients with persistent febrile neutropenia or refractory invasive fungal infection. *Antimicrobial Agents and Chemotherapy* **50**, 658-666.

41. Pursley, T. J., Blomquist, I. K., Abraham, J., Andersen, H. F., and Bartley, J. A. (1996) Fluconazole-induced congenital anomalies in three infants. *Clinical Infectious Diseases* **22**, 336-340.
42. Douglas, C., D'ippolito, J., Shei, G., Meinz, M., Onishi, J., Marrinan, J., Li, W., Abruzzo, G., Flattery, A., and Bartizal, K. (1997) Identification of the FKS1 gene of *Candida albicans* as the essential target of 1, 3-beta-D-glucan synthase inhibitors. *Antimicrobial Agents and Chemotherapy* **41**, 2471-2479.
43. Onishi, J., Meinz, M., Thompson, J., Curotto, J., Dreikorn, S., Rosenbach, M., Douglas, C., Abruzzo, G., Flattery, A., and Kong, L. (2000) Discovery of novel antifungal (1, 3)- β -D-glucan synthase inhibitors. *Antimicrobial Agents and Chemotherapy* **44**, 368-377.
44. Bowman, J., Hicks, P. S., Kurtz, M., Rosen, H., Schmatz, D., Liberator, P., and Douglas, C. (2002) The antifungal echinocandin caspofungin acetate kills growing cells of *Aspergillus fumigatus* *in vitro*. *Antimicrobial Agents and Chemotherapy* **46**, 3001-3012.
45. Pfaller, M., Castanheira, M., Lockhart, S., Ahlquist, A., Messer, S., and Jones, R. (2012) Frequency of decreased susceptibility and resistance to echinocandins among fluconazole-resistant bloodstream isolates of *Candida glabrata*. *Journal of Clinical Microbiology* **50**, 1199-1203.
46. Petrikos, G., and Skiada, A. (2007) Recent advances in antifungal chemotherapy. *International Journal of Antimicrobial Agents* **30**, 108-117.
47. Park, S. C., Park, Y., and Hahm, K. S. (2011) The role of antimicrobial peptides in preventing multidrug-resistant bacterial infections and biofilm formation. *International Journal of Molecular Sciences* **12**, 5971-5992.
48. Cannon, R. D., Lamping, E., Holmes, A. R., Niimi, K., Baret, P. V., Keniya, M. V., Tanabe, K., Niimi, M., Goffeau, A., and Monk, B. C. (2009) Efflux-mediated antifungal drug resistance. *Clinical Microbiology Reviews* **22**, 291-321.
49. Sanglard, D., and Odds, F. C. (2002) Resistance of *Candida* species to antifungal agents: molecular mechanisms and clinical consequences. *The Lancet Infectious Diseases* **2**, 73-85.
50. Taff, H. T., Mitchell, K. F., Edward, J. A., and Andes, D. R. (2013) Mechanisms of *Candida* biofilm drug resistance. *Future Microbiology* **8**, 1325-1337.
51. Van Acker, H., Van Dijck, P., and Coenye, T. (2014) Molecular mechanisms of antimicrobial tolerance and resistance in bacterial and fungal biofilms. *Trends in Microbiology* **22**, 326-333.
52. Martins, M., Uppuluri, P., Thomas, D. P., Cleary, I. A., Henriques, M., Lopez-Ribot, J. L., and Oliveira, R. (2010) Presence of extracellular DNA in the *Candida albicans* biofilm matrix and its contribution to biofilms. *Mycopathologia* **169**, 323-331.

53. Baillie, G. S., and Douglas, L. J. (2000) Matrix polymers of *Candida* biofilms and their possible role in biofilm resistance to antifungal agents. *Journal of Antimicrobial Chemotherapy* **46**, 397-403.
54. Ramage, G., Saville, S. P., Thomas, D. P., and Lopez-Ribot, J. L. (2005) *Candida* biofilms: an update. *Eukaryotic Cell* **4**, 633-638.
55. Flemming, H.-C., and Wingender, J. (2010) The biofilm matrix. *Nature Reviews Microbiology* **8**, 623-633.
56. LaFleur, M. D., Kumamoto, C. A., and Lewis, K. (2006) *Candida albicans* biofilms produce antifungal-tolerant persister cells. *Antimicrobial Agents and Chemotherapy* **50**, 3839-3846.
57. Hancock, R. E. W., and Sahl, H. (2006) Antimicrobial and host-defense peptides as new anti-infective therapeutic strategies. *Nature Biotechnology* **24**, 1551-1557.
58. Zasloff, M. (2002) Antimicrobial peptides of multicellular organisms. *Nature* **415**, 389-395.
59. Kasahara, M., Suzuki, T., and Du Pasquier, L. (2004) On the origins of the adaptive immune system: novel insights from invertebrates and cold-blooded vertebrates. *Trends in Immunology* **25**, 105-111.
60. Stotz, H. U., Thomson, J., and Wang, Y. (2009) Plant defensins: defense, development and application. *Plant Signaling & Behavior* **4**, 1010-1012.
61. Powers, J.-P. S., and Hancock, Robert E. W. (2003) The relationship between peptide structure and antibacterial activity. *Peptides* **24**, 1681-1691.
62. Nakamura, T., Furunaka, H., Miyata, T., Tokunaga, F., Muta, T., Iwanaga, S., Niwa, M., Takao, T., and Shimonishi, S. (1988) Tachyplesin, a class of antimicrobial peptide from the hemocytes of the horseshoe crab (*Tachypleus tridentatus*). Isolation and chemical structure. *Journal of Biological Chemistry* **263**, 16709-16713.
63. Zasloff, M. (1987) Magainins, a class of antimicrobial peptides from *Xenopus* skin: Isolation, characterization of two active forms, and partial cDNA sequence of a precursor. *Proceedings of the National Academy of Sciences* **84**, 5449-5453.
64. Selsted, M. E., Novotny, M. J., Morris, W. L., Tang, Y. Q., Smith, W., and Cullor, J. S. (1992) Indolicidin, a novel bactericidal tridecapeptide amide from neutrophils. *Journal of Biological Chemistry* **267**, 4292-4295.
65. Fehlbauer, P., Bulet, P., Chernysh, S., Briand, J. P., Roussel, J. P., and Letellier, L. (1996) Structure-activity analysis of thanatin, a 21-residue inducible insect defense peptide with sequence homology to frog skin antimicrobial peptides. *Proceedings of the National Academy of Sciences* **93**, 1221-1225.
66. Matejuk, A., Leng, Q., Begum, M., Woodle, M., Scaria, P., Chou, S., and Mixson, A. (2010) Peptide-based antifungal therapies against emerging infections. *Drugs of the Future* **35**, 197-231.

67. Nguyen, L. T., Haney, E. F., and Vogel, H. J. (2011) The expanding scope of antimicrobial peptide structures and their modes of action. *Trends in Biotechnology* **29**, 464-472.
68. Brogden, K. A. (2005) Antimicrobial peptides: pore formers or metabolic inhibitors in bacteria? *Nature Reviews Microbiology* **3**, 238-250.
69. Shai, Y. (1999) Mechanism of the binding, insertion and destabilization of phospholipid bilayer membranes by alpha-helical antimicrobial and cell non-selective membrane-lytic peptides. *Biochimica et Biophysica Acta (BBA)-Biomembranes* **1462**, 55-70.
70. Sengupta, D., Leontiadou, H., Mark, Alan E., and Marrink, S. (2008) Toroidal pores formed by antimicrobial peptides show significant disorder. *Biochimica et Biophysica Acta (BBA)-Biomembranes* **1778**, 2308-2317.
71. Pabst, G., Grage, S. L., Danner-Pongratz, S., Jing, W., Ulrich, A. S., Watts, A., Lohner, K., and Hickel, A. (2008) Membrane thickening by the antimicrobial peptide PGLa. *Biophysical Journal* **95**, 5779-5788.
72. Sevcsik, E., Pabst, G., Richter, W., Danner, S., Amenitsch, H., and Lohner, K. (2008) Interaction of LL-37 with model membrane systems of different complexity: influence of the lipid matrix. *Biophysical Journal* **94**, 4688-4699.
73. Epanand, R. M., and Epanand, R. F. (2011) Bacterial membrane lipids in the action of antimicrobial agents. *Journal of Peptide Science* **17**, 298-305.
74. Rokitskaya, T. I., Kolodkin, N. I., Kotova, E. A., and Antonenko, Y. N. (2011) Indolicidin action on membrane permeability: carrier mechanism versus pore formation. *Biochimica et Biophysica Acta (BBA)-Biomembranes* **1808**, 91-97.
75. Haney, E. F., Nathoo, S., Vogel, H. J., and Prenner, E. J. (2010) Induction of non-lamellar lipid phases by antimicrobial peptides: a potential link to mode of action. *Chemistry and Physics of Lipids* **163**, 82-93.
76. Jeu, L., and Fung, H. B. (2004) Daptomycin: a cyclic lipopeptide antimicrobial agent. *Clinical Therapeutics* **26**, 1728-1757.
77. Miteva, M., Andersson, M., Karshikoff, A., and Otting, G. (1999) Molecular electroporation: a unifying concept for the description of membrane pore formation by antibacterial peptides, exemplified with NK-lysin. *FEBS letters* **462**, 155-158.
78. Shi, J., Ross, C. R., Chengappa, M. M., Sylte, M. J., McVey, D. S., and Blecha, F. (1996) Antibacterial activity of a synthetic peptide (PR-26) derived from PR-39, a proline-arginine-rich neutrophil antimicrobial peptide. *Antimicrobial Agents and Chemotherapy* **40**, 115-121.

79. Boman, H. G., Agerberth, B., and Boman, A. (1993) Mechanisms of action on *Escherichia coli* of cecropin P1 and PR-39, two antibacterial peptides from pig intestine. *Infection and Immunity* **61**, 2978-2984.
80. Subbalakshmi, C., and Sitaram, N. (1998) Mechanism of antimicrobial action of indolicidin. *FEMS Microbiology Letters* **160**, 91-96.
81. Lehrer, R. I., Barton, A., Daher, K. A., Harwig, S. S., Ganz, T., and Selsted, M. E. (1989) Interaction of human defensins with *Escherichia coli*. Mechanism of bactericidal activity. *Journal of Clinical Investigation* **84**, 553-561.
82. Kavanagh, K., and Dowd, S. (2004) Histatins: antimicrobial peptides with therapeutic potential. *Journal of Pharmacy and Pharmacology* **56**, 285-289.
83. Kragol, G., Lovas, S., Varadi, G., Condie, B. A., Hoffmann, R., and Otvos, L. (2001) The antibacterial peptide pyrrocoricin inhibits the ATPase actions of DnaK and prevents chaperone-assisted protein folding. *Biochemistry* **40**, 3016-3026.
84. Brötz, H., Bierbaum, G., Leopold, K., Reynolds, Peter E., and Sahl, H. (1998) The lantibiotic mersacidin inhibits peptidoglycan synthesis by targeting lipid II. *Antimicrobial Agents and Chemotherapy* **42**, 154-160.
85. Thevissen, K., Osborn, R. W., Acland, D. P., and Broekaert, W. F. (2000) Specific binding sites for an antifungal plant defensin from Dahlia (*Dahlia merckii*) on fungal cells are required for antifungal activity. *Molecular Plant-Microbe Interactions* **13**, 54-61.
86. Fromtling, R. A., and Abruzzo, G. K. (1989) L-671, 329, a new antifungal agent. *The Journal of Antibiotics* **42**, 174-178.
87. Endo, M., Takesako, K., Kato, I., and Yamaguchi, H. (1997) Fungicidal action of aureobasidin A, a cyclic depsipeptide antifungal antibiotic, against *Saccharomyces cerevisiae*. *Antimicrobial agents and Chemotherapy* **41**, 672-676.
88. Besson, F., and Michel, G. (1984) Action of the antibiotics of the iturin group on artificial membranes. *The Journal of Antibiotics* **37**, 646-651.
89. Paseale, F., Philippe, B., and Lydia, M. (1994) Septic injury of *Drosophila* induces the synthesis of a potent antifungal peptide with sequence homology to plant antifungal peptides. *Journal of Biological Chemistry* **269**, 33159-33163.
90. Vriens, K., Cools, T. L., Harvey, P. J., Craik, D. J., Spincemaille, P., Cassiman, D., Braem, A., Vleugels, J., Nibbering, P. H., and Drijfhout, J. W. (2015) Synergistic activity of the plant defensin HsAFP1 and caspofungin against *Candida albicans* biofilms and planktonic cultures. *PloS One* **10**, e0132701.

91. Overhage, J., Campisano, A., Bains, M., Torfs, E. C. W., Rehm, B. H. A., and Hancock, R. E. W. (2008) Human host defense peptide LL-37 prevents bacterial biofilm formation. *Infection and Immunity* **76**, 4176-4182.
92. Aka, S. T. (2015) Killing efficacy and anti-biofilm activity of synthetic human cationic antimicrobial peptide cathelicidin hCAP-18/LL-37 against urinary tract pathogens. *Journal of Microbiology and Infectious Diseases* **5**, 15-20.
93. Anunthawan, T., de la Fuente-Núñez, C., Hancock, R. E. W., and Klaynongsruang, S. (2015) Cationic amphipathic peptides KT2 and RT2 are taken up into bacterial cells and kill planktonic and biofilm bacteria. *Biochimica et Biophysica Acta (BBA)-Biomembranes* **1848**, 1352-1358.
94. De Brucker, K., Delattin, N., Robijns, S., Steenackers, H., Verstraeten, N., Landuyt, B., Luyten, W., Schoofs, L., Dovgan, B., and Fröhlich, M. (2014) Derivatives of the mouse cathelicidin-related antimicrobial peptide (CRAMP) inhibit fungal and bacterial biofilm formation. *Antimicrobial Agents and Chemotherapy* **58**, 5395-5404.
95. Harris, M. R., and Coote, P. J. (2010) Combination of caspofungin or anidulafungin with antimicrobial peptides results in potent synergistic killing of *Candida albicans* and *Candida glabrata* *in vitro*. *International Journal of Antimicrobial Agents* **35**, 347-356.
96. Tabbene, O., Azaiez, S., Di Grazia, A., Karkouch, I., Ben Slimene, I., Elkahoui, S., Alfeddy, M. N., Casciaro, B., Luca, V., and Limam, F. (2016) Bacillomycin D and its combination with amphotericin B: promising antifungal compounds with powerful antibiofilm activity and wound-healing potency. *Journal of Applied Microbiology* **120**, 289-300.
97. Troskie, A. M., Rautenbach, M., Delattin, N., Vosloo, J. A., Dathe, M., Cammue, B. P. A., and Thevissen, K. (2014) Synergistic activity of the tyrocidines, antimicrobial cyclodecapeptides from *Bacillus aneurinolyticus*, with amphotericin B and caspofungin against *Candida albicans* biofilms. *Antimicrobial Agents and Chemotherapy* **58**, 3697-3707.
98. Haney, E. F., and Hancock, R. E. W. (2013) Peptide design for antimicrobial and immunomodulatory applications. *Peptide Science* **100**, 572-583.
99. Mygind, P. H., Fischer, R. L., Schnorr, K. M., Hansen, M. T., Sönksen, C. P., Ludvigsen, S., Raventós, D., Buskov, S., Christensen, B., and De Maria, L. (2005) Plectasin is a peptide antibiotic with therapeutic potential from a saprophytic fungus. *Nature* **437**, 975-980.
100. Prinsloo, L., Naidoo, A., Serem, J. C., Taute, H., Sayed, Y., Bester, M. J., Neitz, A. W. H., and Gaspar, A. R. M. (2013) Structural and functional characterization of peptides derived from the carboxy-terminal region of a defensin from the tick *Ornithodoros savignyi*. *Journal of Peptide Science* **19**, 325-332.

101. Tam, J. P., Lu, Y. A., and Yang, J. L. (2001) Correlations of cationic charges with salt sensitivity and microbial specificity of cystine-stabilized beta-strand antimicrobial peptides. *Journal of Biological Chemistry* **277**, 50450-50456.
102. Friedrich, C., Scott, M. G., Karunaratne, N., Yan, H., and Hancock, R. E. W. (1999) Salt-resistant alpha-helical cationic antimicrobial peptides. *Antimicrobial Agents and Chemotherapy* **43**, 1542-1548.
103. Ahmad, I., Perkins, W. R., Lupan, D. M., Selsted, M. E., and Janoff, A. S. (1995) Liposomal entrapment of the neutrophil-derived peptide indolicidin endows it with *in vivo* antifungal activity. *Biochimica et Biophysica Acta (BBA)-Biomembranes* **1237**, 109-114.
104. Jayawardene, D. S., and Dass, C. (1999) The effect of N-terminal acetylation and the inhibition activity of acetylated enkephalins on the aminopeptidase M-catalyzed hydrolysis of enkephalins. *Peptides* **20**, 963-970.
105. Nguyen, L. T., Chau, J. K., Perry, N. A., De Boer, L., Zaat, S. A., and Vogel, H. J. (2010) Serum stabilities of short tryptophan-and arginine-rich antimicrobial peptide analogs. *PLoS One* **5**, e12684.
106. Falciani, C., Lozzi, L., Pollini, S., Luca, V., Carnicelli, V., Brunetti, J., Lelli, B., Bindi, S., Scali, S., Di Giulio, A., Rossolini, G. M., Mangoni, M. L., Bracci, L., and Pini, A. (2012) Isomerization of an antimicrobial peptide broadens antimicrobial spectrum to gram-positive bacterial pathogens. *PLoS One* **7**, e46259.
107. Berthold, N., Czihal, P., Fritsche, S., Sauer, U., Schiffer, G., Knappe, D., Alber, G., and Hoffmann, R. (2013) Novel apiadaecin 1b analogs with superior serum stabilities for treatment of infections by gram-negative pathogens. *Antimicrobial Agents and Chemotherapy* **57**, 402-409.
108. Malan, M., Serem, J. C., Bester, M. J., Neitz, A. W. H., and Gaspar, A. R. M. (2015) Anti-inflammatory and anti-endotoxin properties of peptides derived from the carboxy-terminal region of a defensin from the tick *Ornithodoros savignyi*. *Journal of Peptide Science* **22**, 43-51.
109. Taute, H., Bester, M. J., Neitz, A. W. H., and Gaspar, A. R. M. (2015) Investigation into the mechanism of action of the antimicrobial peptides Os and Os-C derived from a tick defensin. *Peptides* **71**, 179-187.
110. Lamichhane, T. N., Abeydeera, N. D., Duc, A.-C. E., Cunningham, P. R., and Chow, C. S. (2011) Selection of peptides targeting helix 31 of bacterial 16S ribosomal RNA by screening M13 phage-display libraries. *Molecules* **16**, 1211-1239.
111. Rodriguez-Tudela, J., Arendrup, M., Barchiesi, F., Bille, J., Chryssanthou, E., Cuenca-Estrella, M., Dannaoui, E., Denning, D., Donnelly, J., and Dromer, F. (2008) EUCAST Definitive Document EDef 7.1: Method for the determination of broth dilution MICs of antifungal agents for fermentative yeasts: Subcommittee on Antifungal Susceptibility Testing (AFST) of the ESCMID European

- Committee for Antimicrobial Susceptibility Testing (EUCAST). *Clinical Microbiology and Infection* **14**, 398-405.
112. Jose, A., Coco, B. J., Milligan, S., Young, B., Lappin, D. F., Bagg, J., Murray, C., and Ramage, G. (2010) Reducing the incidence of denture stomatitis: are denture cleansers sufficient? *Journal of Prosthodontics: Implant, Esthetic and Reconstructive Dentistry* **19**, 252-257.
 113. Li, X., Yan, Z., and Xu, J. (2003) Quantitative variation of biofilms among strains in natural populations of *Candida albicans*. *Microbiology* **149**, 353-362.
 114. Van den Driessche, F., Rigole, P., Brackman, G., and Coenye, T. (2014) Optimization of resazurin-based viability staining for quantification of microbial biofilms. *Journal of Microbiological Methods* **98**, 31-34.
 115. Koley, D., and Bard, A. J. (2010) Triton X-100 concentration effects on membrane permeability of a single HeLa cell by scanning electrochemical microscopy (SECM). *Proceedings of the National Academy of Sciences* **107**, 16783-16787.
 116. Nocker, A., Cheung, C.-Y., and Camper, A. K. (2006) Comparison of propidium monoazide with ethidium monoazide for differentiation of live vs. dead bacteria by selective removal of DNA from dead cells. *Journal of Microbiological Methods* **67**, 310-320.
 117. Kapuscinski, J. (1995) DAPI: a DNA-specific fluorescent probe. *Biotechnic & Histochemistry* **70**, 220-233.
 118. Valko, M., Leibfritz, D., Moncol, J., Cronin, M. T. D., Mazur, M., and Telser, J. (2007) Free radicals and antioxidants in normal physiological functions and human disease. *The International Journal of Biochemistry & Cell Biology* **39**, 44-84.
 119. Wang, H., and Joseph, J. A. (1999) Quantifying cellular oxidative stress by dichlorofluorescein assay using microplate reader. *Free Radical Biology and Medicine* **27**, 612-616.
 120. François, I. E., Bink, A., Vandercappellen, J., Ayscough, K. R., Toulmay, A., Schneiter, R., Van Gyseghem, E., Van den Mooter, G., Borgers, M., and Vandebosch, D. (2009) Membrane rafts are involved in intracellular miconazole accumulation in yeast cells. *Journal of Biological Chemistry*, 32680-32685.
 121. Rautenbach, M., Gerstner, G. D., Vlok, N. M., Kulenkampff, J., and Westerhoff, H. V. (2006) Analyses of dose–response curves to compare the antimicrobial activity of model cationic α -helical peptides highlights the necessity for a minimum of two activity parameters. *Analytical Biochemistry* **350**, 81-90.
 122. Boheim, G. (1974) Statistical analysis of alamethicin channels in black lipid membranes. *Journal of Membrane Biology* **19**, 277-303.

123. François, I. E., Thevissen, K., Pellens, K., Meert, E. M., Heeres, J., Freyne, E., Coesemans, E., Viellevoye, M., Deroose, F., and Martinez Gonzalez, S. (2009) Design and synthesis of a series of piperazine-1-carboxamide derivatives with antifungal activity resulting from accumulation of endogenous reactive oxygen species. *ChemMedChem: Chemistry Enabling Drug Discovery* **4**, 1714-1721.
124. Brandenburg, L., Merres, J., Albrecht, L., Varoga, D., and Pufe, T. (2012) Antimicrobial peptides: multifunctional drugs for different applications. *Polymers* **4**, 539-560.
125. Yacoub, H. A., Elazzazy, A. M., Abuzinadah, O. A., Al-Hejin, A. M., Mahmoud, M. M., and Harakeh, S. M. (2015) Antimicrobial activities of chicken β -defensin (4 and 10) peptides against pathogenic bacteria and fungi. *Frontiers in Cellular and Infection Microbiology* **5**, 1-10.
126. Bals, R., Wang, X., Wu, Z., Freeman, T., Bafna, V., Zasloff, M., and Wilson, J. M. (1998) Human beta-defensin 2 is a salt-sensitive peptide antibiotic expressed in human lung. *Journal of Clinical Investigation* **102**, 874-880.
127. García, J.-R. C., Krause, A., Schulz, S., Rodríguez-Jiménez, F.-J., Klüver, E., Adermann, K., Forssmann, U., Frimpong-Boateng, A., Bals, R., and Forssmann, W.-G. (2001) Human β -defensin 4: a novel inducible peptide with a specific salt-sensitive spectrum of antimicrobial activity. *The FASEB Journal* **15**, 1819-1821.
128. Goldman, M. J., Anderson, G. M., Stolzenberg, E. D., Kari, U. P., Zasloff, M., and Wilson, J. M. (1997) Human β -defensin-1 is a salt-sensitive antibiotic in lung that is inactivated in cystic fibrosis. *Cell* **88**, 553-560.
129. Douglas, L. J. (2003) *Candida* biofilms and their role in infection. *Trends in Microbiology* **11**, 30-36.
130. Coenye, T., De Prijck, K., Nailis, H., and Nelis, H. (2011) Prevention of *Candida albicans* biofilm formation. *The Open Mycology Journal* **5**, 9-20.
131. Uppuluri, P., Pierce, C. G., and López-Ribot, J. L. (2009) *Candida albicans* biofilm formation and its clinical consequences. *Future Microbiology* **4**, 1235-1237.
132. Paulone, S., Ardizzoni, A., Tavanti, A., Piccinelli, S., Rizzato, C., Lupetti, A., Colombari, B., Pericolini, E., Polonelli, L., and Magliani, W. (2017) The synthetic killer peptide KP impairs *Candida albicans* biofilm *in vitro*. *PLoS One* **12**, e0181278.
133. Delattin, N., De Brucker, K., Craik, D. J., Cheneval, O., Fröhlich, M., Veber, M., Girandon, L., Davis, T. R., Weeks, A. E., Kumamoto, C., Cos, P., Coenye, T., De Coninck, B., Cammue, B. P. A., and Thevissen, K. (2014) The plant-derived decapeptide OSIP108 interferes with *Candida albicans* biofilm formation without affecting cell viability. *Antimicrobial Agents and Chemotherapy* **58**, 2647-2656.

134. Rautenbach, M., Troskie, A. M., and Vosloo, J. A. (2016) Antifungal peptides: To be or not to be membrane active. *Biochimie* **130**, 132-145.
135. Brana, C., Benham, C., and Sundstrom, L. (2002) A method for characterising cell death *in vitro* by combining propidium iodide staining with immunohistochemistry. *Brain Research Protocols* **10**, 109-114.
136. Hawser, S. P., and Douglas, L. J. (1994) Biofilm formation by *Candida* species on the surface of catheter materials in vitro. *Infection and Immunity* **62**, 915-921.
137. Baillie, G. S., and Douglas, L. J. (1999) Role of dimorphism in the development of *Candida albicans* biofilms. *Journal of Medical Microbiology* **48**, 671-679.
138. Prasad, V., Semwogerere, D., and Weeks, E. R. (2007) Confocal microscopy of colloids. *Journal of Physics: Condensed Matter* **19**, 113102-113126.
139. Marchetti, M. A., Weinberger, M., Murakami, Y., Burhans, W. C., and Huberman, J. A. (2006) Production of reactive oxygen species in response to replication stress and inappropriate mitosis in fission yeast. *Journal of Cell Science* **119**, 124-131.
140. Lee, J., Koo, N., and Min, D. B. (2004) Reactive oxygen species, aging, and antioxidative nutraceuticals. *Comprehensive Reviews in Food Science and Food Safety* **3**, 21-33.
141. Valko, M., Leibfritz, D., Moncol, J., Cronin, M. T., Mazur, M., and Telser, J. (2007) Free radicals and antioxidants in normal physiological functions and human disease. *The International Journal of Biochemistry & Cell Biology* **39**, 44-84.
142. Droge, W. (2002) Free radicals in the physiological control of cell function. *Physiological Reviews* **82**, 47-95.
143. Aerts, A. M., François, I. E., Meert, E. M., Li, Q.-T., Cammue, B. P., and Thevissen, K. (2007) The antifungal activity of RsAFP2, a plant defensin from *Raphanus sativus*, involves the induction of reactive oxygen species in *Candida albicans*. *Journal of Molecular Microbiology and Biotechnology* **13**, 243-247.
144. Hwang, B., Hwang, J.-S., Lee, J., and Lee, D. G. (2011) The antimicrobial peptide, psacothasin induces reactive oxygen species and triggers apoptosis in *Candida albicans*. *Biochemical and Biophysical Research Communications* **405**, 267-271.
145. Maurya, I. K., Pathak, S., Sharma, M., Sanwal, H., Chaudhary, P., Tupe, S., Deshpande, M., Chauhan, V. S., and Prasad, R. (2011) Antifungal activity of novel synthetic peptides by accumulation of reactive oxygen species (ROS) and disruption of cell wall against *Candida albicans*. *Peptides* **32**, 1732-1740.

146. Helmerhorst, E. J., Troxler, R. F., and Oppenheim, F. G. (2001) The human salivary peptide histatin 5 exerts its antifungal activity through the formation of reactive oxygen species. *Proceedings of the National Academy of Sciences* **98**, 14637-14642.
147. Mello, E. O., Ribeiro, S. F., Carvalho, A. O., Santos, I. S., Da Cunha, M., Santa-Catarina, C., and Gomes, V. M. (2011) Antifungal activity of PvD1 defensin involves plasma membrane permeabilization, inhibition of medium acidification, and induction of ROS in fungi cells. *Current Microbiology* **62**, 1209-1217.
148. Phillips, A. J., Sudbery, I., and Ramsdale, M. (2003) Apoptosis induced by environmental stresses and amphotericin B in *Candida albicans*. *Proceedings of the National Academy of Sciences* **100**, 14327-14332.
149. Perrone, G. G., Tan, S.-X., and Dawes, I. W. (2008) Reactive oxygen species and yeast apoptosis. *Biochimica et Biophysica Acta (BBA)-Molecular Cell Research* **1783**, 1354-1368.
150. Lee, H., Hwang, J.-S., and Lee, D. G. (2017) Scolopendin, an antimicrobial peptide from centipede, attenuates mitochondrial functions and triggers apoptosis in *Candida albicans*. *Biochemical Journal* **474**, 635-645.
151. Cho, J., and Lee, D. G. (2011) Oxidative stress by antimicrobial peptide pleurocidin triggers apoptosis in *Candida albicans*. *Biochimie* **93**, 1873-1879.
152. Lee, J., and Lee, D. G. (2014) Melittin triggers apoptosis in *Candida albicans* through the reactive oxygen species-mediated mitochondria/caspase-dependent pathway. *FEMS Microbiology Letters* **355**, 36-42.
153. Cursino, L., Chartone-Souza, E., and Nascimento, A. M. A. (2005) Synergic interaction between ascorbic acid and antibiotics against *Pseudomonas aeruginosa*. *Brazilian Archives of Biology and Technology* **48**, 379-384.
154. Khalil, O. A. K., de Faria Oliveira, O. M. M., Velloso, J. C. R., de Quadros, A. U., Dalposso, L. M., Karam, T. K., Mainardes, R. M., and Khalil, N. M. (2012) Curcumin antifungal and antioxidant activities are increased in the presence of ascorbic acid. *Food Chemistry* **133**, 1001-1005.
155. Ojha, R., Manzoor, N., and Khan, L. (2009) Ascorbic acid modulates pathogenicity markers of *Candida albicans*. *International Journal of Microbiology Research* **1**, 19-24.
156. Bates, D., Su, L., Yu, D., Chertow, G., Seger, D., Gomes, D., Dasbach, E., and Platt, R. (2001) Mortality and costs of acute renal failure associated with amphotericin B therapy. *Clinical Infectious Diseases* **32**, 686-693.
157. Morici, P., Fais, R., Rizzato, C., Tavanti, A., and Lupetti, A. (2016) Inhibition of *Candida albicans* biofilm formation by the synthetic lactoferricin derived peptide hLF1-11. *PLoS One* **11**, e0167470.

158. Dathe, M., Nikolenko, H., Klose, J., and Bienert, M. (2004) Cyclization increases the antimicrobial activity and selectivity of arginine-and tryptophan-containing hexapeptides. *Biochemistry* **43**, 9140-9150.
159. Yu, H.-Y., Tu, C.-H., Yip, B.-S., Chen, H.-L., Cheng, H.-T., Huang, K.-C., Lo, H.-J., and Cheng, J.-W. (2011) Easy strategy to increase salt resistance of antimicrobial peptides. *Antimicrobial Agents and Chemotherapy* **55**, 4918-4921
160. Lupetti, A., Paulusma-Annema, A., Welling, M. M., Dogterom-Ballering, H., Brouwer, C. P., Senesi, S., van Dissel, J. T., and Nibbering, P. H. (2003) Synergistic activity of the N-terminal peptide of human lactoferrin and fluconazole against *Candida* species. *Antimicrobial Agents and Chemotherapy* **47**, 262-267.
161. Cools, T. L., Struyfs, C., Drijfhout, J. W., Kucharíková, S., Lobo Romero, C., Van Dijck, P., Ramada, M. H., Bloch Jr, C., Cammue, B., and Thevissen, K. (2017) A linear 19-mer plant defensin-derived peptide acts synergistically with caspofungin against *Candida albicans* biofilms. *Frontiers in Microbiology* **8**, 2051-2064.
162. Cho, J., and Lee, D. G. (2011) The antimicrobial peptide arenicin-1 promotes generation of reactive oxygen species and induction of apoptosis. *Biochimica et Biophysica Acta (BBA)-General Subjects* **1810**, 1246-1251.
163. Madeo, F., Fröhlich, E., and Fröhlich, K.-U. (1997) A yeast mutant showing diagnostic markers of early and late apoptosis. *The Journal of Cell Biology* **139**, 729-734.

7. Appendix

Table 7.1: Components of double strength (2X) RPMI-1640 2% glucose^a for anti-planktonic assay.

Component	Final concentration ^b (g/L)
RPMI-1640 with L-glutamine, phenol red and without sodium bicarbonate	20.80
3-(N-morpholino) propanesulfonic acid (MOPS)	69.06
Glucose	36.00

^aAdjust to pH 7.0 with sodium hydroxide (NaOH).

^bFinal concentration in 1 L.

Table 7.2: Components of single strength RPMI-1640^a for biofilm studies.

Component	Final concentration ^b (g/L)
RPMI-1640 with L-glutamine, phenol red and without sodium bicarbonate	10.40
3-(N-morpholino) propanesulfonic acid (MOPS)	34.53

^aAdjust to pH 7.0 with sodium hydroxide (NaOH).

^bFinal concentration in 1 L.

Table 7.3: Components of 10 mM phosphate buffered saline (PBS)^a for biofilm studies.

Component	Final concentration ^b (g/L)
Sodium chloride (NaCl)	8.00
Potassium chloride (KCl)	0.20
Disodium hydrogen orthophosphate (Na ₂ HPO ₄)	1.44
Potassium dihydrogen orthophosphate (KH ₂ PO ₄)	0.24

^aAdjust to pH 7.4 with hydrochloric acid (HCl).

^bFinal concentration in 1 L.